Journal of Geochemical Exploration 278 (2025) 107845

Contents lists available at ScienceDirect

Journal of Geochemical Exploration

journal homepage: www.elsevier.com/locate/gexplo

The fundamentals of rare earth element ion adsorption clay deposits: A mineral systems approach for exploration

Samantha C. Russo [a,b,*], Ignacio González-Álvarez [b,c,d], Helen A. Cocker [b], Alex J. McCoy-West [a,b]

[a] IsoTropics Geochemistry Laboratory, Earth and Environmental Science, James Cook University, Townsville, QLD 4811, Australia
[b] Economic Geology Research Centre, James Cook University, Townsville, QLD, Australia
[c] CSIRO, Mineral Resources, Discovery Program, Perth 6151, Western Australia, Australia
[d] University of Western Australia, Centre for Exploration Targeting, Perth, Western Australia, Australia

ARTICLE INFO

Keywords:
Rare earth elements
Ion Adsorption clays
Mineral Exploration
REE mobility
Surface Processes
Critical Zone
Cover

ABSTRACT

The exponential growth of demand for 'green-technologies' requires significantly increased production of critical elements, including rare earth elements (REE). Some of the most significant (and largest) REE deposits are associated with carbonatites. However, carbonatites are predominantly light-(L)REE-enriched, which has implications for meeting global heavy-(H)REE demand. As a result, REE ion adsorption clay deposits (IACD), which are examples of intense weathering, have sparked international interest as a HREE source (~80 % of global HREE are sourced from IACD). Therefore, this study presents a comprehensive review of REE IACD to understand their constraints, global distribution, and main features while applying a mineral systems approach.

The REE source for IACD, although typically granitic, is more diverse than traditionally thought, with the weathering of local igneous, metamorphic, and sedimentary rocks and external fluids (e.g., hydrothermal fluids and basinal brines) and lithologies (e.g., transport of weathering constituents rather than an in-situ source) supplying the REE required for IACD formation. Following the weathering of REE-rich source material, REE are liberated and mobilised in the weathering profile through pH-dependent complexation with ligands (e.g., F^-, CO_3^{2-}, SO_4^{2-}, PO_4^{3-}) or as hydrated REE species. The nature of the source (e.g., relative LREE- or HREE-enrichment) and fluids within the weathering profile (e.g., pH and ligand concentrations) control REE fractionation and relative LREE and HREE enrichment of a IACD. Once mobilised, REE are adsorbed out of solution and enriched onto clay minerals (e.g., kaolinite and halloysite), a process strongly controlled by pH and the physicochemical characteristics of the clays present, with REE adsorption most favourable under circumneutral conditions. To preserve REE enrichment (and IACD formation) through clay adsorption, a low erosional setting is required. Climates with excessive rainfall (e.g., tropical humid climates) may be problematic for REE IACD preservation through geological time, where excessive rainfall results in clay dissolution and saprolite collapse. The conceptual model provided in this study develops a framework that will be built upon in the coming years as our knowledge of these deposit types and global exploration continues.

1. Introduction

The exponential growth in demand for advanced-technology and the social shift to green technology requires increased production of "critical elements", such as rare earth elements (REE; Abraham, 2015; Australian Government, 2023; Cherepovitsyn and Solovyova, 2022; Goodenough et al., 2018), owing to their unique magnetic, phosphorescent, and catalytical properties (Balaram, 2019; Wall, 2021). Rare earth elements are crucial for renewable energy and digital developments, high-technology defence capabilities and for achieving the United Nations sustainable development goals (SDG), such as affordable and clean energy (SDG 7), sustainable cities (SDG 11), and responsible consumption and production (SDG 12; Ilankoon et al., 2022). However, these SDG also depend on a diverse supply chain, which is an eminent concern amidst rising geopolitical tensions where few countries dominate the supply chain for specific commodities (e.g., Brazil, ~90 % and China,

* Corresponding author at: IsoTropics Geochemistry Laboratory, Earth and Environmental Science, James Cook University, Townsville, QLD 4811, Australia.
E-mail address: samantha.russo@my.jcu.edu.au (S.C. Russo).

https://doi.org/10.1016/j.gexplo.2025.107845
Received 6 September 2024; Received in revised form 16 April 2025; Accepted 10 June 2025
Available online 12 June 2025

~70 % of the global Nb and REE supply, respectively; USGS, 2024).

Rare earth elements are defined by the International Union of Pure and Applied Chemistry (IUPAC) as elements consisting of the 15 lanthanides (i.e. La to Lu) as well as scandium (Sc) and yttrium (Y), most of which have very similar chemo-physical properties as a result of uniformity in their electronic configuration and their 3^+ oxidation state (Cicconi et al., 2021; Henderson, 1984). Therefore, REE often occur naturally in 'groups' rather than 'singularly' or in 'combinations' of REE. However, in diverse pH, redox (otherwise referred to as Eh, which is a measurement of reduction or oxidation potential measured in volts) and temperature conditions, REE can behave differently from one another. This study will refer to REE as the lanthanides (La, Ce, Pr, Nd, Sm, Eu, Gd, Tb, Dy, Ho, Er, Tm, Yb, Lu) plus Y. Additionally, rare earth oxides (REO) and total rare earth elements (∑REE) will be referred to throughout the text. Promethium and Sc are excluded from these definitions due to the lack of a stable Pm nuclei (Castor and Hedrick, 2006) and differing chemo-physical properties of Sc relative to REE (Van Gosen et al., 2017; Williams-Jones and Vasyukova, 2018). Unlike their name, REE are not considered rare in the Earth's crust and are more common than other commodities, such as Au, Ag and Pt (e.g., in Upper Continental Crust, ∑ REE = 150 ppm, Au = 1.5 ppb, Ag = 53 ppb, and Pt = 0.5 ppb; Rudnick and Gao, 2003). Instead, their name is attributed to the rarity in finding economically viable concentrations of REE (USGS, 1973; Voncken, 2016), as well as the difficulty in separating REE from each other and other elements (Eggert, 2011). Their 'rarity' and the processing complexity of REE-rich minerals creates concern for meeting increasing global REE demand, particularly for elements such as Nd and Dy that are expected to have a demand increase of 700 % and 2600 %, respectively, over the next 25years, in comparison to the current average annual production increase of 6–8 % (Abraham, 2015; Cherepovitsyn and Solovyova, 2022).

Rare earth element deposits are categorised into high-temperature deposits (primary deposits), such as carbonatites, alkaline complexes, pegmatites, calc-silicate, hydrothermal deposits/unconformity related deposits, and low-temperature deposits (secondary deposits), such as seafloor deposits, supergene deposits, heavy mineral sands (HMS), and ion adsorption clay deposits (IACD; Balaram, 2019; González-Álvarez et al., 2021; Wall, 2021). Some of the largest global high-temperature REE deposits include: (1) Bayan Obo, China (480 kt; average grade = 6 wt% REO; Drew et al., 1990; Keller and Anderson, 2018; Wall, 2021); (2) Mountain Pass, USA (> 200 kt; average grade = 8.9 wt% REO; Castor, 2008a; Castor, 2008b); and (3) Dulacao, China (81 kt; average grade = 5.21 wt% REO; Liu and Hou, 2017); whereas significant low-temperature REE deposits include: (1) Mount Weld, Australia (17.7 Mt.; average grade = 8.0 wt% REO; Lottermoser, 1990; Lynas Rare Earths, 2023; Wall, 2021); and (2) Araxá, Brazil (22 Mt.; average grade = 3.02 wt% REO; Neumann and Medeiros, 2015; Takehara et al., 2016). Nevertheless, China remains the leading producer of REE and accounts for ~70 % of global production, followed by the United States accounting for ~15 % (USGS, 2024).

Carbonatites, although some of the most significant REE deposits globally, are typically LREE-enriched and contain high concentrations of environmental contaminants (U and Th) that are hosted in common REE host minerals (e.g., monazite and xenotime; Dostal, 2017; Goodenough et al., 2018; Hoshino et al., 2016). Despite their lower grades relative to REE carbonatites, 'lateritic' REE IACD have sparked interest as a result of their low U and Th contents, more efficient extraction methods through less aggressive reagent salts (e.g., ammonium sulfate) and relative HREE-enrichments, where REE IACD contribute 80 % of global HREE production (Gupta and Krishnamurthy, 1992; Li et al., 2019; Schulze et al., 2017; Tang et al., 2021; Yaraghi et al., 2019). The majority of confirmed and mined REE IACD are currently located in South China (e.g., Zudong deposit; 0.2 Mt.; average grade = 0.098–0.107 wt%; Chu et al., 2024; Huang et al., 1989; Li et al., 2017), with the exception of few localities in Brazil (e.g., Serra Verde deposit; 458 Mt.; average grade = 0.098 wt%; Santana and Botelho, 2022; Santana et al., 2015; Ward, 2017), Madagascar (e.g., the weathering profile associated with the Ambohimirahavavy igneous complex; 628 Mt.; average grade = 0.089 wt%; Borst et al., 2020; Estrade et al., 2019; Ram et al., 2019), Uganda (e.g., Makuutu deposit; 532 Mt.; average grade = 0.064 wt%; Ionic Rare Earths LTD, 2022) and Australia (e.g., Koppamurra and Deep Leads deposits; 186 and 52 Mt., respectively; average grades = 0.071 and 0.081 wt%, repsectively; ABx Group, 2023a; ABx Group, 2023b; Löhr et al., 2024; Trench et al., 2025). This study presents a comprehensive review of REE IACD to understand their constraints, global distribution, and main features while applying a mineral systems approach to improve global exploration. It provides an in-depth examination of the fundamentals of REE IACD, focusing on: (1) sources of REE, (2) mechanisms of REE mobilisation, (3) REE adsorption processes, and (4) factors contributing to the preservation of REE ore bodies. This research introduces a new REE IACD model to aid in understanding and enhancing global REE mineral exploration, highlighting areas that require further research.

2. Rare earth element ion adsorption clay deposits: context

2.1. Chemical weathering

Ion adsorption clay deposits are examples of soft-rock REE deposits, where chemical weathering has liberated REE from REE-bearing minerals and facilitated the mobilisation and adsorption of REE onto clay minerals (e.g., kaolinite and halloysite) within a weathering profile (Borst et al., 2020; Cocker, 2014; Huang et al., 2021; Kanazawa and Kamitani, 2006; Li et al., 2019; Li et al., 2017; Sanematsu and Watanabe, 2016; Zhao et al., 2022). The weathering intensity of a weathering profile increases upwards towards the surface (Fig. 1), with the lowermost horizon comprising unweathered basement rock. As weathering progresses, the unweathered basement rock transitions into saprock, which exhibits alteration of <20 % of weatherable minerals and preservation of the primary fabric. The saprock transitions into saprolite, where >20 % of weatherable minerals are altered and the primary fabric

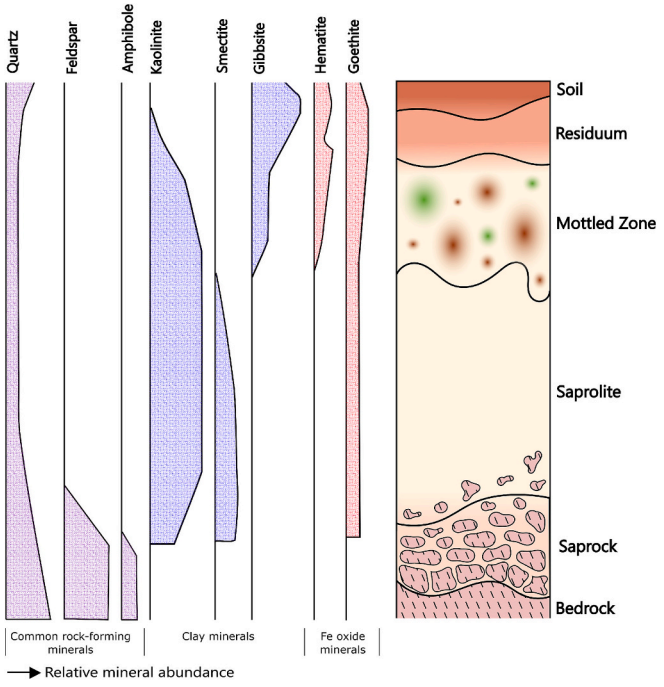

Fig. 1. Simplified weathering profile with terminology and mineral distributions for intermediate to felsic rocks under humid conditions. Relative mineral distributions based on proportions provided in Anand and Paine (2002), Sadleir and Gilkes (1976) and Anand (1998) for granitic and felsic andesite bauxite profiles from the Darling Range, Western Australia.

is still preserved. The primary fabric is eventually destroyed with more progressive weathering as the saprolite transitions into mottled zones and residuum of ferruginous, aluminous or siliceous horizons and soil generation (Fig. 1; Butt et al., 2000; Butt and Zeegers, 1992; Eggleton, 2001; Wright, 1994). Mineral proportions throughout a weathering profile are reflective of the kinetic stability of minerals, where kaolinite, hematite, goethite and/or gibbsite are considered more kinetically stable in upper horizons than the original primary minerals (Butt et al., 2000; Nahon, 1991).

Chemical weathering has traditionally been described as more rapid under tropical and humid climates with increased rainfall, biogenic activity, and weathering kinetics (Bourman, 1993; Gleeson et al., 2003; Taylor et al., 1992), and extensive weathering outside of these domains often attributed to paleoclimate weathering (Cocker, 2014; Elias, 2002; Gleeson et al., 2003). However, equally important mineral-weathering factors, such as parent material, tectonics, topography, drainage, pH and time also facilitate weathering (Bourman, 1993; Gleeson et al., 2003; Lasaga et al., 1994; Taylor et al., 1992; Wilson, 2004). Therefore, the assumption that tropical and humid paleoclimates facilitated extensive chemical weathering in 'unfavourable' glacial and wet, cool-to-cold climatic domains in Norway (Goldschmidt, 1928), North America (Reynolds and Johnson, 1972), and Australia (Bird and Chivas, 1988; Taylor et al., 1992) neglects equally important mineral-weathering factors. As a result, REE IACD, and other 'lateritic' deposits, may occur under a wider range of climatic domains than traditionally thought. Nevertheless, it is important to understand how climate influences the formation of secondary minerals during REE IACD formation, where humid climates favour the formation of 1:1 clays (e.g., kaolinite and halloysite), and can result in the formation of gibbsite through desilication, and drier climates favour the formation of 2:1 clays (e.g., smectite; Butt et al., 2000; Butt and Zeegers, 1992; Deepthy and Balakrishnan, 2005; Tardy, 1992).

2.2. Global distribution and features

The majority of confirmed REE IACD are clustered in present-day warm temperate climates in southeast Asia, specifically in China (Fig. 2; Table 1; Table A1), a consequence of decades-worth of exploration in the area. Improved global exploration of REE IACD has resulted in the discovery of deposits in equatorial and warm temperate climates across Brazil, Uganda, Malawi, Madagascar, and Australia (ABx Group, 2023a; ABx Group, 2023b; Ionic Rare Earths LTD, 2022; Löhr et al., 2024; Sanematsu and Watanabe, 2016; Santana and Botelho, 2022; Santana et al., 2015). Although chemical weathering occurs more rapidly under warmer climatic conditions (Bourman, 1993; Gleeson et al., 2003; Taylor et al., 1992), intense weathering can occur under a wider range of climates than traditionally appreciated (Bird and Chivas, 1988; Goldschmidt, 1928; Reynolds and Johnson, 1972; Taylor et al., 1992). Therefore, the formation (and discoveries) of REE IACD should not be limited to these 'favourable' climates, where colder (snow) climates show potential for REE IACD (as suggested by studies conducted in Finland; Al-Ani and Sarapää, 2009; Al-Ani et al., 2009; Sarapää and Sarala, 2013). Nevertheless, clustering of REE IACD in China is also attributed to its unique geological setting, where large-scale extension during the Mesozoic facilitated fast magma generation and possible REE-enriched lithologies (namely A-type granites) in the area (Zhao et al., 2021). Although confirmed REE IACD in China are associated with a variety of basement rocks (Table 1; Table A1), the majority are associated with granitic rocks (e.g. Bachi, Renju, Dazhou, Guposhan, Dingnan, Gangxia and Zudong deposits; Chu et al., 2024; Huang et al., 1989; Li et al., 2017).

The predominance of granitic rocks as REE IACD sources is attributed to the abundance of REE-bearing accessory phases (e.g., apatite, allanite, titanite and bastnaesite) that are susceptible to weathering, which liberate REE for clay (e.g., kaolinite and halloysite) adsorption. Alongside China, granitic rocks are also common source rocks in Brazilian (e.g., the Carina, Serra Verde, and Caldeira deposits; Aclara, 2023; Meteoric Resources, 2023; Santana and Botelho, 2022; Santana et al., 2015;

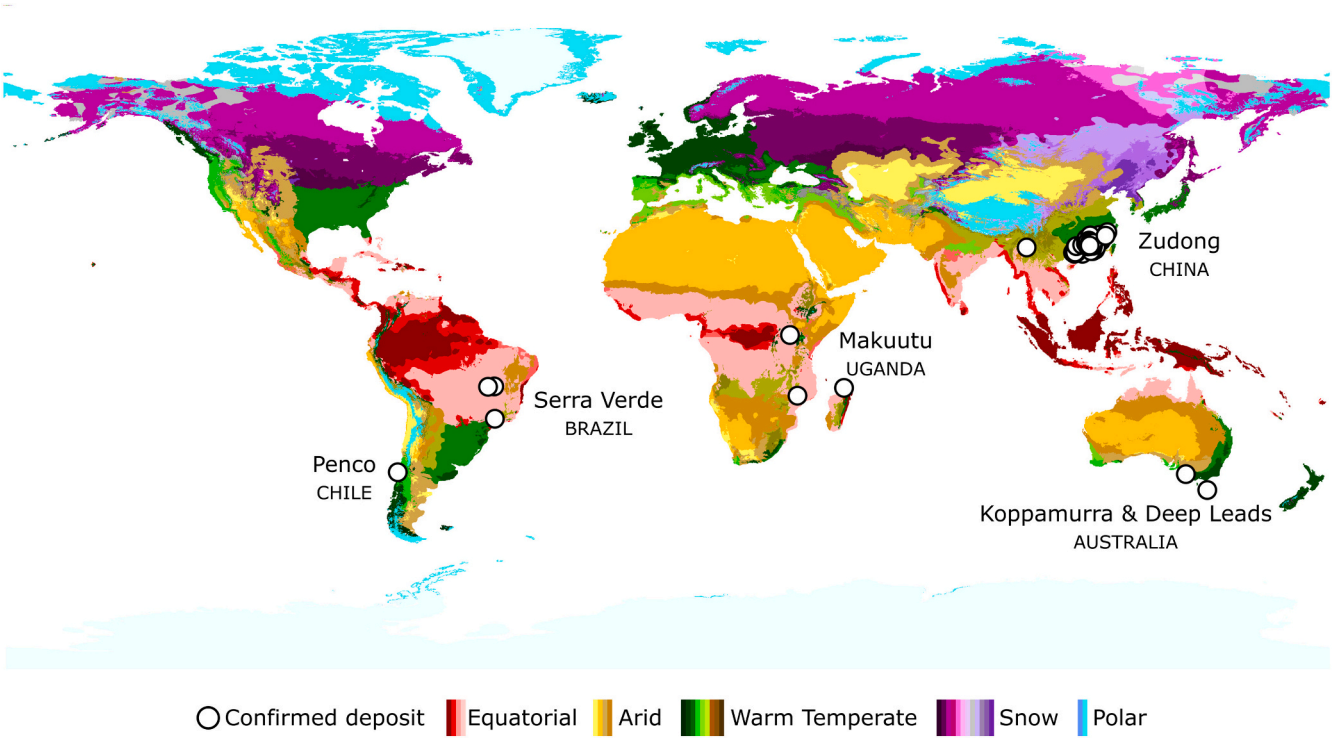

Fig. 2. Global distribution of confirmed (white circles) REE IACD with updated Koppen-Grieger climatic classifications derived from Rubel et al. (2017). Refer to Kottek et al. (2006) for detailed climatic zone legend. Refer to Table A1 in the Appendix for information on all deposit localities.

Table 1
Summary of 30 most significant confirmed REE IACD globally.

Deposit Name	Company	Latitude	Longitude	Continent	Country	State/ Province	Age (Ma)	Geology	Climatic domain	Resource and grade	Exchangeable content (%)	Relative LREE or HREE enrichment	Clay minerals	Reference
Ampasindava	Harena Resources & REENova	−13.8006	48.1717	Africa	Madagascar	Diana			Equatorial with dry winter	628 Mt @ 0.089 wt%	60–75		Kaolinite, halloysite, illite, smectite	Borst et al. (2020); Moldoveanu and Papangelakis (2013); Ram et al. (2019)
Mulanje	Gold Canyon Resources Inc. and Japan Oil, Gas and Metals National Corporation	−15.9144	35.535	Africa	Malawi	Southern Malawi		Hornbende-biotite gneiss intruded by syenite plutons	Equatorial to arid to warm temperate				Kaolinite	Le Couteur (2011); Orris et al. (2018); Sanematsu and Watanabe (2016)
Makuutu	Rwenzori Rare Metals & Ionic Rare Earths	0.5442	33.5042	Africa	Uganda				Equatorial monsoonal	532 Mt @ 0.064 wt%	75			Ionic Rare Earths LTD (2022); Liu et al. (2023a)
Carina	Aclara	−13.3992	−46.7717	Americas	Brazil	Goias		Leucogranite and biotite granite	Equatorial with dry winter	168 Mt @ 0.151 wt%	30	LREE-enriched		(Aclara, 2023)
Serra Verde	Serra Verde	−13.4994	−48.4667	Americas	Brazil	Goias		A-type granite	Equatorial with dry winter	458 Mt @ 0.098 wt%*			Kaolinite with minor smectite	Serra Verde Group (2024)
Caldeira	Meteoric Resources	−22.17	−46.62	Americas	Brazil	Minas Gerais	80	Syenite	Warm temperate with cool and dry summer to equatorial	409 Mt @ 0.263 wt%	75			Meteoric Resources (2023)
Penco	Aclara	−36.6758	−72.9719	Americas	Chile	BioBio		Granitoid	Warm temperate with hot and dry summer	27.5 Mt @ 0.229 wt%	22			Aclara (2022)
Bachi		24.75	115.7619	Asia	China	Guangdong	162	Biotite granite	Warm temperate with humid and hot summer to warm and dry summer	1.35 Mt @ 0.10–0.38 wt %	75–80	LREE-enriched		Chu et al. (2024); Li et al. (2017)
Gonghe		22.5833	112.8833	Asia	China	Guangdong	201.3–174.7	Biotite monazite	Warm temperate with humid and hot summer to warm and	0.28 Mt @ 0.151 wt%	63	LREE-enriched		Chu et al. (2024)

(*continued on next page*)

Table 1 (*continued*)

Deposit Name	Company	Latitude	Longitude	Continent	Country	State/ Province	Age (Ma)	Geology	Climatic domain	Resource and grade	Exchangeable content (%)	Relative LREE or HREE enrichment	Clay minerals	Reference
									dry summer					
Renju		24.7778	115.8133	Asia	China	Guangdong	100.5–66	Granite and rhyolite	Warm temperate with humid and hot summer to warm and dry summer	0.01 Mt @ 0.153–0.197 wt%	87.3	LREE-enriched		Chu et al. (2024); Li et al. (2017)
Shenggongzhai		24.7781	115.7892	Asia	China	Guangdong			Warm temperate with humid and hot summer to warm and dry summer	0.06 Mt @ 0.113 wt%	65	LREE-enriched		Chu et al. (2024)
Sishui		24.7611	116.0194	Asia	China	Guangdong			Warm temperate with humid and hot summer to warm and dry summer	0.03 Mt @ 0.1–0.115 wt %		LREE-enriched		Chu et al. (2024)
Wujingfu				Asia	China	Guangdong	139	Biotite monazite	Warm temperate with humid and hot summer to warm and dry summer	0.07 Mt @ 0.11–0.153 wt%	75	LREE-enriched		Chu et al. (2024); Li et al. (2017)
Yousheng		24.5083	115.0764	Asia	China	Guangdong			Warm temperate with humid and hot summer to warm and dry summer	0.01 Mt @ 0.171 wt%	80	LREE-enriched		Chu et al. (2024)
Zuokeng		24	113.8078	Asia	China	Guangdong			Warm temperate with humid and hot summer to warm and dry summer	0.11 Mt @ 0.124 wt%	60	LREE-enriched		Chu et al. (2024)

(*continued on next page*)

Table 1 (*continued*)

Deposit Name	Company	Latitude	Longitude	Continent	Country	State/ Province	Age (Ma)	Geology	Climatic domain	Resource and grade	Exchangeable content (%)	Relative LREE or HREE enrichment	Clay minerals	Reference
Dazhou		23.2667	110.5494	Asia	China	Guangxi		Granite	Warm temperate with humid and hot summer to warm and dry summer	0.53 Mt @ 0.144 wt%	72.38	LREE-enriched		Chu et al. (2024); Li et al. (2017)
Ganchong-Songshan		22.9	110.3167	Asia	China	Guangxi			Warm temperate with humid and hot summer to warm and dry summer	0.12 Mt @ 0.113 wt%	85	LREE-enriched		Chu et al. (2024)
Guposhan				Asia	China	Guangxi	151, 154	Biotite granite	Warm temperate with humid and hot summer to warm and dry summer	0.11 Mt @ 0.076–0.201 wt%	40–60	LREE-enriched		Chu et al. (2024); Li et al. (2017)
Huashan		24.5333	111.0833	Asia	China	Guangxi			Warm temperate with humid and hot summer to warm and dry summer	0.16 Mt @ 0.1–0.181 wt %	55–70	LREE-enriched		Chu et al. (2024)
Nuodong		23.0314	111	Asia	China	Guangxi			Warm temperate with humid and hot summer to warm and dry summer	0.18 Mt @ 0.15 wt%	70	LREE-enriched		Chu et al. (2024)
Zhongcun		22.9461	110.9122	Asia	China	Guangxi			Warm temperate with humid and hot summer to warm and dry summer	0.22 Mt @ 0.122 wt%	80	LREE-enriched		Chu et al. (2024)
Dingnan				Asia	China	Jiangxi	172	Biotite granite	Warm temperate with humid and hot	0.8 Mt @ 0.06–0.15 wt %	40–60	LREE-enriched		Chu et al. (2024); Li et al. (2017)

(*continued on next page*)

Table 1 (*continued*)

Deposit Name	Company	Latitude	Longitude	Continent	Country	State/ Province	Age (Ma)	Geology	Climatic domain	Resource and grade	Exchangeable content (%)	Relative LREE or HREE enrichment	Clay minerals	Reference
									summer to warm and dry summer					
Gangxia		25.2528	115.4281	Asia	China	Jiangxi	432	Biotite granite	Warm temperate with humid and hot summer to warm and dry summer	20 Mt @ 0.08–0.14 wt %		LREE-enriched		Chu et al. (2024); Li et al. (2017)
Heling				Asia	China	Jiangxi	97.3 (tuff), 96.7 (granite porphyry)	Granite and rhyolitic tuff	Warm temperate with humid and hot summer to warm and dry summer	0.24 Mt @ 0.157 wt%	75	LREE-enriched		Chu et al. (2024); Li et al. (2017)
Nanqiao		24.75	115.7667	Asia	China	Jiangxi	131, 95	Quartz syenite	Warm temperate with humid and hot summer to warm and dry summer	1.02 Mt @ 0.125–0.278 wt%	48	LREE-enriched		Chu et al. (2024); Li et al. (2017)
Shatou		24.6667	115	Asia	China	Jiangxi			Warm temperate with humid and hot summer to warm and dry summer	0.08 Mt @ 0.05–0.535 wt%	45	LREE-enriched		Chu et al. (2024)
Zudong		24.8333	114.8625	Asia	China	Jiangxi	168	Muscovite granite	Warm temperate with humid and hot summer to warm and dry summer	0.2 Mt @ 0.098–0.107 wt%	40–80	HREE-enriched		Chu et al. (2024); Huang et al. (1989); Li et al. (2017)
Koppamurra	Australian Rare Earth	−37.185	140.9611	Australia	Australia	South Australia		Limestone basement	Warm temperate with hot	186 Mt @ 0.071 wt%			Smectite with minor kaolinite	Australian Rare Earths (2023);

(*continued on next page*)

Table 1 (*continued*)

Deposit Name	Company	Latitude	Longitude	Continent	Country	State/ Province	Age (Ma)	Geology	Climatic domain	Resource and grade	Exchangeable content (%)	Relative LREE or HREE enrichment	Clay minerals	Reference
Deep Leads	Elements Limited ABX group	−41.5072	146.7736	Australia	Australia	Tasmania	170	with granitic source Dolerite and alkali basalt	and dry summer Warm temperate, humid with warm summer	52 Mt @ 0.081 wt%	50			Barakos et al. (2022) ABx Group (2023a); ABx Group (2023b)

*Reported in REE (wt%).

Serra Verde Group, 2024) and Chilean REE IACD (e.g., the Penco deposit; Aclara, 2022). However, exploration in Malawi (e.g., the Mulanje deposit; Le Couteur, 2011; Orris et al., 2018; Sanematsu and Watanabe, 2016), Uganda (e.g., the Makuutu deposit; Ionic Rare Earths LTD, 2022) and Australia (e.g., Koppamurra and Deep Leads; ABx Group, 2023a; ABx Group, 2023b; Löhr et al., 2024) suggests that the source of REE IACD is more diverse than currently appreciated, with metamorphic, sedimentary and external sources all capable of forming REE IACD. The diversity of source rocks, alongside other processes that influence REE IACD formation (i.e., mobility, adsorption, and preservation of REE enrichment within a weathering profile) are investigated in this study using the mineral systems approach to improve both our scientific understanding and global exploration efforts.

3. Rare earth element IACD in the Mineral Systems Framework

The mineral systems approach is a holistic framework developed by Magoon and Dow (1991) stating that when the entire mineral system of a deposit is understood it provides a larger exploration target than the characteristics of the mineralised deposit alone. Originally developed for the petroleum industry, the mineral systems approach has been successfully implemented for a range of mineral exploration contexts (Knox-Robinson and Wyborn, 1997; McCuaig et al., 2010; McCuaig and Hronsky, 2014; Wyborn et al., 1994), such as prospecting for REE in carbonatites and alkaline complexes (Aranha et al., 2022a; Aranha et al., 2022b), uranium in surficial environments (Chudasama et al., 2018), hydrothermal nickel (González-Álvarez et al., 2010) and magmatic nickel sulfides (Porwal et al., 2010). To gain a more complete understanding of REE IACD and aid future exploration, the mineral systems approach will be applied here to characterise the different aspects of REE IACD formation, which include: (1) REE source, (2) REE mobility, (3) REE adsorption, and (4) preservation of a REE ore body.

3.1. REE source

Rare earth elements enriched within REE IACD are traditionally thought to be sourced from weathered granitic rocks, however, this section explores the diversity of REE IACD sources that includes local igneous, metamorphic, and sedimentary rocks (with REE concentrations of diverse rock types provided in Table 2) and external REE-rich fluids

Table 2
Rare earth element concentrations of diverse rock types.

Rock type	Major rock-forming minerals	Common accessory minerals	Total REE (ppm)
Igneous			
Basalt	Plagioclase, pyroxene and olivine	Minor apatite and titanite	118.80 [a]
Syenite	Feldspar, pyroxene, amphibole and biotite	Zircon, apatite and titanite	405.80 [b]
Granite	Feldspar, quartz, mica and amphibole		267.80 [a]
I-type		Zircon, apatite, titanite and allanite	
S-type		Zircon, apatite, monazite and xenotime	
A-type		Fluorite, fluorocarbonate, titanite and zircon, minor monazite and xenotime	
Sedimentary			
Sandstone	Quartz	Zircon, apatite, monazite, xenotime and allanite	249.70 [b]

Modified from Jaireth et al. (2014). References: (a) Krauskopf and Bird (1995) and (b) Turekian and Wedepohl (1961).

(e.g., hydrothermal fluids) and weathering constituents that are transported through wind and water media (Huang et al., 1989; Huang et al., 2021; Ishihara et al., 2008; Li et al., 2017; Löhr et al., 2024; Moreno et al., 2006; Pain and Ollier, 1995; Sanematsu and Watanabe, 2016; Santana and Botelho, 2022; Sengupta and Gosen, 2016; Simonson, 1995; Taylor and Eggleton, 2001). This section also examines the importance of understanding how weathering affects various rock types, with particular emphasis on the mineral phases that release REE during this process (e.g., REE-bearing accessory minerals, such as apatite, allanite and REE-(fluoro)carbonates; Estrade et al., 2019; Li et al., 2022; Sanematsu and Watanabe, 2016; Zhao et al., 2022). The nature of the various sources (e.g., local and external rocks and fluids) are also investigated to understand how relative LREE- and HREE-enrichment of the source rock can control the REE patterns observed within the weathering profile.

3.1.1. *Weathering susceptibility of common REE-bearing minerals*

Rare earth element-bearing minerals, such as REE-(fluoro)carbonates, allanite, and titanite, have been suggested to be the most dominant source minerals of REE in REE IACD as a result of their susceptibility to weathering (Estrade et al., 2019; Li et al., 2022; Li et al., 2019; Li et al., 2017; Sanematsu and Watanabe, 2016; Zhao et al., 2022). Weathering of REE-(fluoro)carbonates to form REE enriched weathering profiles is observed in the weathering profile associated with the Serra Douranda Granite, Brazil (Santana and Botelho, 2022; Ward, 2017), as well as numerous studies indicating the high solubility of REE-(fluoro)carbonates in acidic soil water (Goldich, 1938; Huang et al., 1989; Sanematsu et al., 2016; Sanematsu et al., 2013). Similarly, allanite, titanite and apatite are also reported to dissolve during weathering (Banfield and Eggleton, 1989; Dou et al., 2023; Price et al., 2005a), whereas minerals such as thorite, zircon, and some REE-phosphates (e.g., monazite, xenotime) are considered more resistant (Fig. 3; Goldich, 1938; Li et al., 2017; Sanematsu et al., 2016; Sanematsu and Watanabe, 2016). However, organic acids have been shown to increase the weathering susceptibility of these more resistant minerals (e.g., monazite), where organic acids promote mineral weathering through, proton-promoted dissolution, forming inner-sphere complexes to liberate elements, and forming aqueous metal-ligand complexes (Corbett et al., 2017; Drever and Stillings, 1997; Furrer and Stumm, 1986; Ganor et al., 2009; Goyne et al., 2010; Lazo et al., 2017; Stumm, 1997; Tan, 1986).

Allanite and titanite are more susceptible to weathering as a result of their complex solid solutions that allow isomorphic substitution of REE^{3+} for Ca^{2+} or Na^{+} (Ercit, 2002; Foley and Ayuso, 2013; Miyawaki, 1995; Shannon, 1976). In contrast, minerals such as zircon, that exhibit simpler chemical substitution (i.e., in zircon, REE^{3+} substitutes for Th^{4+} or Zr^{4+}) are less likely to have their stability compromised by isomorphic substitution. Additionally, metamictisation (i.e., radiation damage by high concentrations U and Th) of allanite also increases weathering susceptibility, therefore contributing to the release of REE into meteoric waters and adsorbing them onto clays within weathering profiles (Price et al., 2005a).

Although metamictisation also occurs in zircon grains, the annealing nature of zircon is unlikely to contribute significant adsorbed REE proportions, restoring the crystallinity and weathering resistance of metamict grains (Carroll, 1953; Delattre et al., 2007; Du et al., 2012; Ewing, 1994; Geisler, 2002; Herrmann et al., 2021; Rubin et al., 1993; Ueda, 1957). Similar observations are seen in REE-bearing phosphate minerals (e.g. apatite, monazite, and xenotime), where metamict apatite is more susceptible to weathering as a result of its amorphous state, and monazite and xenotime remain stable with preserved crystallinity (Sanematsu and Watanabe, 2016; Ueda, 1957). However, when apatite does dissolve during weathering, the released PO_4^{2-} ligands can interact with mobilised REE^{3+} in solution and precipitate more stable REE-phosphate minerals such as rhabdophane and/or florencite (Banfield and Eggleton, 1989; Köhler et al., 2005; Sanematsu and Watanabe, 2016). Therefore, parent rocks with high P_2O_5 contents are potentially problematic for the formation of REE IACD, where common REE-bearing phosphate minerals (e.g., monazite and xenotime) are resistant to weathering (Bern et al., 2017). Alternatively, alteration fluids and weathering events may dissolve and reprecipitate REE-bearing minerals that are more susceptible to weathering, relative to their precursor mineral phases (Banfield and Eggleton, 1989; Huang et al., 2021).

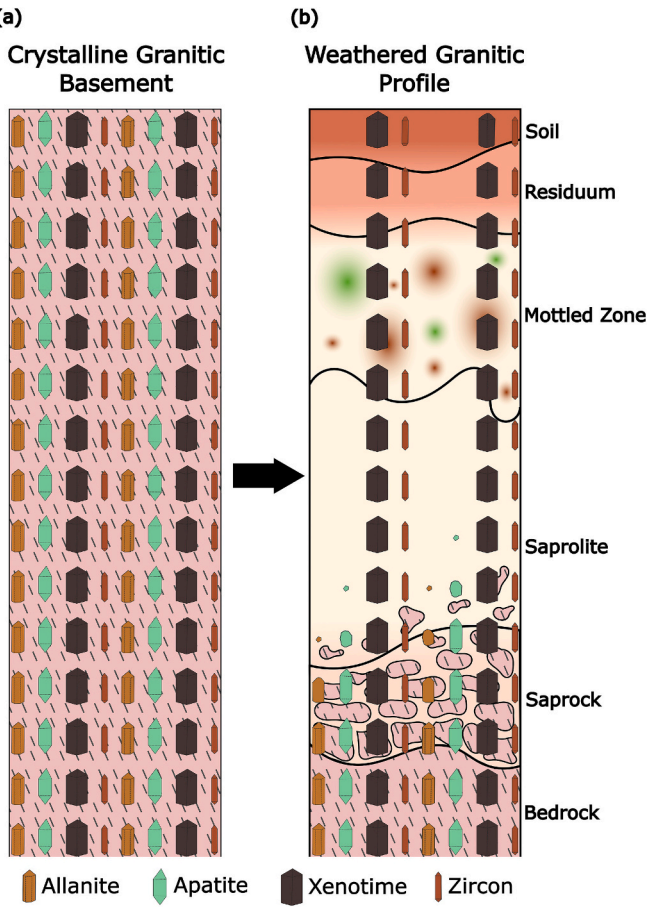

Fig. 3. Schematic diagram demonstrating the weathering susceptibility of some common REE-bearing accessory phases (a) Distibution of accessory phases (e.g., apatite, allanite, xenotime, and zircon) within unweathered crystalline granitic basement. (b) During weathering, apatite and allanite are easily dissolved, whereas, xenotime and zircon are relatively resistant to weathering. As a result, more susceptible minerals (i.e., apatite and allanite) contribute to the REE budget of the weathering profile while more resistant minerals (i.e., xenotime and zircon) retain their original REE endowment.

3.1.2. *Local basement rocks*

3.1.2.1. Granitic source rocks. Granitic rocks are presented in the literature as the predominant source rocks for REE IACD, attributed to their high proportions of feldspar and mica minerals that alter easily into clay minerals combined with the presence of REE-rich accessory phases that release REE into solution when weathered (Chu et al., 2024; Kanazawa and Kamitani, 2006; Li et al., 2017; Sanematsu and Watanabe, 2016). Although major granite (and other rock) forming minerals (e.g., feldspar, micas, and amphiboles) contribute to the REE budget of the regolith, their contributions are minimal compared to REE-rich accessory phases (i.e., (fluoro)carbonates and phosphates) that comprise up to 95 % of the REE budget (Bea, 1996; Peter Gromet and Silver, 1983). Rare earth element-rich accessory phases form through fractional crystallisation and/or secondary alteration events (i.e., deuteric metasomatism) and control the relative LREE- or HREE-enrichment of the regolith through their weathering susceptibility (e.g., apatite easily weathers and liberates LREE and MREE into the weathering profile;

Table 3
Common REE-bearing accessory minerals and their weathering susceptibility.

Mineral	Formula	LREE or HREE enriched	Reported range of REO (wt%)	Weathering rate (mol/m2/s)
Halide				
Fluorite	$(Ca,Ln)F_2$	LREE or HREE		10^{-14} [d]
(Fluoro)carbonate				
Bastnasite	$LnCO_3F$	LREE	67–75 [a]	
Parisite	$CaLn_2(CO_3)_2F_2$	LREE	61–63 [a]	
Synchisite	$CaLn(CO_3)_2F$	LREE	51 [b]	
Oxide				
Aeschynite	$(Ln,Ca,Fe,Th)(Ti,Nb)_2(O,OH)_6$		24–48 [a]	
Cerianite	$(Ce,Th)O_2$	LREE	63–81 [a,b]	
Fergusonite	$(Ln,Y)NbO_4$	HREE	46–53 [a]	
Perovskite	$(Ca,Ln)TiO_3$	LREE	≤37 [c]	
Pyrochlore	$(Ca,Na,Ln)_2Nb_2O_6(OH,F)$	LREE		
Samarskite	$(Ln,U,Fe)_3(Nb,Ta,Ti)_5O_{16}$	HREE	18 [a]	
Phosphate				
Apatite	$Ca_5(PO_4)_3(F,Cl,OH)$	LREE	≤ 19 [b]	10^{-11} [e]
Crandallite	$CaAl_3(PO_4)_2(OH)_5$	LREE		
Florencite	$LnAl_3(PO_4)_2(OH)_6$	LREE	32 [a]	
Monazite	$(Ln,Th)PO_4$	LREE	51–71 [a, b]	
Rhabdophane	$LnPO_4$	LREE	c. 65 [a]	10^{-15} - 10^{-14} [f]
Xenotime	YPO_4	HREE	61–74 [a]	
Silicate				
Allanite	$(Y,Ln,Ca,Th)_2(Al,Fe)_3(SiO_4)_3(OH)$	LREE	21–39 [a]	10^{-11}–10^{-10} [g]
Britholite	$(Ln,Th,Ca)_5(SiO_4,PO_4)_3(OH,F)$	LREE	32–53 [a]	
Eudialyte	$Na_4(Ca,Ln)_2(Fe,Mn,Y)ZrSi_8O_{22}(OH,Cl)_2$	HREE	≤ 8 [a]	
Gadolinite	$LnFeBe_2Si_2O_{10}$	HREE	39–48 [a]	
Garnet	$(Ca,Ln,Fe,Mg,Mn,Y)_3(Al,Cr,Fe,Mn,Ti,V,Zr)_2(Si,Al)_3O_{12}$	HREE		10^{-11} - 10^{-10} [g,h]
Sphene/ Titanite	$(Ca,Ln)TiSiO_5$	LREE or HREE	≤ 4 [a]	
Zircon	$(Zr,Ln)SiO_4$	HREE	≤ 4 [a]	

References: (a) Webmineral composition (www.webmineral.com), (b) Castor and Hedrick (2006), (c) Weng et al. (2013), (d) Palandri and Kharaka (2004), (e) Price et al. (2020), (f) Ma et al. (2011), (g) Price et al. (2005b), and (h) Price et al. (2008).

Table 3; Huang et al., 1989; Ishihara et al., 2008; Li et al., 2017; Sanematsu and Watanabe, 2016; Santana and Botelho, 2022). Therefore, it is important to consider the variability of REE-rich accessory minerals in local granitic sources and how this influences the REE budget of the source and regolith, and its prospectivity for REE IACD.

Granitic rocks are mostly categorised as either I-, S- or A-type, which represent igneous-, sedimentary- and anorogenic-derived granites, respectively. Although, M-type (mantle-derived) granites also exist, they are rare and will omitted from this discussion. I-type granites, which are derived from igneous protolith, are metaluminous to weakly peraluminous with high SiO_2, CaO, MgO and Na_2O contents, and are undersaturated in Al_2O_3 and K_2O relative to other granite types (Chappell, 1974; Chappell and White, 2001; Qiu et al., 2023). Accessory phases in I-type granites are generally zircon, apatite, titanite and allanite (Bea, 1996; Chappell, 1974; Chappell and White, 2001; Fu et al., 2019; Li et al., 2007; Sanematsu et al., 2015). I-type granites are relatively prospective for REE IACD as a result of easily weatherable accessory phases (except for crystalline zircon) that release REE into the weathering profile. Consequently, REE IACD type mineralisation has been observed following the weathering of I-type granites, such as weathering profiles associated with the transitional I- to S-type Kata Beach granite in Phuket, Thailand (Sanematsu et al., 2013) and I-type granites at Maran, Pahang and Mersing, Johor in Malaysia (Tohar et al., 2024).

S-type granites, on the other hand, are peraluminous granites that formed from a sedimentary protolith, containing oversaturated SiO_2 and relatively high Al_2O_3 and low Na_2O (Chappell, 1974; Chappell and White, 2001). Common accessory minerals in S-type granites include zircon, apatite, tourmaline, monazite, and xenotime (Bea et al., 1994; Chappell, 1974; Chappell and White, 2001; Fu et al., 2019; Zhou et al., 2006). Strongly peraluminous S-type granites contain elevated P, which may inhibit the formation of REE IACD with the presence of weathering-resistant monazite and xenotime phases (Bea et al., 1992; Chappell, 1974; Chappell and White, 2001; Oelkers and Poitrasson, 2002; Oelkers et al., 2008; Sanematsu et al., 2015). Although phosphate-rich phases, such as monazite, are more susceptible to weathering in the presence of organic acids (Corbett et al., 2017; Goyne et al., 2010; Lazo et al., 2017), liberated PO_4^{3-} in weathering profile fluids may inhibit REE mobilisation (and adsorption) through REE complexing and precipitation (Byrne et al., 1991; Johannesson et al., 1995; Lee and Byrne, 1992). However, S-type granites may be more prospective than originally thought, where weathering-susceptible phosphate-rich accessory phases, such as apatite, contribute significantly to the REE budget of a weathering profile (Fu et al., 2019).

A-type granites are typically anorogenic or anhydrous, as characterised by their lack of orogenic or transitional tectonic fabric and low water contents. A-type granites are variably peralkaline and are high in SiO_2, F, S and REE, and contain low Al_2O_3, CaO and MgO contents (Bailey and Hampton, 1990; Eby, 1990; Patiño Douce, 1997; Qiu et al., 2023). As a result of their characteristically high fluoride contents (e.g., with most A-type granites indicating an excess of 1000 ppm F; Collins et al., 1982), A-type granites typically contain fluoride-rich accessory phases, such as fluorite and fluorocarbonate, although titanite and zircon are also common (Collins et al., 1982; Fu et al., 2019; Price et al., 1999; Wang et al., 2015b; Wang et al., 2014; Whalen et al., 1987). Monazite and xenotime may also be present in A-type granites, although these accessory phases are rarer with low P contents (Broska and Petrík, 2008; Broska et al., 2004). Several A-type granite locations have been considered prospective for REE IACD formation including the regolith associated with the Serra Douranda, Pedra Branca, the Madeira granite, Brazil, and granites in the Bachi area, Guangdong in China (Botelho and Moura, 1998; Costa et al., 2020; da Silva Alves et al., 2018; Marini et al., 1992; Zhao et al., 2021). However, higher volatile contents in melts of A-type granites (i.e., F) can inhibit REE enrichment through distortion of crystalline melt frameworks (Mahood and Hildreth, 1983; Sawka et al., 1984). Alternatively, high F in A-type granites may promote the dissolution of resistant minerals (e.g., quartz and zircon), and therefore liberation of REE, through the formation of hydrofluoric acid (i.e., HF; da Silva Alves et al., 2018). However, the presence of F-rich source rocks and surrounding lithologies may be problematic where F-rich fluids might inhibit REE adsorption through the formation of REE-fluoride precipitates (Itoh et al., 1984; Sassani and Shock, 1993; Wood, 1990). Nevertheless, the concentration of F^- required to form REE-fluoride precipitates may not be typical for surface waters and groundwaters associated with A-type granite weathering (discussed in subsequent sections). Therefore, A-type granites appear to be particularly favourable for REE IACD formation.

Aside from the prospectivity of different granitic rock types for REE IACD formation, it is also important to recognise processes that facilitate relative LREE- or HREE-enrichments, given only 3 % of granites globally are HREE-enriched (Fan et al., 2023) and even fewer have the potential to form HREE deposits. Studies on the HREE-enriched Zudong and LREE-enriched Guanxi deposits, China, suggest that HREE enrichment is the product of deuteric metasomatism during melt evolution or hydrothermal overprinting and LREE enrichment is the product of fractional

crystallisation (Fan et al., 2023; Huang et al., 1989; Li and Zhou, 2024; Li et al., 2017). However, LREE enrichment in the Dignan and Wuliting granites, China, and the Serra Sourada granite, Brazil, and their associated weathering profiles are the products of secondary/hydrothermal processes rather than fractional crystallisation (Ishihara et al., 2008; Santana and Botelho, 2022; Santana et al., 2015). Therefore, LREE-rich granites are formed through magmatic (i.e., fractional crystallisation) and/or hydrothermal processes (i.e., deuteric metasomatism), whereas HREE-rich granites are largely the product of hydrothermal processes (as supported by Nb/Ta and K/Rb ratios, where Nb/Ta < 5 and K/Rb $<$ 150 are indicative of hydrothermal systems; Li et al., 2017). Nevertheless, relative LREE and HREE enrichments in weathering profiles are also facilitated by the weathering susceptibility of accessory REE-rich minerals. For example, S-type granites are likely to produce LREE-enriched deposits in the presence of weatherable LREE-rich phases (e.g., apatite) and weathering-resistant HREE-rich mineral phases (e.g., xenotime; Fu et al., 2019).

3.1.2.2. Basaltic source rocks. Although REE-bearing accessory phases (e.g., apatite and titanite) can enrich REE in basaltic magmas and rocks, REE partition coefficients in accessory phases tend to increase with increasing polymerisation (Prowatke and Klemme, 2005; Prowatke and Klemme, 2006a; Prowatke and Klemme, 2006b; Watson and Green, 1981). Additionally, REE-bearing accessory phases are typically more unstable/soluble in mafic melts and therefore unlikely to contribute to the REE budget significantly (Forst and Lindsley, 1992; Frost et al., 2001; Harrison and Watson, 1984; Kohn, 2017; London et al., 1999; Mysen et al., 1981; Watson and Capobianco, 1981; Wones, 1989; Xirouchakis and Lindsley, 1998). However, major basaltic rock-forming minerals, such as clinopyroxene and plagioclase, have higher partition coefficients (e.g., $D_{Nd} = 0.4–0.6$ and 0.1–0.15, respectively; Bindeman and Davis, 2000; Hill et al., 2000) relative to other rock forming minerals within these rock types, such as olivine (e.g., olivine $D_{Nd} < 0.0002$; Ionov et al., 2002; Sun and Liang, 2013), and can host significant REE concentrations. Alongside higher partition coefficients, high mineral proportions of clinopyroxene and plagioclase in basaltic rocks and their relatively low weathering resistance (e.g., diopside has a weathering rate of 10–11 mol/m2/s at pH 6 and 25°C, whereas albite and anorthite have a weathering rate of 10–12 and 10–7 mol/m2/s at pH 5, respectively; White and Brantley, 1995; Wilson, 2004) suggest that basaltic rocks can serve as a source for REE IACD.

Despite limited examples of REE IACD from basaltic sources, the deposit associated with the Emeishan basalt, China, demonstrates its potential as a source rock (Dai et al., 2010; Yang et al., 2008; Zhao et al., 2017; Zhou et al., 2013). Although XRD, SEM-EDS and trace element analyses suggest that intermediate acid volcanic rocks in the region and hydrothermal alteration contributed to the source, REE patterns and Sr isotope compositions of the weathering profile are comparable to the Emeishan basalt (Zhang et al., 2010; Zhou et al., 2013). Similarly, although secondary REE-bearing phases (i.e., REE-carbonates and -phosphates) precipitated from hydrothermal alteration contributed to the REE budget of the profile, easily weatherable primary REE-bearing rock-forming minerals may have also contributed to the budget (such as clinopyroxene and plagioclase; Wang et al., 2015a; Zhao et al., 2017; Zhou et al., 2013). Nevertheless, the potential of basaltic rocks for REE IACD formation remains relatively underexplored.

3.1.2.3. Metamorphic source rocks. Similar to granitic and basaltic source rocks, REE-bearing minerals in metamorphic rocks are a potential source for REE IACD development. Although metamorphism is unlikely to upgrade whole-rock REE concentrations, it can redistribute REE between minerals through the instability/stability of REE-bearing minerals at various metamorphic grades (Bea and Montero, 1999; Bingen et al., 1996; Cullers et al., 1974; Janots et al., 2018; Mulrooney and Rivers, 2005; Villaseca et al., 2003). For example, Bingen et al. (1996) found that during the transition from amphibolite to granulite metamorphic facies in orthogneisses from southwestern Norway, M-HREE contents of apatite increased with progressive metamorphism alongside decreasing modal abundances (i.e. dissolution) of titanite, hornblende and biotite. In contrast, increased LREE contents in monazite with increasing metamorphic grade were attributed to the breakdown of allanite. Nevertheless, metamorphism controls the stability of minerals, and therefore the redistribution (and concentration) of REE into more/less weathering susceptible phases. One of the most significant metamorphic-derived REE IACD is the Ningdu deposit, China, where the metamorphic sandstone source constitutes weathering and fragmentation of granitoids in the area (Huang et al., 2021). Hydrothermal alteration of the metamorphic bedrock aided in the concentration of >50 % of REE in the bedrock as rhabdophane and REE-epidote, with precursor metamorphism concentrating the other 40 % of REE in the bedrock through the crystallisation of epidote and titanite (Huang et al., 2021). Both processes (i.e., hydrothermal alteration and metamorphism) significantly contributed to the REE budget of the regolith. Therefore, the reorganisation of REE during metamorphism, particularly from sedimentary rocks, suggests that metamorphic rocks can be prospective sources for REE IACD development.

3.1.3. External sources including fluids and sedimentary components

Aside from local igneous, metamorphic and (meta-)sedimentary rocks, non-local processes, such as enrichment facilitated by fluids (i.e., hydrothermal fluids and basinal brines) and source materials transported by sedimentary processes (wind and/or water transport), can promote REE IACD formation. Hydrothermal alteration can facilitate the breakdown of weathering resistant minerals and the enrichment of REE into more easily dissolvable phases (e.g., Ningdu deposit, China; Huang et al., 2021). Additionally, hydrothermal fluids may also introduce REE to the system and contribute to the REE budget of the weathering profile (as speculated in the weathering profile associated with the Emeishan basalt, China; Zhao et al., 2017). Alongside hydrothermal fluids, basinal brines also modify REE-bearing accessory phases, resulting in remobilisation and redistribution of REE to the system as reflected by the Mesoproterozoic Belt-Purcell Supergroup in North America, which hosts sedimentary and mafic intrusive rocks (González-Álvarez and Kerrich, 2010; González-Álvarez and Kerrich, 2011; González-Álvarez et al., 2006; Kyser et al., 2000). However, the influence of basinal brines in the context of REE IACD is understudied and not well constrained at present.

Despite limited research on the influence of aeolian input in the REE IACD context, previous studies have investigated the contribution of aeolian sediments to weathering profiles and suggest that aeolian sediments are most significant in settings where local chemical weathering and/or erosion is relatively slow (Babechuk et al., 2015; Brimhall et al., 1988; Ferrier et al., 2011; Heckman and Rasmussen, 2011; Lawrence et al., 2013; Shi et al., 2023; Vázquez-Ortega et al., 2015). Rare earth element transport by meteoric water (e.g., fluvial systems), on the other hand, has been demonstrated by recent studies focusing on REE IACD formation and mineralisation at the Koppamurra and Deep Leads deposits in Australia (ABx Group, 2023a; ABx Group, 2023b; Löhr et al., 2024). At the Koppamurra deposit, REE and clay materials are unlikely to be sourced from local igneous or metasedimentary rocks but rather eroded material from granites in the Lachlan Orogen that were deposited in a lagoon-estuarine system and later weathered by tectonic uplift and shoreline progradation (Bowler et al., 2006; Löhr et al., 2024; Marx and Kamber, 2010; Murray-Wallace et al., 2018). The Deep Leads deposit, although associated with weathering of dolerite and alkali basalt in the area, demonstrates thicker and higher-grade mineralisation within paleochannels (ABx Group, 2023a; ABx Group, 2023b). Therefore, geochemical dispersion processes at the surface, driven by the lateral flow of meteoric water, can transport and accumulate REE away from the original basement source. As a result, sedimentary processes (e.g., aeolian and fluvial transport) and a diversity of fluids (e.g., meteoric waters, hydrothermal, and basinal brines) can facilitate or enhance the

prospectivity of REE IACD. However, these geological processes require further research to better constrain their systematics, which is out of the scope for this study.

3.2. (Physico)chemical mobility of REE during weathering

Following the dissolution of REE-bearing minerals during weathering, REE are mobilised and dispersed both laterally and vertically within the stratigraphy via meteoric water (Lottermoser, 1990; McQueen and Scott, 2008; Phillips et al., 2019; Verplanck, 2017). The groundwater table migrates based on weather events (e.g., flood and drought) and influences the vertical and lateral transport of REE, where during high rainfall (and flooding events) the weathering profile is saturated and promotes elemental transport (Carrillo-González et al., 2006; Ollier and Pain, 1996). High rainfall, alongside erosional effects, can result in hillslope processes where topographic highs and lows are prominent (Fig. 4; see Section 3.4). Li et al. (2020) suggests that erosional runoff from the ridgetop at the Bankeng REE IACD in south China promoted ore formation at the footslopes, where groundwater likely played a major role in transporting REE. However, extensive lateral transport can result in lower grades and inhibit ore formation (Verplanck, 2017).

Fluid transport in weathering profiles is either diffusive or dispersive. Diffusive transport is controlled by concentration gradients (i.e., molecules from high concentration regions moving to low concentration regions), whereas dispersive transport is controlled by variable fluid velocities in pore spaces (where pore space sizes vary along flow paths; Carrillo-González et al., 2006; Hemond and Fechner, 2022; Rose, 1973; Steefel and Lasaga, 1992). Diffusive transport typically dominates low-clay systems (e.g., acidic sandy soils) where adsorption processes are insignificant, and dispersive transport typically dominates high-clay systems (e.g., REE IACD) where adsorption is more prevalent with heterogenously distributed adsorption sites (Carrillo-González et al., 2006; Delolme et al., 2004; Gerritse, 1996; Steefel and Lasaga, 1992). Nevertheless, both diffusion and dispersion follow preferential flow pathways created by natural processes (e.g., cracking and shrinking of soils and macropores by flora and fauna), resulting in chemical weathering as fluids interact with minerals (Ollier and Pain, 1996). Therefore, the interplay of physical and chemical factors both influence fluid mobility and distribution of REE in weathering profiles.

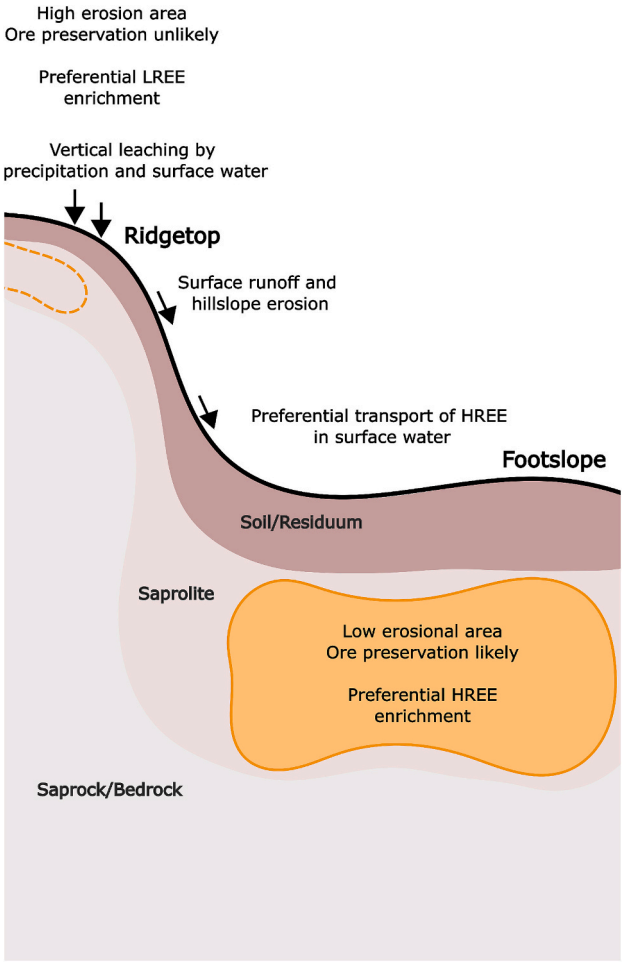

Fig. 4. Schematic diagram displaying topographic effects on the development of weathering profiles, and therefore the preservation of REE IACD. At topographic highs (ridgetops) weathering profiles are poorly developed due to excessive erosion, whereas at topographic lows (footslopes) weathering profiles are well developed due to minimal erosion and transported material contributed by ridgetops. Therefore, footslopes provide a more ideal environment for the development and preservation of REE IACD.

Chemical controls on REE mobilisation include redox, pH, ligand concentration and ionic strength. Temperature also affects REE mobilisation, for example, REE-chloride complexes are less stable than REE-fluoride complexes at 25°C but behave similarly at temperatures above 150°C (Haas et al., 1995; Migdisov et al., 2019; Migdisov et al., 2016; Migdisov and Williams-Jones, 2014; Williams-Jones et al., 2012; Wood, 1990). However, negligible differences in the stability of REE complexes are observed at ambient temperatures relevant to weathering processes associated with REE IACD, therefore further discussion on temperature-dependent stability is outside of the scope for this study. Regarding redox, the majority of the REE are monovalent (i.e. REE^{3+}) and therefore unaffected by redox variations, except for Ce (with oxidation states 3^+ and 4^+), which is strongly controlled by oxic and anerobic horizons in the weathering profile. In oxic upper regions of weathering profiles, Ce is oxidised to Ce^{4+} and subsequently forms cerianite (CeO_2) or is coprecipitated with Mn, resulting in negative anomalies of adsorbed Ce in the upper weathered profile (Braun et al., 1990; Marsh, 1991; Verplanck, 2017). However, in reducing lower regions of weathering profiles, Ce predominantly occurs as Ce^{3+} and behaves like the other LREE.

Additionally, pH, ligand concentration and ionic strength strongly control REE speciation in meteoric fluids, where REE occur as either hydrated cations (i.e., REE^{3+}) or as complexes with organic and inorganic ligands (i.e., REEHS, $REEF^{2+}$; $REECO_3^+$, $REEPO_4$, $REESO_4^+$, where HS refers to humic substances) with the dominant species dependent on pH (Haas et al., 1995; Johannesson and Lyons, 1994; Johannesson et al., 2004; Li et al., 2022; Nestmeyer and McCoy-West, 2025; Wood, 1990). In acidic meteoric fluids (pH < ~5.5), REE are predominantly simple hydrated cations, $LnSO_4^+$ and LnF^{2+} (where Ln refers to REE; Gimeno Serrano et al., 2000; Li et al., 2022; Lozano et al., 2019; Wood, 1990). However, under circumneutral (pH = ~5.5–7.2) and alkaline groundwaters (pH > ~7.2), REE-carbonate, −phosphate, and -hydroxide species become more significant (Johannesson et al., 1996; Johannesson et al., 2000; Wood, 1990). Speciation of REE also facilitates REE fractionation, with HREE forming stronger complexes with carbonate ions than LREE and are therefore more easily retained in solution (Luo and Byrne, 2004; Millero, 1992). Therefore, it is crucial to assess the stability and solubility of these complexes in meteoric fluids, as well as their influence on REE mobilisation and fractionation in a REE IACD context.

3.2.1. Influence of organic REE complexes

Organic ligands, namely humic substances, which comprise humic acids (HA) and fulvic acids (FA), are significant for REE complexation in natural waters with appreciable organic matter (e.g., dissolved organic carbon (DOC) content >0.7 mg/L; Ingri et al., 2000; Tang and Johannesson, 2003; Tanizaki et al., 1992; Viers et al., 1997). Rare earth element-HS complexes fractionate REE through a phenomenon referred to as REE loading, where low REE/DOC and high REE/DOC ratios result in preferential HREE- and middle REE (Sm, Eu and Gd)-HS complexes, respectively (Marsac et al., 2010; Pourret et al., 2007c; Stern et al., 2007;

Table 4
Stability constants (logβ values) of various REE complexes at 25 °C at zero ionic strength.

Ligand	SO_4^{2-}				F-				OH-				Cl-	NO_3^-	CO_3 2-		HCO_3^-	$H_2PO_4^-$	PO_4 3-	
nth order	1			2	1		2	3	1		2	3	4	1	1	1	2	1	1	2
Reference	a	b	c	b	c	f	e		c	d				c					g	
La	3.62	3.50 ± 0.04	3.21	1.85 ± 0.07	3.12	3.85	6.65	8.69	5.1	5.34	9.86	14.09	15.14	0.29	0.58	6.82	11.31	2.02	2.5	10.96 ± 0.11	17.63 ± 0.29
Ce		3.48 ± 0.03	3.29	1.75 ± 0.1	3.28	4.19	7.27	9.52	5.6	5.59	11.62	15.85	17.22	0.31	0.69	6.95	11.5	1.95	2.43	11.35 ± 0.09	18.48 ± 0.30
Pr	3.62	3.58 ± 0.03	3.27	1.86 ± 0.7	3.48	4.25	7.38	9.67	5.6	5.73	10.73	15.36	18.39	0.32	0.69	7.03	11.65	1.89	2.37	11.60 ± 0.10	19.08 ± 0.29
Nd	3.64	3.43 ± 0.05	3.26	1.74 ± 0.08	3.56	4.34	7.54	9.89	5.67	5.84	10.96	15.59	18.9	0.32	0.79	7.13	11.8	1.83	2.31	11.78 ± 0.09	19.50 ± 0.28
Sm		3.52 ± 0.09	3.28	1.67 ± 0.10	3.58	4.39	7.63	10.02	5.81	6.04	11.49	16.08	20.97	0.3	0.78	7.3	12.11	1.75	2.23	12.11 ± 0.06	20.42 ± 0.15
Eu	3.66	3.54 ± 0.03	3.37	1.78 ± 0.09	3.63	4.45	7.74	10.16	5.83	6.1	11.62	16.58	21.47	0.28	0.83	7.37	12.24	1.6	2.21	12.22 ± 0.04	20.66 ± 0.09
Gd	3.66	3.48 ± 0.04	3.25	1.73 ± 0.10	3.75	4.57	7.96	10.46	5.79	6.07	11.62	16.71	21.6	0.28	0.47	7.44	12.39	1.72	2.2	12.2	20.71
Tb	3.64	3.74 ± 0.05	3.2	1.9 ± 0.05	3.85	4.66	8.13	10.68	5.98	6.14	11.82	16.91	21.8	0.27	0.51	7.5	12.52	1.71	2.19	12.39 ± 0.07	21.02 ± 0.12
Dy	3.61	3.43 ± 0.03	3.15	1.75 ± 0.10	3.89	4.69	8.18	10.76	6.04	6.19	11.9	17.16	22.5	0.27	0.15	7.55	12.65	1.72	2.2	12.52 ± 0.10	21.22 ± 0.17
Y		3.34 ± 0.08		2 ± 0.08																	
Ho	3.59	3.38 ± 0.04	3.16	1.6 ± 0.2	3.95	4.74	8.27	10.88	6.01	6.22	11.93	17.43	22.47	0.27	0.25	7.59	12.77	1.73	2.21	12.59 ± 0.13	21.27 ± 0.22
Er	3.59	3.41 ± 0.04	3.15	1.78 ± 1.10	3.98	4.76	8.31	10.93	6.15	6.27	12.04	17.64	23.4	0.28	0.15	7.63	12.88	1.76	2.24	12.69 ± 0.17	21.41 ± 0.31
Tm	3.59	3.41 ± 0.05	3.07	1.80 ± 0.10	3.99	4.78	8.35	10.98	6.19	6.32	12.11	17.81	23.3	0.27	0.2	7.66	13	1.79	2.27	12.82 ± 0.20	21.57 ± 0.38
Yb	3.59	3.33 ± 0.06	3.06	1.72 ± 0.09	4.02	4.8	8.38	11.03	6.22	6.4	12.25	18.14	23.3	0.16	0.25	7.67	13.08	1.84	2.32	12.94 ± 0.22	21.79 ± 0.44
Lu	3.59	3.49 ± 0.09	3.01	1.8 ± 0.2	4.05	4.83	8.44	11.1	6.24	6.41	12.65	18.14	24.05	−0.03	0.56	7.7	13.2	1.9	2.38	12.99 ± 0.23	21.90 ± 0.45

References: **(a)** Powell (1974), **(b)** Izatt et al. (1969), **(c)** Millero (1992), **(d)** (Haas et al., 1995), **(e)** Sassani and Shock (1993), **(f)** Smith and Martell (1989), and **(g)** Lee and Byrne (1992).

Tang and Johannesson, 2010a). Rare earth element fractionation through humic substances is also controlled by molecular weight, where high molecular weight HA forms stronger complexes with MREE and low molecular weight FA forms stronger complexes with HREE (Pourret et al., 2007a; Sonke and Salters, 2006; Tang and Johannesson, 2003; Tang and Johannesson, 2010a). However, REE loading can alter the properties and behaviour of HS, such as the structure and charge distribution, affecting the overall binding capacity and availability for complexing (Marsac et al., 2010; Marsac et al., 2015; Yamamoto et al., 2010). Nonetheless, aspects such as pH, as well as competition of other ligands (e.g., CO_3^{2-}) and cation metal species (e.g., Fe and Al) also influence REE complexation.

Regarding pH, the pH of a system controls the solubility of REE-HS complexes, where FA are soluble at all pH levels and HA are soluble at pH >2 (Gaffney et al., 1996). Additionally, the pH of a system controls the availability of competing inorganic ligands (e.g., CO_3^{2-}), where organic complexing is often outcompeted by inorganic ligands with more stable REE complexes when DOC is low (e.g., DOC <0.7 mg/L; Tang and Johannesson, 2003; Tang and Johannesson, 2010a). The abundance of metal cations (e.g., Al and Fe) also inhibits REE complexing onto humic substances. Therefore, in natural waters with relatively high DOC, such as river waters (global average DOC for river water ranges between 4 and 6 mg/L; Degens, 1982), humic substances are considered significant for REE complexation, whereas for low DOC natural waters (e.g., groundwater, where average DOC = 0.7 mg/L; Leenheer et al., 1974), humic substances are insignificant for REE complexing (Tang and Johannesson, 2003). As a result of the prominence of organic-poor natural waters (e.g., groundwater) in the mobilisation, deposition and preservation of REE in REE IACD, further discussion of humic substances is considered out of the scope for this study. However, the role of humic substances of mobility and deposition (in the case of colloids) should not be disregarded for organic-rich systems (Ingri et al., 2000; Pokrovsky et al., 2006; Tang and Johannesson, 2003; Tanizaki et al., 1992; Viers et al., 1997).

3.2.2. *Stability of inorganic REE complexes in systems and the influence of dissociation constants*

Stability constants (logβ) indicate whether a complex is stable in solution and its degree of stability. A negative logβ value favours the reactants, whereas a positive logβ value favours the products, with larger negative and positive values indicating more stable reactants and products, respectively. Eq. (1) shows a first order REE-fluoride complex (LnF^{2+}), where a negative logβ would indicate a preference for Ln^{3+} and F^- (reactants), but a positive logβ would indicate a preference for LnF^{2+} (products). It is also important to consider the order of the complex (e.g. first, second, or third order which for REE-fluoride complexes are LnF^{2+}, LnF_2^+, and LnF_3, respectively, Eqs. (1)–(3)), where different orders exhibit different stabilities (Eqs. (4)–(6), where [X] refers to concentration of X in the system).

$$Ln^{3+} + F^- \rightarrow LnF^{2+} \quad (1)$$

$$LnF^{2+} + F^- \rightarrow LnF_2{}^+ \quad (2)$$

$$LnF_2{}^+ + F^- \rightarrow LnF_3 \quad (3)$$

$$\beta_{F,1} = \frac{[LnF^{2+}]}{[Ln^{3+}][F^-]}, \quad (4)$$

$$\beta_{F,2} = \frac{[LnF_2^+]}{[LnF^{2+}][F^-]} \quad (5)$$

$$\beta_{F,3} = \frac{[LnF_3]}{[LnF_2^+][F^-]} \quad (6)$$

Stability constants for various REE complexes at 25 °C at zero ionic

strength are provided in Table 4. The stability of complexes is partly controlled by electronegativity, where 'hard' ions are more compatible and stable with other 'hard' ions, and 'soft' ions with 'soft' ions (Pearson, 1988; Pearson and Gray, 1963; Wood, 1990). 'Hard' ions are generally ions with smaller ionic radii that have large HOMO/LUMO (highest occupied vs. lowest unoccupied molecular orbitals) energy gaps that favour ionic bonding, whereas 'soft' ions generally have larger ionic radii with smaller HOMO/LUMO energy gaps where bonding is typically covalent. REE are 'hard' cations that are compatible with 'hard' anions, such as fluoride, carbonate, sulfate, hydroxides, and phosphate ions, rather than 'soft' anions, such as chloride and nitrate (Pearson, 1988; Pearson and Gray, 1963; Wood, 1990). However, LREE are considered 'softer' than HREE and are slightly more compatible with chloride and nitrate anions. Nevertheless, REE complexation with 'hard' anions is significant for REE mobilisation, and potentially fractionation.

Dissociation constants (logD), which refer to whether an acid or base in solution is likely to dissociate or not, also strongly controls REE mobilisation. Dissociation constants indicate whether ligands are available to complex with REE and whether there are pH controls on REE complexation. Similar to stability constants, a negative logD value indicates preference for the reactants and a positive logD indicates preference for the products. Eqs. (7) and (8) show the dissociation (and calculation) of HF into H^+ and F^-. The logD of HF is −3.2 (Shock et al., 1989), indicating that the dissociation of HF is pH controlled and that HF is favoured under acidic conditions. Therefore, REE-fluoride complexes are typically not major complexes for REE mobilisation at acidic pH, except for where there are high concentrations of F^- or low concentrations of competing ions (e.g., Al^{3+} and SO_4^{2-}) in solution (Gimeno Serrano et al., 2000; Johannesson and Lyons, 1995; Migdisov and Williams-Jones, 2014; Shock et al., 1989).

$$HF \rightarrow H^+ + F^- \quad (7)$$

$$D_{HF} = [H^+][F^-] \quad (8)$$

For dissociation constants, similar to stability constants, orders for some complexes need to be considered, such as phosphoric acid (Eqs. (9) to (14)), where H_3PO_4, $H_2PO_4^-$, and HPO_4^{2-} are first, second, and third order complexes, respectively, with each stage of dissociation. Dissociation constants for common acids and bases in surface waters are provided in Table 5.

$$H_3PO_4 \rightarrow {H_2PO_4}^{2-} + H^+ \quad (9)$$

$${H_2PO_4}^- \rightarrow {HPO_4}^{2-} + H^+ \quad (10)$$

$${HPO_4}^{2-} \rightarrow {PO_4}^{3-} + H^+ \quad (11)$$

Table 5
Dissociation constants (logD) of various acids, that control REE complexation, at 25 °C at zero ionic strength.

Complex	nth order	Reference	logD
H_2SO_4	1	h	3.29
HSO_4^-	2	a, g	−1.99
HF	1	b	−3.2
H_2O	1	f	−14
HCl	1	a	6.1
HNO_3	1	e	1.29
H_2CO_3	1	c	−6.38
HCO_3^-	2	c	−10.32
H_3PO_4	1	d	−2.15
$H_2PO_4^-$	2	d	−7.2
HPO_4^{2-}	3	d	−12.38

References: (a) Helgeson (1969), (b) Shock et al. (1989), (c) Firsching and Mohammadzadei (1986), (d) Firsching and Brune (1991), (e) Ziouane and Leturcq (2018), (f) Verma (2003), (g) Marshall and Jones (1966), and (h) Petković (1982).

$$D_{H3PO4} = [H_2PO_4^-][H^+] \quad (12)$$

$$D_{H2PO4-} = [HPO_4^{2-}][H^+] \quad (13)$$

$$D_{HPO4\ 2-} = [PO_4^{3-}][H^+] \quad (14)$$

3.2.2.1. Chloride and nitrate complexes. Chloride and nitrate ions, often considered 'soft' anions, have a reduced affinity for the 'hard' REE cations than other common anions (e.g., flouride, carbonate and hydroxide; Pearson, 1988; Pearson and Gray, 1963; Wood, 1990). While chloride and nitrate will preferentially complex with LREE, which are considered 'softer' than HREE, it is unlikely to cause significant REE fractionation in solution where there is competition with 'hard' ions and limited availability of chloride and nitrate (Pearson, 1988; Pearson and Gray, 1963; Wood, 1990). Rare earth element-chloride complexes typically occur as first order complexes (e.g., $LnCl^{2+}$) in surface waters. However, at higher temperatures in hydrothermal fluids (Migdisov and Williams-Jones, 2014) or in brines with salinities greater than seawater (salinities >35 ppt, such as the Deep-Basin Brine aquider in the Palo Duro basin, Texas, USA; Gammons et al., 1996; Gosselin et al., 1992; Wood, 1990) chloride complexes become more significant and give rise to second order REE-chloride ($LnCl_2^+$) complexes. However, the diversity of REE-chloride complexes in hydrothermal fluids and brines is outside the scope of this manuscript and will not be discussed further.

Rare earth element-chloride complexes are most influential at acidic pH where there is limited competition with more stable 'hard' ligands (e.g., carbonate and hydroxide ions), which are dominant at circumneutral and alkaline pH (Gosselin et al., 1992; Wood, 1990). Additionally, pH does not control the availability of Cl^- in solution (log D_{HCl} = 6.1), allowing REE-chloride complexes to form under acidic conditions. However, chloride complexes are unlikely to transport appreciable REE in surface waters and groundwater systems with their relatively low stability and low availability in solution, where the global mean Cl^- concentration of groundwater is 24 ppm (Wood et al., 2022). This is supported by aqueous speciation modelling of surface waters and groundwater within this study, which demonstrated insignificant REE-chloride complexes (< 1 % of REE complexation) in aqueous media that contained <17 ppm Cl^- (Fig. 5).

Rare earth element-nitrate complexes are slightly more stable than REE-chloride complexes and are typically present as first order ($LnNO_3^{2+}$) complexes in groundwater and surface water (Table 4; Fig. 5; Millero, 1992; Wood, 1990). Similar to chloride complexes, nitrate complexes are considered negligible for REE transport (Janssen and Verweij, 2003; Shand et al., 2005; Sikakwe et al., 2018; Smedley, 1991). This is attributed to their relatively low stability constants and the low availability of NO_3^- (Wood, 1990; Wood et al., 2022).

3.2.2.2. Carbonate, fluoride, sulfate, phosphate, and hydroxide complexes. Carbonate, fluoride, sulfate, hydroxide, and phosphate ligands are examples of 'hard' ligands that are compatible with REE (HREE more than LREE), based on their high stability constants (Table 4). Rare earth element transport through carbonate complexing is supported in REE IACD systems by the simultaneous liberation (and availability) of REE^{3+} and CO_3^{2-} in solution through the dissolution of REE-(fluoro)carbonate minerals during weathering. Carbonate complexes have been widely studied concerning their complexation with REE under circumneutral and alkaline conditions (Biddau et al., 2002; Johannesson and Lyons, 1994; Johannesson et al., 1995; Johannesson et al., 2000; Zwicker et al., 2022). Rare earth element-carbonate (and -bicarbonate) complexes are strongly controlled by pH, with dissociation constants (logD) of H_2CO_3 and HCO_3^- are −6.4 and − 10.3, respectively (Table 5; Firsching and Mohammadzadei, 1986), and are therefore significant under circumneutral to alkaline conditions. Rare earth element-carbonate complexes are generally present as first order ($LnCO_3^+$) and second order ($Ln(CO_3)_2^-$) complexes, which are pH dependent (Wood, 1990). Bicarbonate

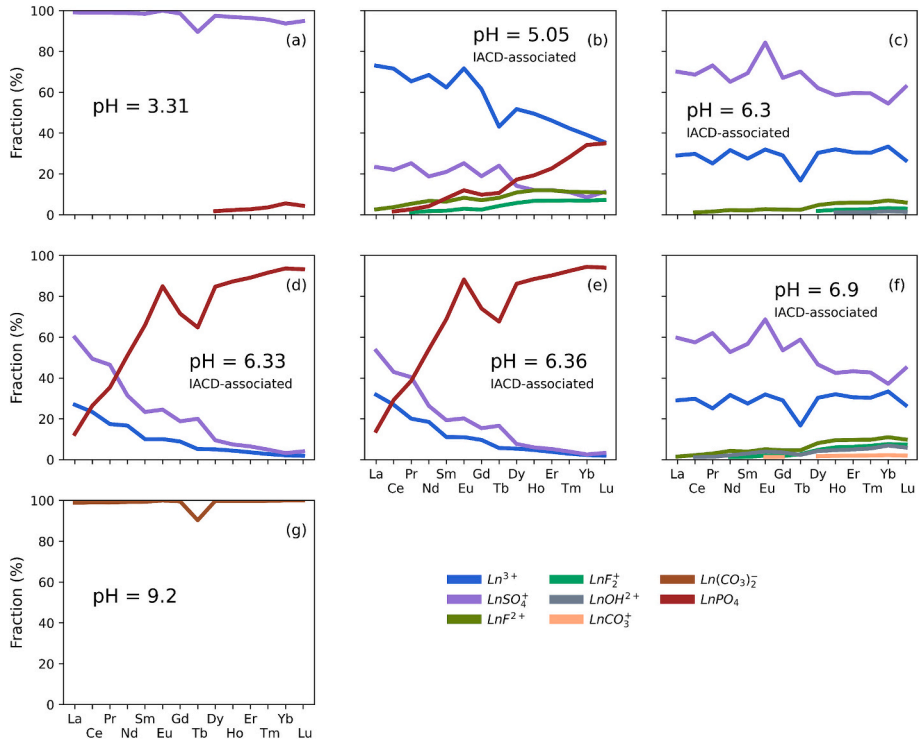

Fig. 5. Speciation of REE in a global selection of surface waters and groundwaters demonstrating the pH control on REE transport, including samples in proximity to known IACD. Speciation modelling was performed using PHREEQC. Species that contributed <1 % of an element were considered insignificant to REE transport and were omitted. (a) Non-REE IACD-associated groundwater in the shale bedrock, Cross River Basin and Niger Delta Region, Nigeria (Nganje et al., 2017) indicating dominance of REE-sulfate species at acidic conditions. (b, d, e) REE IACD-associated groundwater from the Quijaing River Basin, Zhejiang Province, China (Liu et al., 2023b) showing speciation (and fractionation) is controlled by (minor) REE-fluoride, hydrated REE, REE-sulfate, and REE-phosphate species at slightly acidic to circumneutral pH. (c, f) REE IACD-associated groundwater from meta-sediments and granites from Uganda, respectively (Owor et al., 2021) showing speciation is largely controlled by REE-sulfate and hydrated REE species (in the absence of phosphate data) under circumneutral conditions with influence of REE-hydroxide and REE-carbonate species increasing with increasing pH. (g) Non-REE IACD-associated groundwater from the Main Ethiopian Rift in the Ethiopian Volcanic Terrain (Ayenew, 2005) demonstrating the dominance of REE-carbonate species (in the absence of phosphate data) at alkaline pH. Refer to Appendix for full description of databases used for stability of complexes and groundwater and surface waters data used for speciation modelling.

complexes may also be present as first order complexes ($LnHCO_3^{2+}$), however, these complexes are less abundant and stable compared to carbonate complexes. For example, REE-carbonate speciation in surface waters and groundwaters of Ottana-Orani area, Sardinia, Italy, showed $Ln(CO_3)^{2-}$ dominates at pH > 7.5 and $LnCO3^+$ at pH between 6.5 and 7.5 (Biddau et al., 2002). Similar findings are observed in the alkaline saline waters (pH ~ 9.8) of Mono Lake, California, USA, where $Ln(CO_3)^{2-}$ accounted for >99 % of REE speciation (Johannesson and Lyons, 1994). Additionally, aqueous speciation modelling performed within this study using surface waters and groundwaters with varying pH, ligand concentration, and association with REE IACD, also found REE-carbonate species to be dominant in circumneutral to alkaline waters (more information on the PHRREQC modelling performed within this study is provided in Section 4.1 and within the Appendix; Fig. 5). Carbonate complexes are also responsible for fractionating REE in solution, where HREE are often retained in solution as HREE-carbonate complexes and LREE preferentially adsorbed onto clays (Table 4; Johannesson et al., 1999; Millero, 1992; Su et al., 2017). Therefore, pH (and availability of carbonate ions) can control REE patterns throughout the weathering profile, and thus relative LREE- and HREE-enrichments of REE IACD.

Fluoride complexes, similar to carbonate complexes, support REE transport in REE IACD formation context through simultaneous liberation of REE^{3+} and F^- during dissolution of REE-(fluoro)carbonates. Rare earth element-fluoride complexes also facilitates REE fractionation in solution, where stability increases with atomic number (i.e., LuF^{2+} is more stable than LaF^{2+}; Table 4; Millero, 1992; Sassani and Shock, 1993; Smith and Martell, 1989; Wood, 1990). The stability of REE-fluoride complexes also increases with complexation number, for example first (LnF^{2+}), second (LnF_2^+) and third order (LnF_3) complexes. However, the formation of ordered REE-fluoride complexes is largely controlled by temperature, pH and F^- concentration (Migdisov and Williams-Jones, 2014). Rare earth element-fluoride complexes are most significant at circumneutral conditions and are unlikely to transport significant REE in acidic or alkaline systems where the availability of F^- is suppressed (i.e., $\log D_{HF} = -3.2$; Shock et al., 1989) and competition with more stable complexes is magnified, respectively (Migdisov et al., 2016; Migdisov and Williams-Jones, 2014; Shakeri et al., 2015; Wood, 1990; Zwicker et al., 2022). However, the relatively low concentration of F^- in surface waters and groundwaters (i.e., global mean concentration of F- in groundwater is 0.23 ppm; Wood et al., 2022) suggests that these ions have minimal impact on REE mobilisation for IACD, as supported by aqueous speciation modelling (Fig. 5). However, if present in significant concentrations, fluoride complexes may inhibit REE IACD formation through forming insoluble third order REE-fluoride complexes (Itoh et al., 1984; Migdisov et al., 2016; Migdisov and Williams-Jones, 2014; Wood, 1990).

Unlike REE-fluoride and -carbonate complexes, REE-sulfate complexes are unlikely to fractionate REE in solution (Table 4; Izatt et al., 1969; Millero, 1992; Powell, 1974). Sulfate complexes are most influential under acidic conditions, where there is minimal competition with more stable complexes (e.g., carbonate and phosphate complexes) and pH dependence on SO_4^{2-} availability in solution (i.e., logD of H_2SO_4 and HSO_4^- are 3.29 and − 1.99, respectively; Helgeson, 1969; Marshall and Jones, 1966; Petković, 1982). Sulfate complexes are typically present as first order ($LnSO_4^+$) complexes, however, second ($Ln(SO_4)_2^-$) and third

order complexes ($Ln(SO_4)_3^{3-}$) may be present where there are anomalous SO_4^{2-} concentrations in solution (global mean concentration of SO_4^{2-} in groundwater is 31 ppm; Pourret et al., 2007b; Welch et al., 2009; Wood, 1990; Wood et al., 2022). As supported by aqueous speciation modelling, REE speciation in acidic and circumneutral surface waters and groundwaters are dominated by first order complexes (e.g. accounting for up to ~90–100 % of REE speciation in groundwater with pH = 3.31; **Fig. 5**a). Therefore, it is suggested that REE-sulfate complexes are significant for forming REE IACD at acidic and circumneutral conditions.

Phosphate complexes, on the other hand, predominantly form first order complexes ($LnPO_4$) or second order complexes ($Ln(PO_4)_2^{3-}$) when surface waters and groundwaters exceed PO_4^{2-} concentrations of 10^{-6} M (Lee and Byrne, 1992). Availability of free PO_4^{2-} species is controlled by pH (Table 5), therefore REE-phosphate complexes are more prevalent under circumneutral and alkaline conditions. Complexation with hydrogen phosphate ($LnHPO_4^{2-}$) and dihydrogen phosphate ($LnH_2PO_4^{2-}$) may also form under acidic regimes (pH < 6; Wood, 1990), however, these complexes are outcompeted by sulfate and/or fluoride ligands with higher stability constants and concentrations (Table 4). First order REE-phosphate complexes remain significant, particularly for HREE, under pH conditions between ~6.5–9 (Byrne et al., 1991; Lee and Byrne, 1992) as demonstrated by speciation modelling within this study (Fig. 5). However, phosphate complexes may inhibit REE transport due to the insolubility of $LnPO_4$ (Johannesson et al., 1995; further discussed in Section 3.2.2).

Hydroxide ligands in solution can facilitate REE fractionation with preferential complexing with HREE (Table 4; Haas et al., 1995; Millero, 1992), particularly in solutions with pH > 6 (Wood, 1990). The order of the hydroxide complex is strongly controlled the atomic number of REE, pH (and the availability of OH- in solution, where logD of $H_2O = -14$; Table 5; Verma, 2003) and the stability of the complex (Table 4; Haas et al., 1995; Millero, 1992). Aqueous speciation modelling demonstrates that $LnOH^{2+}$ complexes have limited significance for REE complexation between pH 6.3 and 6.9 (Fig. 5). However, Lee and Byrne (1992) found that $Ln(OH)_3$ complexes were significant at alkaline pH between 9 and 10, and Zwicker et al. (2022) found that $Ln(OH)_3$ and $Ln(OH)_4^-$ complexes were significant for LREE and HREE, respectively, in hyperalkaline (pH ~11–12) spring waters, southern Spain. Nevertheless, it is important to understand the effect of hydroxide complexes on REE transport, and REE IACD formation, particularly under alkaline conditions where $Ln(OH)_3$ complexes may form REE precipitates (discussed further in subsequent sections; Das et al., 2023; Diakonov et al., 1998; Lee and Byrne, 1992).

3.2.2.3. Hydrated REE cations. Rare earth elements in surface water and groundwater also mobilise as hydrated cation species (Ln^{3+}). Hydrated REE species typically form under acidic and circumneutral conditions where the metal ion maintains its complete hydration sphere and there is limited competition between ligands (e.g., carbonate, fluoride, phosphate and hydroxide ligands; Johannesson et al., 2004; Tan et al., 2014; Tang and Johannesson, 2003), as confirmed by the aqueous speciation modelling herein (Fig. 5). However, with increased SO_4^{2-} (and PO_4^{2-}) concentrations, hydrated REE cations become the second or third most significant species in solution. Hydrated REE cations themselves do not fractionate REE. Although when other fractionating ions (such as carbonate, fluoride, phosphate, and hydroxide ions) are present in solution, LREE will preferentially exist as hydrated Ln^{3+} species, while HREE will preferentially complex with ions. Nevertheless, under acidic conditions, where there is minimal competition with other ligands, hydrated REE cations can transport appreciable REE, with minimal fractionation.

3.2.3. Solubility of inorganic REE complexes during chemical weathering

Solubility of a complex determines whether the complex will be retained (and transported) in solution or will be precipitated out. Solubility constant ($logK_{sp}$) values for a range of common complexes are provided in Table 6. Negative $logK_{sp}$ values favour the reactants and positive $logK_{sp}$ values favour the products. Eqs. (15) and (16) below demonstrate the calculation of solubility constants using $LnPO_4$ as an example:

$$LnPO_4 \leftrightarrow Ln^{3+} + PO_4^{3-} \quad (15)$$

$$K_{sp} = \left[Ln^{3+}\right]\left[PO_4^{3-}\right] \quad (16)$$

Solubility constants are only applied to complexes with neutral charge, for example the first order phosphate complex ($LnPO_4$), which has a neutral charge. Therefore, based on solubility constants ($logK_{sp} = \sim -25$; Table 6; Fig. 6) and the dominance of $LnPO_4$ in aqueous modelling at circumneutral pH (Fig. 5), first order REE-phosphate complexes in natural waters will facilitate REE phosphate precipitation and inhibit REE enrichment in REE IACD (Banfield and Eggleton, 1989; Bern et al., 2017; Firsching and Brune, 1991; Johannesson et al., 1995; Sanematsu and Watanabe, 2016). Other complexes such as third order REE-fluoride (LnF_3) and REE-hydroxide ($Ln(OH)_3$) have also been shown to inhibit REE mobilisation in a multitude of geological contexts through the formation REE precipitates, as expressed by low solubility products (Hassas et al., 2021; Lee and Byrne, 1992; Migdisov et al., 2016; Migdisov and Williams-Jones, 2014; Wood, 1990). Despite the insignificance of third order REE-fluoride complexes according to modelling within this study (Fig. 5), it is suggested that natural waters with high F^- concentrations, sourced from surrounding F-rich lithologies, may inhibit REE transport and clay adsorption through the formation of REE fluoride (LnF_3) precipitates. As for hydroxide ions, it is possible that hyperalkaline fluids facilitate hydrolysis and inhibit REE IACD formation.

3.3. Deposition (and adsorption) of REE onto clay minerals

Following REE mobility and transport, REE are adsorbed out of meteoric fluids onto clay mineral surfaces (e.g., kaolinite and halloysite). Adsorption of REE onto clays is controlled by surface physicochemical properties of the clays, such as surface charge, specific surface area (SSA), and cation exchange capacity (CEC), which are strongly controlled by the structural layering of clays and pH (Bergaya et al., 2006; Coppin et al., 2002; Coppin et al., 2003; Laveuf and Cornu, 2009). Redox conditions also influence REE adsorption onto clays, where isomorphically substituted cations (e.g., Fe) enhance the cation exchange capacity through reduction or oxidation (Stucki, 2013). However, redox effects on REE adsorption onto clay minerals are relatively understudied in the REE IACD context and will be omitted from further discussion. Therefore, this section delves into the surface physicochemical properties of clays and pH controls on REE adsorption.

3.3.1. General structure of clays in REE IACD

Kaolinite and halloysite are recorded as the most dominant clay minerals in REE IACD, however, it is not uncommon for smectite (technically montmorillonite), vermiculite, and illite to be present, each of which have different physiochemical properties (Borst et al., 2020; He et al., 2023; Li and Zhou, 2023; Ram et al., 2019; Sanematsu and Watanabe, 2016; Theng, 2012; Wang et al., 2024; Yang et al., 2019). Clays are classified depending on the layering of silica-tetrahedra sheets (referred to as T sheets) and Al- or Mg-octahedra sheets (referred to as O sheets; Fig. 7; Bergaya et al., 2006; Schoonheydt and Johnston, 2011). Clays with a 1:1 structure such as kaolinite and halloysite, exhibit TO layering (i.e., where a T sheet is coupled with an O sheet in a layer), whereas 2:1 clays, such as smectite, vermiculite, and illite, exhibit TOT layering (i.e., where an O sheet is 'sandwiched' between two T sheets within a layer; Fig. 7; Al-Ani and Sarapää, 2008; Bergaya et al., 2006; Schoonheydt and Johnston, 2011). The sequencing of T and O sheets within layers of clays influences the surface charge, SSA and CEC of clays, effecting their ability to adsorb REE.

Table 6
Solubility constants ($logK_{sp}$) values of various REE complexes at 25 °C.

Ligand	SO_4^{2-}	F^-	OH^-	Cl^-	NO_3^-	CO_3^{2-}	PO_4^{3-}
Reference	a	b	c	d	e	f	g
La	−5.08	−20.5	−21.79	3.79	4.09	−29.91 ± 0.05	−26.15 ± 0.52
Ce	−3.22	−19.8	−23.93		4.30		
Pr	−1.56	−18.8	−21.75		4.22	−33.19 ± 0.26	−26.06 ± 0.18
Nd	−3.03	−19.3	−24.39	3.81	4.08	−34.1 ± 0.48	−25.95 ± 0.06
Sm	−5.95	−19	−23.56	3.68	3.96	−34.41 ± 0.53	−25.99 ± 0.05
Eu		−18.9	−23.27		3.88	−35.03 ± 0.25	−25.75 ± 0.27
Gd	−4.28	−18.6	−25.29	3.65	4.00	−35.45 ± 0.05	−25.39 ± 0.23
Tb		−18.5	−24.76		4.07	−34.86 ± 0.65	−25.07 ± 0.03
Dy		−18.1	−28.02	3.67	4.13	−33.97 ± 0.19	−25.15 ± 0.07
Y	−1.38	−18.4	−27.89		4.35	−31.52 ± 0.52	−24.76 ± 0.14
Ho	−2.79	−18	−26.38		4.23	−32.8 ± 1.2	−25.57 ± 0.46
Er	−1.03	−17.8	−26.65	3.74	4.37	−28.25 ± 0.32	−25.78 ± 0.45
Tm		−17.6	−25.19		4.54	−31.58 ± 0.28	−26.05 ± 0.06
Yb	0.80	−17.2	−26.64	3.84	4.72	−31.67 ± 0.78	−26.17 ± 0.01
Lu		−16.9			4.76	−32.16 ± 0.24	−25.39 ± 0.03

Values are for complexes with zero ionic strength. References: (**a**) Spedding and Jaffe (1954), (**b**) Itoh et al. (1984), (**c**) Diakonov et al. (1998), (**d**) Saeger et al. (1960), (**e**) Maksimov et al. (2019), (**f**) Firsching and Mohammadzadei (1986), and (**g**) Firsching and Brune (1991).

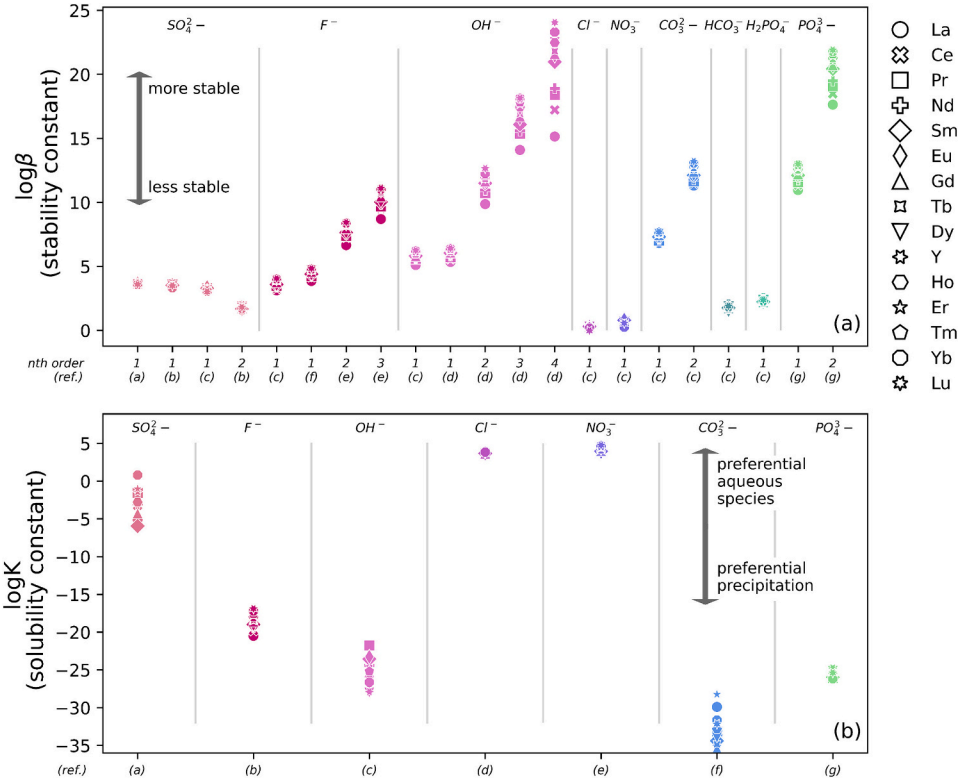

Fig. 6. Stability (a) and solubility (b) constants of REE complexes: sulfate, fluoride, hydroxide, chloride, nitrate, carbonate, bicarbonate, dihydrogen phosphate and phosphate. Increasingly positive logβ values indicate more stable complexes, whereas increasingly positive logK values indicate preferential solution-based complexation. These figures show that sulfate, fluoride, hydroxide, carbonate, and phosphate ions form stable complexes with REE. The main purpose of this figure is to show that REE-fluoride, −hydroxide, −carbonate, and-phosphate complexes fractionate REE (i.e., forming more stable complexes with HREE relative to LREE). References for (a) and (b) are provided in the footnotes of Tables 4 and 6, respectively.

3.3.1.1. Clay minerals 1:1 (kaolinite and halloysite). Cation exchange capacity is a physiochemical property of clay minerals that controls the total capacity of clays to adsorb exchangeable cations (such as, REE). Generally, the CEC of a clay mineral increases with increasing SSA and decreasing particle size (Joussein et al., 2005; Ma and Eggleton, 1999; Yukselen and Kaya, 2006). However, CEC is strongly controlled by isomorphic substitutions within the clay mineral structure, effecting the overall surface charge of the mineral and its affinity for cations (Avena et al., 2003; Bleam, 1990; Yang et al., 2016). The structure of kaolinite (Fig. 7) inhibits isomorphic substitution within the T and O sheets where strong hydrogen bonds form between the T and O sheets, resulting in limited space to host water molecules and/or cations (as supported by the layer charge of <0.01 in Table 4; Borst et al., 2020; Schoonheydt and Johnston, 2011; Skibińska, 2017; Uddin, 2008). Nevertheless, the CEC of clay is also controlled by pH through either protonation or deprotonation under acidic and alkaline conditions, respectively (Bergaya et al., 2006; Ma and Eggleton, 1999; Theng, 2012). Regarding kaolinite, cation adsorption is facilitated on the basal (OH) surfaces of the O sheets, where CEC increases with higher pH through the substitution of H^+ ions with REE^{3+} (Ma and Eggleton, 1999). The influence of pH on REE

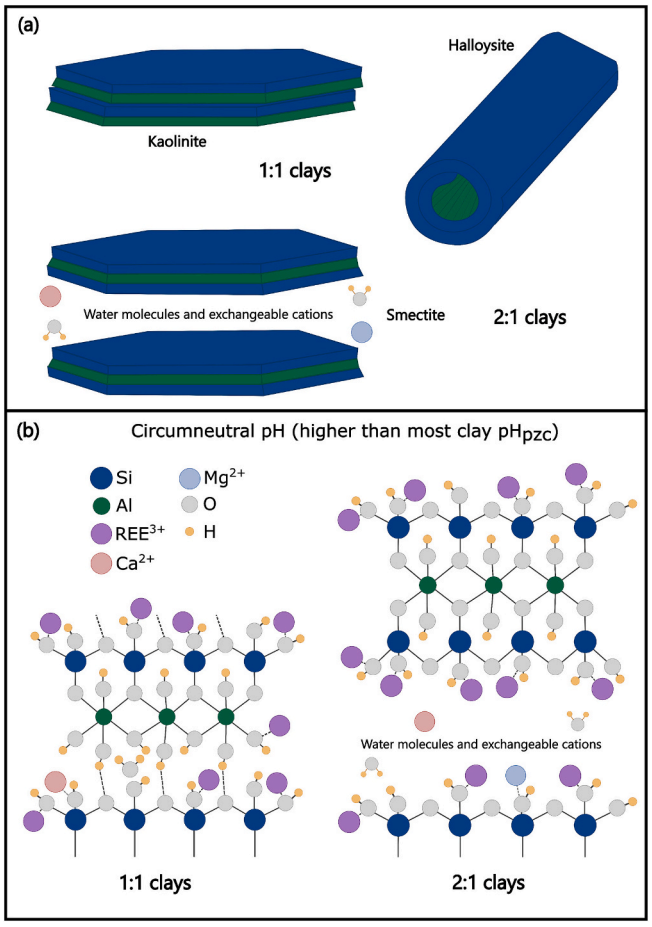

Fig. 7. Schematic diagram of the (a) structure and (b) REE adsorption onto 1:1 clays (i.e., kaolinite and halloysite) and 2:1 clays (e.g., smectite). Tetrahedral layers of 1:1 and 2:1 clays facilitate REE adsorption where the pH of the system exceeds the pH_{pzc} of the clay (refer to Table 5), resulting in hydroxyls that promote Van der Waal bonding. Rare earth elements may also adsorb to edge hydroxyl sites of the octahedral layer (green). 2:1 clays typically have larger basal spacing between tetrahedral layers that is typically filled with water molecules and exchangeable cations (e.g., Ca^{2+}). As a result of the larger basal spacing between layers, 2:1 clays tend to have higher surface charge sites, facilitating a higher adsorption capacity for REE. (For interpretation of the references to colour in this figure legend, the reader is referred to the web version of this article.)

adsorption onto kaolinite (and other clays) is further explained by the point of zero charge (pH_{pzc}), a unique pH value where a clay exerts a neutral charge at specific temperature, pressure, solution composition (and ionic strength), and particle shape (Chorover, 2023; Theng, 2012). The median pH_{pzc} for kaolinite is reported to be a pH of ~2–6.5 (Herrington et al., 1992; Kosmulski, 2018; Theng, 2012), therefore, under most natural systems kaolinite is negatively charged and facilitates REE (Ln^{3+}) adsorption.

Halloysite, unlike kaolinite, occurs as either a hydrated or dehydrated halloysite, causing large variability in the CEC (Table 7; Fig. 7). The main distinction between hydrated and dehydrated halloysite is the presence of a hydrated interlayer between TO layers, typically occupied by water molecules and/or cations (Skibińska, 2017; Yang et al., 2016). The hydrated interlayer in halloysite alters the charge of the mineral and increases the CEC, therefore increasing adsorption of REE. Similarly, halloysite is more susceptible to isomorphic substitution, typically substitution of Al for Mg, Fe or Ti in the octahedral layer, affecting the surface charge and thus CEC (Ouyang et al., 2018; Skibińska, 2017; Tarì et al., 1999; Theng, 2012). Nevertheless, similar to kaolinite, the CEC of halloysite is strongly controlled by pH and readily adsorbs REE, where some natural systems observe a pH_{pzc} as low as 2 (Kosmulski, 2018).

3.3.1.2. Clay minerals 2:1 (smectite, vermiculite and illite). Clays with a 2:1 structure (Fig. 7), such as smectite (montmorillonite), vermiculite, and illite, typically possess larger surface charges, increased CEC and REE adsorption, relative to 1:1 clays (Table 7; Bergaya et al., 2011; Brigatti et al., 2006; Kraepiel et al., 1999; Schoonheydt and Johnston, 2011; Wang et al., 2017). Higher adsorption capacities of 2:1 clays are the result of hydrated interlayers incorporated into the clay structure and isomorphic substitution within the hydrated interlayer and/or within the T and O sheets. Isomorphic substitution of 2:1 clays typically results in an overall negative charge that attracts cations, such as REE^{3+}, and results in pH-independent REE adsorption, particularly under low ionic strength conditions (Borisover and Davis, 2015; Coppin et al., 2002; Han et al., 2023; Ma and Eggleton, 1999; Theng, 2012; Yang et al., 2019). Experimental work by Coppin et al. (2002) reported pH-independent REE adsorption onto smectite at low ionic strength (experiments performed using 0.025M $NaNO_3$ at 25°C and pH values ranging from 3 to 9), whereas kaolinite under the same conditions exhibited pH-dependent REE adsorption. However, at high ionic strength conditions (0.5 M $NaNO_3$ at 25°C and pH values ranging from 3 to 9), both smectite and kaolinite demonstrated pH-dependent REE adsorption (Coppin et al., 2002). Differences in pH-independent and -dependent REE adsorption between 2:1 and 1:1 clay behaviour under low and high ionic strength conditions is attributed to the overall negative charge of 2:1 clay, as further explained by 'double layer theory'. The double layer theory considers two layers of ion adsorption onto clays minerals: (1) the stern layer, which refers to the inner layer where ions are directly adsorbed onto clay surfaces, and (2) the diffuse layer, which refers to the outer layer where ions are less strongly attracted to the clay surface (Jayadeva and Sridharan, 1982; Laird, 2006; Stern, 1924). Under low ionic strength conditions, reduced competition between ions for adsorption onto the clay surface results in a larger diffuse layer, reducing the sensitivity of surface changes to pH changes (and consequently H^+ competition; Callaghan and Ottewill, 1974; Çelik, 2004; Jayadeva and Sridharan, 1982; Sondi et al., 1996). Therefore,

Table 7
Common clay minerals in REE IACD and their physicochemical properties.

Layer Type	1:1		2:1		
Group	Kaolinites		Smectites	Micas	Vermiculites
Clay mineral	Kaolinite	Halloysite	Montmorillonite	Illite	Vermiculite
SSA (m^2/g)	10–20 [a]	50-60[h]	50–100 [a]	50–100 [a]	10–800 [a]
Basal spacing (Å)	7.2 [b]	7.2–10 [c]	9.8–20 [b]	10 [a]	10–25 [b]
CEC (meq/100 g)	3–15 [d]	5–50 [d]	70–100 [d]	10–40 [d]	100–150 [d]
pH_{pzc}	2–6.5 [e]	~2 [e]	2.50–5.50 [f]	2.2–4.30 [f]	
Layer charge	<0.01 [g]		0.5–1.2 [g]	1.4–2.0 [g]	1.2–1.8 [g]

Abbreviations: SSA = specific surface area; CEC = cation exchange capacity; pH_{pzc} = pH at point of zero charge.
References: (**a**) Belghazdis and Hachem (2022), (**b**) Kumari and Mohan (2021), (**c**) Al-Ani and Sarapää (2008), (**d**) (Carroll, 1959), (**e**) Kosmulski (2018), (**f**) Yu et al. (2021), (**i**) (Uddin, 2008), (h) (Joussein et al., 2005).

based on the low ionic strength nature of most surface waters and groundwaters, it is suggested that REE adsorption onto 2:1 clays is more likely controlled by layer charges (and isomorphic substitution) rather than pH. Additionally, although layer charges in 2:1 clays potentially facilitate greater REE adsorption (through increased CEC) relative to 1:1 clays, this may compromise ore processing (as further discussed in Section 4.2.4). Therefore, it is recommended to understand the clay mineralogy, and the intersection between physical and chemical controls on REE adsorption, unique to a deposit.

3.4. Preservation of REE IACD

Preservation of REE IACD is controlled by chemical (e.g., chemical leaching) and mechanical processes (e.g., erosion due to surface runoff, topographic gradients, subsidence, and tectonic activity), where both are addressed in this section with focus on climate, landscape evolution and sedimentary dynamics. Kaolinite is often the major clay mineral detected in REE IACD (Borst et al., 2020; He et al., 2023; Li and Zhou, 2023; Ram et al., 2019; Sanematsu and Watanabe, 2016; Wang et al., 2024; Yang et al., 2019), therefore the formation and dissolution of kaolinite significantly affects REE IACD development, controlling REE adsorption and ore body preservation. Elevated kaolinite proportions form in weathering profiles through intense chemical weathering, particularly by high rainfall. However, excessive rainfall also promotes kaolinite dissolution and saprolite collapse, causing significant implications for preserving weathering profiles and REE IACD. Early studies on Hawaiian soils demonstrated that excessive annual rainfall (64–89 cm) resulted in decreasing kaolinite contents through dissolution (Dean, 1947; Sherman, 1949; Tanada, 1942). Weathering profiles in Malawi (McFarlane, 1992) and Australia (Butt, 1985) show dissolution of kaolinite at pH < 5, which became more aggressive at pH < 4 (Butt, 1985; Garrels and Christ, 1965; Norton, 1973). As a result, dissolution of kaolinite in weathering profiles is more prevalent under excessive rainfall, where the initial pH of rainwater is generally 5.5–6.5 but can be as low as 3.5 in upper layers through interactions with organic acids and soil CO_2 (Norton, 1973). Dissolution of kaolinite in weathering profiles facilitates lateral movement through saprolite collapse and potentially results in lower grades of REE (Aleva, 1983; McFarlane, 1992; Verplanck, 2017; Wayland, 1934). The dissolution of kaolinite (and other clay minerals) in weathering profiles is also facilitated by internal drainage system changes. Impervious clay-rich zones throughout the weathering profile result in stagnation and oversaturation of surface waters, promoting the dissolution of clays and lateral movement (Mohr and Pendleton, 1944; Sherman, 1949). Consequently, climates with excessive rainfall (i.e., tropical humid climates) may not be ideal for REE IACD preservation.

Lateral movement in weathering profiles also occurs in drier climates where mechanical processes (e.g., direct surface runoff) are more influential in redistributing weathering products (Li et al., 2020; McFarlane, 1992). Li et al. (2020) stated that hillslope processes (including runoff erosion, creep, and landslides) mobilise and transport REE from ridgetops to footslopes, resulting in less mature profiles and inhibiting REE IACD preservation (Fig. 4). However, Braun et al. (2018) found that topographic effects generate insignificant REE loss in the saprolite of ridgetops, whereas pedogenic REE losses were more significant and potentially promote vertical mobilisation at the footslopes with longer residence times. Nevertheless, these processes facilitate REE fractionation where ridgetops are preferentially enriched in LREE and footslopes are preferentially enriched in HREE in subtropical areas (Li et al., 2020; Liu et al., 2022). This fractionation is suggested to be a function of the subsurface throughflow and/or groundwater chemistry, where ligands in fluids (e.g., carbonate ions) remobilise and retain HREE in solution as a result of higher affinities (Johannesson et al., 1999; Li et al., 2022; Millero, 1992; Su et al., 2017). Therefore, understanding landscape evolution (drainage dynamics through time), climatic conditions (intense weathering versus moderate weathering conditions), and sedimentary dynamics is fundamental in assessing prospectivity for REE IACD.

Mechanical surface processes that are responsible for preserving weathering profiles (and REE IACD) include glacial activity (ice movement), sea-level changes, and tectonic activity (Anand and De Broekert, 2005; Braun et al., 2016; Fairbridge and Finkl, 1980; González-Álvarez et al., 2016a; González-Álvarez et al., 2016b; Kleman et al., 2008; Marquette et al., 2004; Stroeven et al., 2002; Taylor and Howard, 1999). For example, in southern Western Australia, between the Yilgarn Craton plateau and the coastline, the preservation of weathering profiles are influenced by the downward tilting of the Australia Plate, and therefore sea level changes, from the Late Cretaceous to the Eocene (González-Álvarez et al., 2016a; González-Álvarez et al., 2016b). These sea level variations led to the erosion of previously weathered profiles and the development of newer weathering profles that are significantly younger than their more distal counterparts in the Yilgarn craton, and are not affected by tectonic induced erosional processes. This process also promoted landscape changes including topographic highs, uneven basement, and flat regions as a result of erosional and depositional effects. Tectonic activity, alongside sea-level changes, also controls topography and the depth of weathering through the disaggregation of bedrock (Arrowsmith et al., 1996; Maitra et al., 2020; St. Clair et al., 2015). Active tectonic landscapes promote erosion, which can disrupt the preservation and development of weathering profiles and REE IACD through the removal or alteration of REE-bearing clays by sedimentary processes (e.g., reactivation of fluvial and coastal systems). Additionally, tectonism can redirect groundwater flows and alter the chemical architecture of the landscape at depth (Braun et al., 2016; Butt et al., 2000; Pope, 2015). Glacial activity may also inhibit weathering profile and REE IACD preservation through ice-sheet erosion (as observed in Baffin Island, eastern Canadian Arctic; Refsnider and Miller, 2013).

4. Discussion

4.1. Considerations when undertaking aqueous speciation modelling

Aqueous speciation of REE in surface waters and groundwaters from China (Liu et al., 2023b), Uganda (Owor et al., 2021), Ethiopia (Ayenew, 2005), and Nigeria (Nganje et al., 2017) were modelled using PHREEQC (Fig. 5). These localities were selected based on their association with a confirmed REE IACD and/or potential occurrence, as well as their variability in pH and anion concentrations (more information is provided within the Appendix). The robustness of this modelling depends on the quality of the geochemical data and database variables used. Inconsistencies between databases is considered a limitation in PHREEQC modelling where data is taken from various literature sources without internal consistency and there is no systematic attempt to determine its suitability (Parkhurst and Appelo, 2013). Therefore, in this study internal inconsistencies were minimised by compiling and developing a database using stability and dissociation constants from Blanc et al. (2012), Tables 4 and 5 (referenced database with datasets and information on how to access the database are provided in the Appendix). For simplicity all geochemical data of surface water and groundwater used was modelled at $25^{\circ}C$, although this may not represent the true natural temperature of the waters. However, minor differences in ambient temperature in a low ionic strength systems are considered negligible in assessing REE mobility trends for REE IACD development, as demonstrated by the negligible differences in phosphate solubility at $23^{\circ}C$ ($\log K_{NdPO4} = -25.8$; Cetiner et al., 2005) and $25^{\circ}C$ ($\log K_{NdPO4} = -25.95$; Firsching and Brune, 1991).

A further complication was incomplete geochemical data for the relevant anions for some water samples used in the modelling (e.g. Cl^{-}, F^{-}, SO_4^{2-}, PO_4^{3-}, HCO_3^{-}/CO_3^{2-}, NO_3^{-}). For example, groundwaters from Uganda did not include NO_3^{-} or PO_4^{3-} concentrations (Owor et al., 2021). Where anion concentrations are missing from the datasets, these ligands

were not included in the modelling, therefore aqueous speciation in these media should be interpreted with caution. The aqueous speciation performed herein may also potentially overestimate the proportions of some complexes given other cations (i.e., Ca^{2+}, Mg^{2+}, Al^{3+} and Fe^{3+}) that compete with REE complexing (Gimeno Serrano et al., 2000; Johannesson et al., 1996; Tang and Johannesson, 2003) were omitted from modelling for simplicity. Additionally, because of the limited trace element geochemical data available for most water samples, global average REE concentrations in groundwater (Noack et al., 2014) were used rather than measured REE concentrations at each location. Nonetheless, the speciation modelling performed herein (Fig. 5) serves as a guide to better understand REE mobility in the context of REE IACD formation.

4.2. Understanding REE IACD in the natural systems

4.2.1. Implications of diverse REE sources

It is reported that granitic rocks are the most common source rocks for REE IACD (Chu et al., 2024; Huang et al., 1989; Li et al., 2019; Li et al., 2017; Sanematsu and Watanabe, 2016; Santana and Botelho, 2022; Santana et al., 2015). However, recent discoveries suggest the source of REE is diverse with examples of metamorphic (e.g., Mulanje deposit, Malawi and Ningdu deposit, China; Huang et al., 2021; Le Couteur, 2011; Orris et al., 2018; Sanematsu and Watanabe, 2016) and sedimentary rocks (e.g., Makuutu deposit, Uganda; Ionic Rare Earths LTD, 2022), as well as fluids (e.g., LREE enrichment in the Serra Dourada granite, and associated weathering profile, by hydrothermal fluid; Santana and Botelho, 2022; Santana et al., 2015) and sedimentary processes (e.g., Koppamurra and Deep Leads deposits, Australia; ABx Group, 2023a; ABx Group, 2023b; Australian Rare Earths, 2023; Löhr et al., 2024). Therefore, it is important to consider the implications of variable source rocks on REE IACD formation, particularly source rocks with high P content. Source rocks that are high in P, such as S-type granites, host most of their REE in weathering resistant phosphate minerals (e.g., monazite and xenotime) that inhibit the release (and therefore, adsorption) of REE during weathering (Bea et al., 1992; Chappell, 1974; Chappell and White, 2001; Oelkers and Poitrasson, 2002; Oelkers et al., 2008; Sanematsu et al., 2015). Although organic acids aid in the dissolution of these resistant minerals (Corbett et al., 2017; Goyne et al., 2010; Lazo et al., 2017), when dissolved these phases liberate both REE^{3+} and PO_4^{3-} into solution and promote the precipitation of REE-phosphates with both high stability and solubility (Figs. 5 and 6; Tables 4 and 6).

Phosphate-rich sources, and surrounding lithologies, influence the chemistry of weathering profiles and sub-surface waters, and control potential REE adsorption and enrichment onto clay minerals. Alternatively, Fu et al. (2019) suggests that P-rich S-type granites are actually prospective but only when apatite serves as the main REE source, a result of its weathering susceptibility relative to other phosphate minerals (e.g., monazite and xenotime). In addition to P-rich sources, F-rich sources (i.e., A-type granites) may also inhibit REE IACD formation, where liberated REE^{3+} and F^- during weathering can form stable and insoluble third order REE-fluoride complexes ($REEF_3$; Fig. 6; Tables 4 and 6). However, $REEF_3$ complexes are not significant in most surface waters and groundwaters (Fig. 5), indicating that F-rich lithologies are less problematic than P-rich lithologies in REE IACD development. Fluoride-rich lithologies may instead be more prospective in developing REE IACD, where the formation of HF accelerates the breakdown of weathering resistance minerals (da Silva Alves et al., 2018). Nevertheless, the potential sources for REE IACD are considered more diverse than traditionally thought.

4.2.2. pH controls on REE mobility in natural waters

Transport of REE in solution in surface water and groundwater are essential for REE IACD formation and is largely controlled by the availability, stability, and solubility of complexes (e.g., REE-sulfate, −fluoride, −phosphate, and -hydroxide complexes). The proportions of specific REE-complexes are largely controlled by pH (Fig. 5), where REE-sulfate and hydrated REE species are most prominent under acidic to circumneutral conditions with minor REE-fluoride complexes (Helgeson, 1969; Johannesson et al., 2004; Marshall and Jones, 1966; Petković, 1982; Tan et al., 2014; Tang and Johannesson, 2003). In contrast, under circumneutral to alkaline pH conditions, REE-fluoride, −hydroxide and -carbonate complexes are more dominant (Biddau et al., 2002; Johannesson and Lyons, 1994; Johannesson et al., 1995; Johannesson et al., 2000; Wood, 1990; Zwicker et al., 2022). Phosphate complexes, although present under most pH conditions, are most favourable under circumneutral to alkaline conditions (pH > 6.5; Byrne et al., 1991; Lee and Byrne, 1992). Phosphate complexes have a strong affinity for MREE and HREE (Table 4), potentially fractionating REE in solution where MREE- and HREE-phosphate complexes precipitate and LREE remain in solution until adsorbed onto clay surfaces (Fig. 5).

Rare earth element-fluoride, −hydroxide and -carbonate complexes also preferentially complex with M-HREE, though not as strongly as phosphate-complexes and are less likely to precipitate out of solution. Nevertheless, pH strongly controls the relative LREE- and HREE-enrichment of weathering profiles and REE IACD irrespective of inherited source rock variations (Fig. 8). For example, at acidic to circumneutral pH, REE in solution are unlikely to fractionate, therefore a LREE- or HREE-rich source rock will likely result in a LREE- or HREE-rich weathering profile at acidic conditions, respectively. In contrast, circumneutral to alkaline conditions can facilitate REE fractionation and result in LREE-enriched weathering profiles from LREE- and HREE-rich source rocks.

A study conducted on REE behaviour in springs and streams on the basaltic island of San Cristóbal, Ecuador, found that pH controlled REE adsorption and fractionation onto colloid metal species (e.g., Fe- and Mn-oxyhydroxides; Larsen et al., 2021). Low pH springs exhibited enrichment of HREE onto the colloids, reflecting preferential adsorption of HREE onto metal species and the prominence of non-fractionating complexes (e.g., REE-sulfate complexes). High pH springs demonstrated preferential adsorption of LREE onto colloids due to the higher stability of soluble HREE complexes (e.g., HREE-carbonate complexes). Additionally, groundwaters from the Carnmenellis area, southwest England, inherited LREE-enriched signatures from the source rocks (e.g., granite and metasediments) in the area (Smedley, 1991). Rare earth elements in the groundwater preferentially existed as free hydrated species or REE-sulfate or -carbonate complexes depending on the activities of the sulfate and carbonate ions. Rare earth element-chloride, −hydroxide, −nitrate, and -phosphate complexes were negligible, suggesting that LREE-enrichment in the groundwater was caused by the absence of strong complexing ligands that would have otherwise retained HREE in solution and preferentially adsorbed LREE onto clay (or other colloidal, such as Fe- and Mn-oxyhydroxide) surfaces (e.g., HREE-enrichment of seawater with a global pH average of 8.07; Byrne and Kim, 1990; Jiang et al., 2019; Smedley, 1991; Tang and Johannesson, 2010b). Therefore, applying this knowledge to REE enrichment onto clays in REE IACD suggests that HREE-enriched deposits require a HREE-rich source and REE mobilised under acidic to circumneutral conditions where concentrations of fractionating complexes (e.g., PO_4^{3-} and CO_3^{2-}) are insignificant.

Additionally, pH influences relative LREE- and HREE-enrichment throughout a weathering profile, where the acidic upper portions are typically LREE-enriched and the circumneutral to alkaline lower portions are more HREE-enriched (Wang et al., 2018; Wang et al., 2023; Yaraghi et al., 2020). During the development of a weathering profile (Fig. 9), weathering is facilitated by acidic rainwater that promotes an acidic environment with the influence of organic acids. However, during periods of elevated precipitation, the relatively more alkaline groundwater table rises and promotes REE fractionation, with HREE preferentially complexed with fluoride, hydroxide, carbonate, and phosphate ligands. Once precipitation ceases and the groundwater table

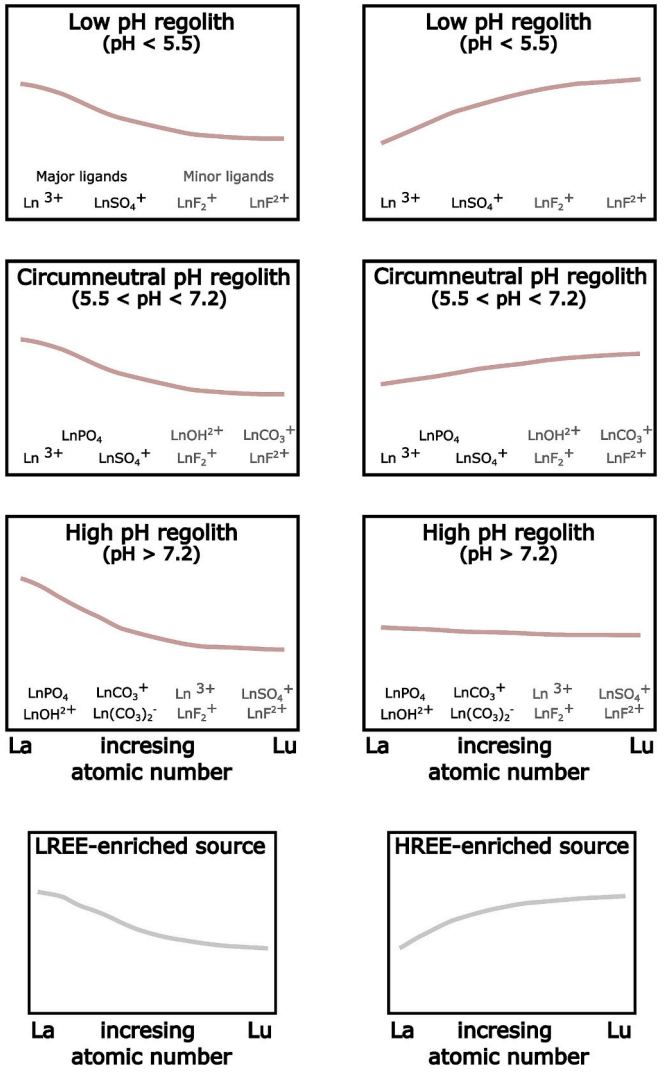

Fig. 8. Stylised REE patterns, excluding Ce and Eu anomalies, of LREE- and HREE-enriched source rocks and their associated regolith profiles under low, circumneutral and high pH conditions. An acidic regime will produce a LREE- and HREE-enriched regolith from a LREE- and HREE-rich source, respectively, as a result of non-fractionating REE complexation. Minor ligands (~1–5 % of total complexation; written in gray) at acidic conditions include first (LnF^{2+}) and second order fluoride complexes (LnF_2^+). Major ligands (≥ 5 % of total complexation; written in black) at acidic conditions include hydrated REE species (Ln^{3+}) and sulfate complexes ($LnSO_4^+$). Circumneutral regimes will produce similar REE patterns to acidic regimes, however fractionating complexes (such as, fluoride, carbonate, phosphate, and hydroxide complexes) become more significant (≥ 1–5 % of total complexation). Alkaline regimes will produce LREE-enriched regolith from LREE- and HREE-rich sources as the presence of fractionating complexes become more dominant (≥ 5 % of total complexation). These fractionating complexes retain soluble HREE in the surface waters and groundwaters, resulting in preferential adsorption of LREE onto clay mineral surfaces. The influence of minor and major ligands under different pH conditions in these stylised REE patterns is based on the PHREEQC modelling undertaken in Fig. 5.

subsequently retreats (along with the preferentially complexed HREE), LREE remain preferentially enriched in the more acidic upper layers of the soil profile and can eventually be adsorbed onto clay minerals (Fig. 9). Heavy REE may also favour in-solution complexation (such as REE-carbonate complexation) with high affinities (Johannesson et al., 1999; Johannesson et al., 2000; Li et al., 2022; Munemoto et al., 2015; Tang and Johannesson, 2010b), therefore resulting in slightly HREE-enriched lower layers when LREE are exhausted. Ultimately, the interplay of precipitation dynamics and regolith development will have a strong influence on the relative LREE or HREE enrichment of a REE IACD.

4.2.3. Adsorption of REE onto clays in natural systems

Clays are rarely pure end-member specimens. The selectivity (and CEC) of natural clays is strongly influenced by clay purity. For example, halloysite-rich soils from northern California exhibited higher than expected CEC for pure kaolin minerals (i.e., kaolinite and halloysite), which is attributed to the minor proportions of 2:1 clays (e.g., smectite; Takahashi et al., 2001). Variability of clay minerals and properties throughout the weathering profile also influences adsorption, as demonstrated at the Zudong deposit, China. The upper horizons of the weathering profile at Zudong reflect a reduced adsorption capacity relative to lower portions as a result of changes in the porosity, SSA, and CEC (and pH_{pzc}) of the clays (Li and Zhou, 2020). Additionally, pH disparities between the upper (acidic) and lower (circumneutral to alkaline) horizons control the adsorption of REE, where a pH range between ~5.5.-6.5 is considered ideal to minimise competition between H^+ and REE^{3+} for adsorption sites and hydrolysis (Huang et al., 2021; Li et al., 2017; Nesbitt, 1979; Sanematsu et al., 2013; Wang et al., 2023; Yang et al., 2019). Nevertheless, the influence of parameters, such as SSA, CEC, pH, clay purity and weathering progression on REE clay adsorption in the REE IACD context remains poorly understood and understudied.

4.2.4. Implications of different clays for REE IACD ore processing

Clay mineral properties, such as SSA and CEC, control the adsorption of REE onto clays, with higher SSA and CEC resulting in higher adsorption. However, these parameters also significantly impact the mining and production of REE concentrates from REE IACD. Alshameri et al. (2019) assessed the adsorption and desorption efficiencies of clay minerals using La^{3+} and Yb^{3+} and demonstrated that adsorption efficiencies followed the order montmorillonite > muscovite > illite > kaolinite, with order attributed to higher clay mineral charges and 2:1 clay impurities (Alshameri et al., 2019; Alshameri et al., 2018; Bergaya et al., 2011; Bhattacharyya and Gupta, 2008; Brigatti et al., 2006; Schoonheydt et al., 2018; Theng, 2012). The highest REE extraction efficiencies from clays showed the inverse relationship (i.e., kaolinite > illite > muscovite > montmorillonite; Alshameri et al., 2019). The observed trend for extraction efficiencies may be the result of pH changes across desorption experiments and hydrolysis of available REE (i.e., pH increased from 4.5 to 5.7 for montmorillonite and muscovite), as well as stronger affinities of REE to higher charge clays (Alshameri et al., 2019; Moldoveanu and Papangelakis, 2013). Consequently, a thorough understanding of the clay mineralogy of any prospective REE IACD is crucial for understanding the leaching protocol required to create REE concentrates.

4.3. Conceptual exploration model for REE IACD

Previous conceptual models developed for REE IACD have focused on regions where there has been extensive REE IACD development (i.e., REE IACD formed from granitic rocks in China; Chu et al., 2024; Li et al., 2017; Sanematsu and Watanabe, 2016) or have been deposit dependent, highlighting characteristics unique to that deposit (e.g., Koppamurra deposit, Australia; Löhr et al., 2024). The conceptual model presented here integrates the above information, while focusing on features from confirmed REE IACD that ubiquitously contribute to REE IACD formation (Fig. 10). The conceptual model is broken up into four separate parts, synthesised below based on the extensive literature review presented in Section 3:

(1) Source of REE: The source rocks that provide the REE required for the formation of REE IACD can originate from either weathered igneous, metamorphic, or sedimentary basement terranes.

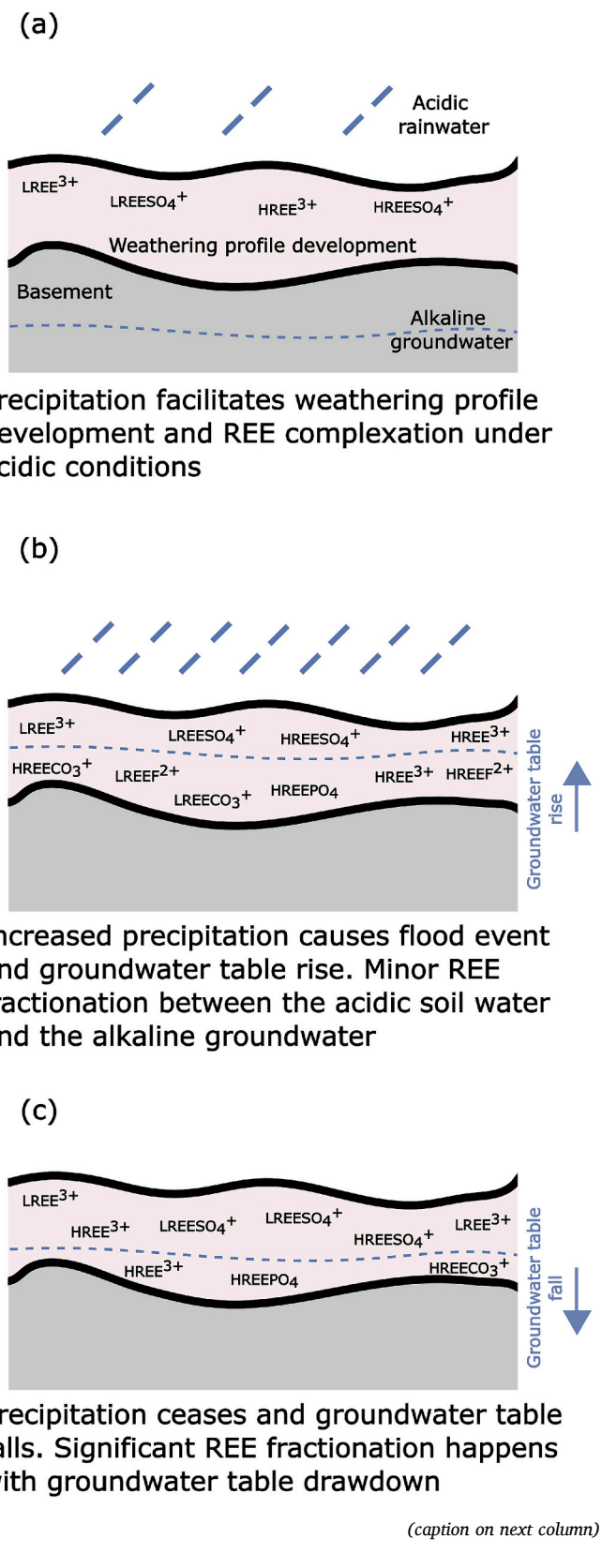

(caption on next column)

Fig. 9. Schematic diagram demonstrating how climatic events (e.g., flooding) influence the groundwater table and facilitate REE fractionation within the weathering profile. (a) Precipitation facilitates weathering (and erosion), resulting in the development of a weathering profile. The acidic nature of the rainwater, alongside organic acids, results in acidic soil water in the upper part of the profile and the predominance of hydrated REE species and REE-sulfate solution complexes. (b) As precipitation increases, the alkaline groundwater table rises and increases the pH of the soil water and promotes complexing with phosphate, fluoride, carbonate, and hydroxyl ions. These ions facilitate minor REE fractionation, where HREE are preferentially retained in alkaline solutions. (c) Precipitation ceases and results in drawdown of the alkaline groundwater table. The higher affinity of HREE with fractionating complexes in alkaline solution results in more extensive REE fractionation, with HREE preferentially drawdown with the groundwater table until eventually adsorbed onto clays in lower horizons of the weathering profile. Therefore, resulting in LREE-enriched upper horizons and HREE-enriched lower horizons typically exhibited within a weathering profile.

Igneous rocks, particularly granites, are the most common sources for REE IACD as evidenced by the multitude of deposits across China (Chu et al., 2024; Huang et al., 1989; Li et al., 2019; Li et al., 2017; Sanematsu and Watanabe, 2016) and Brazil (Aclara, 2023; Santana and Botelho, 2022). However, metamorphic (as exhibited in Ningdu deposit, China and Mulanje deposit, Malawi; Huang et al., 2021; Orris et al., 2018) and sedimentary rocks (Makuutu deposit, Uganda; Ionic Rare Earths LTD, 2022) can also supply REE. In addition to weathered basement, external sources may also contribute to the REE budget, such as hydrothermal fluids (as speculated for the weathering profile associated with the Emeishan basalt, China; Zhao et al., 2017) and fluvial processes (Koppamurra deposit, Australia; Löhr et al., 2024). These external sources can also supply the clay minerals required for REE adsorption.

(2) Mobilisation of REE: Once liberated, REE are mobilised and transported in solution to or within a weathering profile as either complexes with ligands or as hydrated species (Li et al., 2022; Wood, 1990). At acidic to circumneutral pH conditions, hydrated species and REE-sulfate complexes are the most dominant, whereas REE-fluoride and -phosphate complexes are minor. Under circumneutral to alkaline conditions, REE-phosphate, −carbonate, −fluoride, and -hydroxide species become more prominent. These complexes under circumneutral to alkaline conditions may also facilitate REE fractionation, where HREE are preferentially retained in solution and LREE are preferentially adsorbed onto clay surfaces. Therefore, pH strongly controls REE mobility and fractionation, meaning that acidic and circumneutral conditions are ideal for inhibiting preferential HREE soluble complexes.

(3) Adsorption of REE: Following mobilisation, REE are adsorbed onto clay minerals. 1:1 clay minerals (e.g., kaolinite and halloysite) are most commonly observed within these deposit types, however, adsorption is also facilitated by 2:1 clays (e.g., smectite; Borst et al., 2020; Wang et al., 2024; Yang et al., 2019). 2:1 clay minerals typically have higher adsorption capacities than 1:1 clays, however, this is potentially problematic when desorbing REE during mining and processing of REE IACD. Adsorption of REE is strongly controlled by pH, where at acidic conditions adsorption sites are occupied by available H^+ and at alkaline conditions hydrolysis inhibits REE adsorption. Therefore, a slightly acidic to circumneutral pH range (e.g., ~5.5–6.5; Huang et al., 2021) is ideal for REE adsorption and ensures the influence of fractionating ligands (e.g., carbonate and phosphate ions) is minimal.

(4) Preservation of a deposit: To preserve an ore body, a low erosional setting is ideal, therefore tropical climates are not necessarily ideal for long-term REE IACD preservation. Similarly,

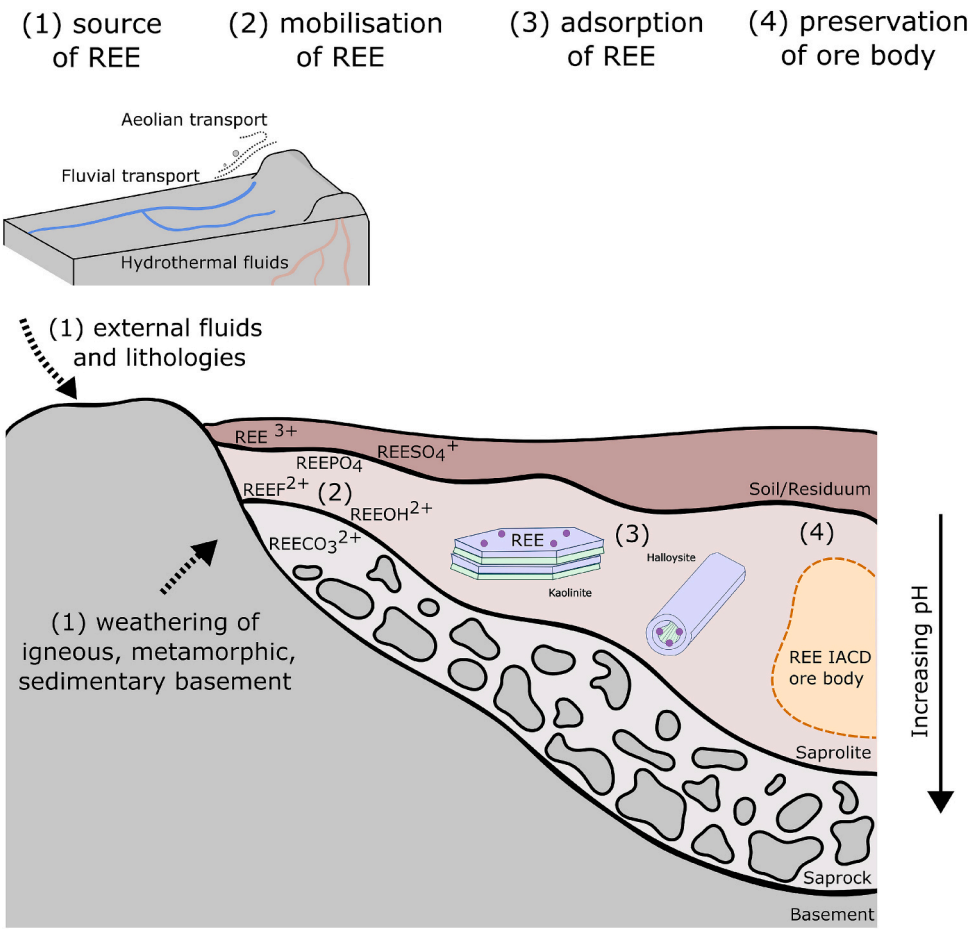

Fig. 10. Stylised mineral system framework for development of a REE IACD. (1) REE source from weathering of basement and/or external fluids or lithologies; (2) mobilisation of REE through complexation with ligands or free hydrated species; (3) adsorption of REE onto clay minerals, such as kaolinite and halloysite; (4) preservation of the ore body under low erosional settings with minimal lateral transport.

mechanical, and chemical processes, such as excessive precipitation, can facilitate saprolite collapse and clay dissolution, resulting in lateral transport. Locations where lateral transport of REE is predicted to be minimal will ensure higher grades of REE in the ore body. Topographic 'highs' and 'lows' (or ridgetops and footslopes, respectively) also have implications given ridgetops represent high erosion settings with large lateral fluxes and footslopes represent low erosion areas with a less prominent lateral flux. Therefore, footslopes are considered more favourable in forming economic REE IACD, particularly HREE-enriched REE IACD (as suggested by the Bankeng deposit, China; Li et al., 2020).

This conceptual model is considered a framework to build upon over the coming years. As the unknowns highlighted in this review become better understood our knowledge can only be improved, aiding in future REE IACD exploration efforts.

4.4. Implications for mineral exploration of REE IACD

Understanding and comparing the genesis, mineralogy, and physicochemical properties of REE IACD across the globe (e.g., Borst et al., 2020; Chu et al., 2024; Huang et al., 1989; Li et al., 2019; Li et al., 2017; Liu et al., 2023a; Löhr et al., 2024; Ram et al., 2019; Sanematsu and Watanabe, 2016) provides insight into different depositional environments and processes that result in REE IACD formation and preservation. Based on the extensive review provided above, the following exploration proxies can be extracted for targeting REE IACD:

(1) Despite warm temperate climates being considered favourable for REE IACD, increased (and improved) global exploration has resulted in confirmed deposits in equatorial and arid climates (e.g., Ampasindava, Mulanje, Makuutu, Carina and Serra Verde deposits; Table 1; Aclara, 2023; Borst et al., 2020; Ionic Rare Earths LTD, 2022; Liu et al., 2023a; Orris et al., 2018; Ram et al., 2019; Sanematsu and Watanabe, 2016; Serra Verde Group, 2024). Additionally, cold climates may also be prospective for REE IACD with anomalous concentrations of adsorbed REE in weathering profiles in Finland reported (Al-Ani and Sarapää, 2009; Al-Ani et al., 2009; Sarapää and Sarala, 2013). As a result, understanding climatic conditions, alongside landscape evolution and drainage dynamics, is fundamental for assessing REE IACD prospectivity.

(2) Topographic 'highs' (or ridgetops) are high erosion settings that facilitate lateral transport, therefore inhibiting REE IACD formation. Topographic 'lows' (or footslopes), on the other hand, may be more prospective for REE IACD with low erosion and relatively minimal lateral transport. These topographic 'highs' and 'lows' may also result in preferentially LREE-enriched ridgetops and HREE-enriched footslopes.

(3) Granitic rocks are the prominent source (particularly A- and I-type granites) for REE IACD because of their high content of feldspar and mica minerals, which are the precursors of clay minerals, and REE-rich accessory phases, which release REE into the profile upon weathering. Metamorphic rocks are also prospective source rocks as a result of the redistribution of REE between minerals, particularly from sedimentary protoliths.

Basaltic rocks, although less common, demonstrate potential as source rocks.

(4) Sedimentary processes driven by the lateral flow of meteoric water can transport REE (and other weathering constituents, such as clay minerals) from their original source location and accumulate them. Additional fluid and wind transport mechanisms can enhance REE mobilisation and deposition (e.g., hydrothermal and basinal brines, and aeolian transport).

(5) Under acidic conditions (pH < 5.5), REE occur predominantly as simple hydrated cations, REE-sulfate and/or -fluoride complexes. Under circumneutral to alkaline conditions (pH 5.5–7.2 and pH > 7.2, respectively), REE-carbonate, −phosphate, and -hydroxide species become more significant. Ligands under circumneutral to alkaline conditions tend to fractionate REE as a result of higher in-solution complex stability amongst HREE, preferentially adsorbing LREE onto clay mineral surfaces. Therefore, circumneutral to alkaline conditions may inhibit the formation of HREE-rich REE IACD from HREE-rich source material.

(6) Kaolinite and halloysite are common clay minerals that host REE adsorption in REE IACD, although smectite, vermiculite, and illite may also be present. It is important to understand the clay mineralogy of a profile, particularly for mining and processing. Although 2:1 clays (e.g., smectite, vermiculite, and illite) adsorb higher proportions of REE relative to 1:1 clays (e.g., kaolinite and halloysite), 2:1 clays have lower desorption efficiencies stifling REE recovery.

By utilising these proxies, explorers can better target areas with high potential for REE IACD, enhancing the efficiency and effectiveness of exploration efforts.

5. Conclusions

Through compiling a comprehensive review and applying the mineral system framework, the following has been proposed:

(1) Granitic rocks are the most common source rock for REE IACD, as exhibited by extensive exploration in China and Brazil. However, mafic to intermediate igneous rocks, as well as metamorphic and sedimentary rocks and external processes are proven sources for deposits across the globe (e.g. China, Brazil, Chile, Malawi, Madagascar, Malawi, Uganda, and Australia). This suggests that the REE (and clay) source materials for REE IACD are more diverse that originally thought. In fact, granitic rocks, particularly those high in phosphate, may inhibit REE IACD formation through low weathering susceptibility of REE phosphate mineral phases (e.g., monazite and xenotime) and the insoluble tendency of REE-phosphate complexes when liberated into surface waters and groundwaters.

(2) Aqueous speciation modelling suggests that pH controls the fractionation of REE and the formation of LREE- and HREE-enriched REE IACD. Under acidic to circumentrual conditions, dominant species such as hydrated REE species and REE-sulfate complexes are unlikely to facilitate REE fractionation. Therefore, weathering of a LREE- and HREE-rich source under acidic to circumentrual conditions will preferentially result in a LREE- and HREE-rich regolith, respectively. However, under circumneutral to alkaline conditions, the presence of fractionating complexes (e.g., REE-carbonate and -phosphate complexes) facilitates REE fractionation and results in a LREE-rich regolith from a LREE- and HREE-rich source rock.

(3) Adsorption of REE is complicated in natural samples, where 2:1 clays (e.g., smectite, vermiculite and illite) can be present in horizons rich with 1:1 clays (e.g., kaolinite and halloysite). This natural contamination of samples can complicate the mining and processing of REE IACD, where REE remain more strongly adsorbed to 2:1 clays than 1:1 clays. Therefore, understanding deposit mineralogy is crucial. Adsorption of REE onto clay is also strongly controlled by pH, where a slightly acidic to circumneutral pH is considered ideal for minimising competition of REE with H^+ at acidic pH and hydrolysis of clays at alkaline pH. A slightly acidic to circumneutral pH also ensures that the influence of fractionating ligands in solution (e.g., REE-carbonate and -phosphate complexes) is minimal helping to facilitate the enrichment of the more critical HREE.

Collectively understanding the REE source, mobility, adsorption and ore body preservation in REE IACD adds to both scientific knowledge and global exploration efforts.

Supplementary data to this article can be found online at https://doi.org/10.1016/j.gexplo.2025.107845.

CRediT authorship contribution statement

Samantha C. Russo: Writing – original draft, Visualization, Validation, Investigation. **Ignacio González-Álvarez:** Writing – original draft, Visualization, Validation, Supervision, Conceptualization. **Helen A. Cocker:** Writing – review & editing, Visualization, Validation, Supervision, Conceptualization. **Alex J. McCoy-West:** Writing – original draft, Visualization, Validation, Supervision, Funding acquisition, Conceptualization.

Declaration of competing interest

The authors declare that they have no known conflict of interest that could have appeared to influence the work reported in this paper.

Acknowledgements

We acknowledge the traditional owners of the land of which this research has been conducted, and we pay our respects to the past, present, and future elders. SCR acknowledges receipt of an Australian Postgraduate PhD Scholarship to complete this work. AMW acknowledges ARC grant DE210101395. Mark Nestmeyer and Anne Kaufmann are thanked for discussions at JCU. This research project was conceived from a CSIRO DISIPA Student Internship undertaken by SCR in 2022. The reviewers and editors are thanked for their insight and comments.

Data availability

No data was used for the research described in the article.

References

Abraham, D.S., 2015. The Elements of Power: Gadgets, Guns, and the Struggle for a Sustainable Future in the Rare Metal Age. Yale University Press.
ABx Group, 2023a. ABx Rare Earth Resources Exceed 50 Million Tonnes.
ABx Group, 2023b. Ree resource triples at Deep Leads, Tasmania, ASX Announcement.
Aclara, 2022. Aclara Provides an Update on the Mineral Resource Estimate at the Penco Module Project.
Aclara, 2023. Aclara announces discovery of 168 Mt ionic clay mineral resources at its Carina module in Goias, Brazil.
Al-Ani, T., Sarapää, O., 2008. Clay and clay mineralogy. In: Physical-Chemical Properties and Industrial Uses, pp. 11–65.
Al-Ani, T., Sarapää, O., 2009. Geochemistry and mineralogy of REE in Virtasalmi kaolin deposits, SE Finland, Geological Survey of Finland, report M19/3231/2009/33.
Al-Ani, T., Sarapää, O., Juhanson, B., 2009. Concentration and residence of rare earth elements (REE) in Kaolin and Weathered Rock of Virtasalmi, Taivalkoski and Puolanka deposits. Eastern Finland. GTK Internal Report. Helsinki, Finland. Geol. Surv. Finl.
Aleva, G., 1983. On weathering and denudation of humid tropical interfluves and their triple planation surfaces. Geol. Mijnb. 62 (3), 383–388.
Alshameri, A., He, H., Zhu, J., Xi, Y., Zhu, R., Ma, L., Tao, Q., 2018. Adsorption of ammonium by different natural clay minerals: Characterization, kinetics and adsorption isotherms. Appl. Clay Sci. 159, 83–93.
Alshameri, A., He, H., Xin, C., Zhu, J., Xinghu, W., Zhu, R., Wang, H., 2019. Understanding the role of natural clay minerals as effective adsorbents and

alternative source of rare earth elements: Adsorption operative parameters. Hydrometallurgy 185, 149–161.
Anand, R., De Broekert, P., 2005. Weathering history, landscape evolution and implications for exploration. In: Anand, R.R., de Broekert, P. (Eds.), Regolith Landscape Evolution Across Australia: A Compilation of Regolith Landscape Case Studies With Regolith Landscape Evolution Models, pp. 2–40.
Anand, R.R., 1998. Regolith-landform Evolution and Geochemical Dispersion From the Boddington Gold Deposit. Cooperative Research Centre for Landscape Evolution & Mineral Exploration, Western Australia.
Anand, R.R., Paine, M., 2002. Regolith geology of the Yilgarn Craton, Western Australia: implications for exploration. Aust. J. Earth Sci. 49 (1), 3–162.
Aranha, M., Porwal, A., González-Álvarez, I., 2022a. Targeting REE deposits associated with carbonatite and alkaline complexes in northeast India. Ore Geol. Rev. 148, 105026.
Aranha, M., Porwal, A., Sundaralingam, M., González-Álvarez, I., Markan, A., Rao, K., 2022b. Rare earth elements associated with carbonatite–alkaline complexes in western Rajasthan, India: exploration targeting at regional scale. Solid Earth 13 (3), 497–518.
Arrowsmith, J.R., Pollard, D.D., Rhodes, D.D., 1996. Hillslope development in areas of active tectonics. J. Geophys. Res. Solid Earth 101 (B3), 6255–6275.
Australian Government, 2023. Critical Minerals Strategy 2023–2030.
Australian Rare Earths, 2023. 2023 Annual & Sustainability Report.
Avena, M.J., Mariscal, M.M., De Pauli, C.P., 2003. Proton binding at clay surfaces in water. Appl. Clay Sci. 24 (1–2), 3–9.
Ayenew, T., 2005. Major ions composition of the groundwater and surface water systems and their geological and geochemical controls in the Ethiopian volcanic terrain. SINET Ethiop. J. Sci. 28 (2), 171–188.
Babechuk, M.G., Widdowson, M., Murphy, M., Kamber, B.S., 2015. A combined Y/Ho, high field strength element (HFSE) and Nd isotope perspective on basalt weathering, Deccan Traps, India. Chem. Geol. 396, 25–41.
Bailey, D., Hampton, C., 1990. Volatiles in alkaline magmatism. Lithos 26 (1–2), 157–165.
Balaram, V., 2019. Rare earth elements: a review of applications, occurrence, exploration, analysis, recycling, and environmental impact. Geosci. Front. 10 (4), 1285–1303.
Banfield, J.F., Eggleton, R.A., 1989. Apatite replacement and rare earth mobilization, fractionation, and fixation during weathering. Clay Clay Miner. 37 (2), 113–127.
Barakos, G., Dyer, L., Hitch, M., 2022. The long uphill journey of Australia's rare earth element industry: challenges and opportunities. Int. J. Min. Reclam. Environ. 36 (9), 651–670.
Bea, F., 1996. Residence of REE, Y, Th and U in granites and crustal protoliths; implications for the chemistry of crustal melts. J. Petrol. 37 (3), 521–552.
Bea, F., Montero, P., 1999. Behavior of accessory phases and redistribution of Zr, REE, Y, Th, and U during metamorphism and partial melting of metapelites in the lower crust; an example from the Kinzigite Formation of Ivrea-Verbano, NW Italy. Geochim. Cosmochim. Acta 63 (7–8), 1133–1153.
Bea, F., Fershtater, G., Corretgé, L.G., 1992. The geochemistry of phosphorus in granite rocks and the effect of aluminium. Lithos 29 (1), 43–56.
Bea, F., Pereira, M., Corretgé, L., Fershtater, G., 1994. Differentiation of strongly peraluminous, perphosphorus granites: the Pedrobernardo pluton, central Spain. Geochim. Cosmochim. Acta 58 (12), 2609–2627.
Belghazdis, M., Hachem, E.-K., 2022. Clay and clay minerals: a detailed review. International Journal of Recent Technology and Applied Science 4 (2), 54–75.
Bergaya, F., Theng, B.K.G., Lagaly, G., Theng, B.K.G., 2006. Handbook of clay science. In: Developments in Clay Science, vol. 1. Elsevier Science & Technology, Amsterdam.
Bergaya, F., Jaber, M., Lambert, J.F., 2011. Clays and clay minerals. In: Rubber-Clay Nanocomposites: Science, Technology, and Applications, pp. 1–44.
Bern, C.R., Yesavage, T., Foley, N.K., 2017. Ion-adsorption REEs in regolith of the Liberty Hill pluton, South Carolina, USA: an effect of hydrothermal alteration. J. Geochem. Explor. 172, 29–40.
Bhattacharyya, K.G., Gupta, S.S., 2008. Adsorption of a few heavy metals on natural and modified kaolinite and montmorillonite: a review. Adv. Colloid Interf. Sci. 140 (2), 114–131.
Biddau, R., Cidu, R., Frau, F., 2002. Rare earth elements in waters from the albitite-bearing granodiorites of Central Sardinia, Italy. Chem. Geol. 182 (1), 1–14.
Bindeman, I.N., Davis, A.M., 2000. Trace element partitioning between plagioclase and melt: investigation of dopant influence on partition behavior. Geochim. Cosmochim. Acta 64 (16), 2863–2878.
Bingen, B., Demaiffe, D., Hertogen, J., 1996. Redistribution of rare earth elements, thorium, and uranium over accessory minerals in the course of amphibolite to granulite facies metamorphism: the role of apatite and monazite in orthogneisses from southwestern Norway. Geochim. Cosmochim. Acta 60 (8), 1341–1354.
Bird, M.I., Chivas, A.R., 1988. Stable-isotope evidence for low-temperature kaolinitic weathering and post-formational hydrogen-isotope exchange in permian kaolinites. Chemical Geology: Isotope Geoscience section 72 (3), 249–265.
Blanc, P., Lassin, A., Piantone, P., Azaroual, M., Jacquemet, N., Fabbri, A., Gaucher, E.C., 2012. Thermoddem: a geochemical database focused on low temperature water/rock interactions and waste materials. Appl. Geochem. 27 (10), 2107–2116.
Bleam, W.F., 1990. The Nature of Cation-Substitution Sites in Phyllosilicates. Clay Clay Miner. 38 (5), 527–536.
Borisover, M., Davis, J.A., 2015. Adsorption of inorganic and organic solutes by clay minerals. In: Developments in Clay Science. Elsevier, pp. 33–70.
Borst, A.M., Smith, M.P., Finch, A.A., Estrade, G., Villanova-de-Benavent, C., Nason, P., Marquis, E., Horsburgh, N.J., Goodenough, K.M., Xu, C., 2020. Adsorption of rare earth elements in regolith-hosted clay deposits. Nat. Commun. 11 (1), 1–15.
Botelho, N.F., Moura, M.A., 1998. Granite-ore deposit relationships in Central Brazil. J. S. Am. Earth Sci. 11 (5), 427–438.
Bourman, R.P., 1993. Perennial problems in the study of laterite: a review. Aust. J. Earth Sci. 40 (4), 387–401.
Bowler, J., KoTSONIS, A., Lawrence, C.R., 2006. Environmental evolution of the Mallee region, western Murray Basin. Proc. R. Soc. Victoria 118 (2), 161–210.
Braun, J., Pagel, M., Muller, J., Bilong, P., Michard, A., Guillet, B., 1990. Cerium anomalies in lateritic profiles. Geochem. Cosmochim. Acta 54, 781–795.
Braun, J., Mercier, J., Guillocheau, F., Robin, C., 2016. A simple model for regolith formation by chemical weathering. J. Geophys. Res. Earth 121 (11), 2140–2171.
Braun, J.J., Riotte, J., Battacharya, S., Violette, A., Oliva, P., Prunier, J., Maréchal, J.C., Ruiz, L., Audry, S., Subramanian, S., 2018. REY-Th-U dynamics in the critical zone: combined influence of reactive bedrock accessory minerals, authigenic phases, and hydrological sorting (Mule Hole Watershed, South India). Geochem. Geophys. Geosyst. 19 (5), 1611–1635.
Brigatti, M.F., Galan, E., Theng, B., 2006. Structures and mineralogy of clay minerals. Developments in Clay Science 1, 19–86.
Brimhall, G.H., Lewis, C.J., Ague, J.J., Dietrich, W.E., Hampel, J., Teague, T., Rix, P., 1988. Metal enrichment in bauxites by deposition of chemically mature aeolian dust. Nature 333 (6176), 819–824.
Broska, I., Petrík, I., 2008. Genesis and stability of accessory phosphates in silicic magmatic rocks: a Western Carpathian case study. Mineralogia 39 (1–2), 53–66.
Broska, I., Williams, C.T., Uher, P., Konečný, P., Leichmann, J.r., 2004. The geochemistry of phosphorus in different granite suites of the Western Carpathians, Slovakia: the role of apatite and P-bearing feldspar. Chem. Geol. 205 (1), 1–15.
Butt, C., 1985. Granite weathering and silcrete formation on the Yilgarn Block, Western Australia. Aust. J. Earth Sci. 32 (4), 415–432.
Butt, C.R.M., Zeegers, H., 1992. Regolith Exploration Geochemistry in Tropical and Subtropical Terrains. In: Handbook of Exploration Geochemistry, v. 4. Elsevier, Amserdam.
Butt, C.R.M., Lintern, M.J., Anand, R.R., 2000. Evolution of regoliths and landscapes in deeply weathered terrain — implications for geochemical exploration. Ore Geol. Rev. 16 (3), 167–183.
Byrne, R.H., Kim, K.-H., 1990. Rare earth element scavenging in seawater. Geochim. Cosmochim. Acta 54 (10), 2645–2656.
Byrne, R.H., Lee, J.H., Bingler, L.S., 1991. Rare earth element complexation by PO43− ions in aqueous solution. Geochim. Cosmochim. Acta 55 (10), 2729–2735.
Callaghan, I., Ottewill, R., 1974. Interparticle forces in montmorillonite gels. Faraday Discuss. Chem. Soc. 57, 110–118.
Carrillo-González, R., Šimůnek, J., Sauvé, S., Adriano, D., 2006. Mechanisms and pathways of trace element mobility in soils. In: Advances in Agronomy. Academic Press, pp. 111–178.
Carroll, D., 1953. Weatherability of zircon. J. Sediment. Res. 23 (2), 106–116.
Carroll, D., 1959. Ion exchange in clays and other minerals. Geol. Soc. Am. Bull. 70 (6), 749–779.
Castor, S.B., 2008a. The Mountain Pass rare-earth carbonatite and associated ultrapotassic rocks, California. Can. Mineral. 46 (4), 779–806.
Castor, S.B., 2008b. Rare Earth Deposits of North America. Resour. Geol. 58 (4), 337–347.
Castor, S.B., Hedrick, J.B., 2006. Rare earth elements. Industrial Minerals and Rocks 7, 769–792.
Çelik, M.S., 2004. Electrokinetic behavior of clay surfaces. In: Interface Science and Technology. Elsevier, pp. 57–89.
Cetiner, Z.S., Wood, S.A., Gammons, C.H., 2005. The aqueous geochemistry of the rare earth elements. Part XIV. The solubility of rare earth element phosphates from 23 to 150 °C. Chem. Geol. 217 (1), 147–169.
Chappell, B.W., 1974. Two contrasting granite types. Pac. Geol. 8, 173–174.
Chappell, B.W., White, A.J., 2001. Two contrasting granite types: 25 years later. Aust. J. Earth Sci. 48 (4), 489–499.
Cherepovitsyn, A., Solovyova, V., 2022. Prospects for the development of the Russian rare-earth metal industry in view of the global energy transition—a review. Energies 15 (1), 387.
Chorover, J., 2023. Surface charge and zero-charge points. In: Goss, M.J., Oliver, M. (Eds.), Encyclopedia of soils in the environment (Second Edition). Academic Press, Oxford, pp. 368–375.
Chu, G., Chen, H., Feng, Y., Wu, C., Li, S., Zhang, Y., Lai, C.-K., 2024. Are South China granites special in forming ion-adsorption REE deposits? Gondwana Res. 125, 82–90.
Chudasama, B., Porwal, A., González-Álvarez, I., Thakur, S., Wilde, A., Kreuzer, O.P., 2018. Calcrete-hosted surficial uranium systems in Western Australia: Prospectivity modeling and quantitative estimates of resources. Part 1 – Origin of calcrete uranium deposits in surficial environments: a review. Ore Geol. Rev. 102, 906–936.
Cicconi, M.R., Le Losq, C., Henderson, G.S., Neuville, D.R., 2021. The redox behavior of rare earth elements. Magma Redox Geochemistry 381–398.
Cocker, M.D., 2014. Lateritic, Supergene Rare Earth Element (REE) Deposits.
Collins, W.J., Beams, S.D., White, A., Chappell, B., 1982. Nature and origin of A-type granites with particular reference to southeastern Australia. Contrib. Mineral. Petrol. 80, 189–200.
Coppin, F., Berger, G., Bauer, A., Castet, S., Loubet, M., 2002. Sorption of lanthanides on smectite and kaolinite. Chem. Geol. 182 (1), 57–68.
Coppin, F., Castet, S., Berger, G., Loubet, M., 2003. Microscopic reversibility of Sm and Yb sorption onto smectite and kaolinite: experimental evidence. Geochim. Cosmochim. Acta 67 (14), 2515–2527.
Corbett, M.K., Eksteen, J.J., Niu, X.Z., Watkin, E.L.J., 2017. Incorporation of indigenous microorganisms increases leaching rates of Rare Earth Elements from Western Australian Monazite. Solid State Phenom. 262, 294–298.

Costa, N., Botelho, N., Garnier, J., 2020. Concentration of rare earth elements in the Faixa Placha tin deposit, Pedra Branca A-Type Granitic Massif, central Brazil, and its potential for ion-adsorption-type REE-Y mineralization. Ore Geol. Rev. 123, 103606.
Cullers, R.L., Yeh, L.-T., Chaudhuri, S., Guidotti, C.V., 1974. Rare earth elements in Silurian pelitic schists from NW Maine. Geochim. Cosmochim. Acta 38 (3), 389–400.
Dai, S., Zhou, Y., Zhang, M., Wang, X., Wang, J., Song, X., Jiang, Y., Luo, Y., Song, Z., Yang, Z., Ren, D., 2010. A new type of Nb (Ta)–Zr(Hf)–REE–Ga polymetallic deposit in the late Permian coal-bearing strata, eastern Yunnan, southwestern China: possible economic significance and genetic implications. Int. J. Coal Geol. 83 (1), 55–63.
Das, G., Lencka, M.M., Liu, J., Anderko, A., Riman, R.E., Navrotsky, A., 2023. Modeling phase equilibria and speciation in aqueous solutions of rare earth elements with hydroxide and organic ligands. J. Chem. Thermodyn. 186, 107125.
Dean, L.A., 1947. Differential thermal analysis of HAWAIIAN soils. Soil Sci. 63 (2).
Deepthy, R., Balakrishnan, S., 2005. Climatic control on clay mineral formation: evidence from weathering profiles developed on either side of the Western Ghats. Journal of Earth System Science 114 (5), 545–556.
Degens, E.T., 1982. Transport of Carbon and Minerals in Major World Rivers Part 1, Proceedings of a Workshop Arranged by Scientific Committee on Problems of the Environment (SCOPE) and the United Nations Environment Programme (UNEP), 1982. Humburg University.
Delattre, S., Utsunomiya, S., Ewing, R.C., Boeglin, J.-L., Braun, J.-J., Balan, E., Calas, G., 2007. Dissolution of radiation-damaged zircon in lateritic soils. Am. Mineral. 92 (11−12), 1978–1989.
Delolme, C., Hébrard-Labit, C., Spadini, L., Gaudet, J.-P., 2004. Experimental study and modeling of the transfer of zinc in a low reactive sand column in the presence of acetate. J. Contam. Hydrol. 70 (3–4), 205–224.
Diakonov, I.I., Ragnarsdottir, K.V., Tagirov, B.R., 1998. Standard thermodynamic properties and heat capacity equations of rare earth hydroxides:: II. Ce(III)-, Pr-, Sm-, Eu(III)-, Gd-, Tb-, Dy-, Ho-, Er-, Tm-, Yb-, and Y-hydroxides. Comparison of thermochemical and solubility data. Chem. Geol. 151 (1), 327–347.
Dostal, J., 2017. Rare Earth Element Deposits of Alkaline Igneous Rocks, Resources.
Dou, J., Wang, C.Y., Xing, Y., Tan, W., Zhao, Z., 2023. Redistribution of REE in granitic bedrocks during incipient weathering: insights into the role of groundwater in the formation of regolith-hosted REE deposit. Contrib. Mineral. Petrol. 178 (10), 69.
Drever, J., Stillings, L., 1997. The role of organic acids in mineral weathering. Colloids Surf. A Physicochem. Eng. Asp. 120 (1–3), 167–181.
Drew, L.J., Qingrun, M., Weijun, S., 1990. The Bayan Obo iron-rare-earth-niobium deposits, Inner Mongolia, China. Lithos 26 (1), 43–65.
Du, X., Rate, A.W., Gee, M.A.M., 2012. Redistribution and mobilization of titanium, zirconium and thorium in an intensely weathered lateritic profile in Western Australia. Chem. Geol. 330-331, 101–115.
Eby, G.N., 1990. The A-type granitoids: a review of their occurrence and chemical characteristics and speculations on their petrogenesis. Lithos 26 (1–2), 115–134.
Eggert, R.G., 2011. Minerals go critical. Nat. Chem. 3 (9), 688–691.
Eggleton, R., 2001. Glossary of regolith-surficial geology, soils and landscape. CRC LEME Publication, Perth, pp. 144–169.
Elias, M., 2002. Nickel laterite deposits-geological overview, resources and exploitation. In: Giant Ore Deposits: Characteristics, Genesis and Exploration, 4. CODES Special Publication, pp. 205–220.
Ercit, T.S., 2002. The mess that is “allanite”. Can. Mineral. 40 (5), 1411–1419.
Estrade, G., Marquis, E., Smith, M., Goodenough, K., Nason, P., 2019. REE concentration processes in ion adsorption deposits: evidence from the Ambohimirahavavy alkaline complex in Madagascar. Ore Geol. Rev. 112, 103027.
Ewing, R.C., 1994. The metamict state: 1993—the centennial. Nucl. Instrum. Methods Phys. Res., Sect. B 91 (1–4), 22–29.
Fairbridge, R.W., Finkl, C.W., 1980. Cratonic Erosional Unconformities and Peneplains. J. Geol. 88 (1), 69–86.
Fan, C., Xu, C., Shi, A., Smith, M.P., Kynicky, J., Wei, C., 2023. Origin of heavy rare earth elements in highly fractionated peraluminous granites. Geochim. Cosmochim. Acta 343, 371–383.
Ferrier, K.L., Kirchner, J.W., Finkel, R.C., 2011. Estimating millennial-scale rates of dust incorporation into eroding hillslope regolith using cosmogenic nuclides and immobile weathering tracers. J. Geophys. Res. Earth 116 (F3).
Firsching, F.H., Brune, S.N., 1991. Solubility products of the trivalent rare-earth phosphates. J. Chem. Eng. Data 36 (1), 93–95.
Firsching, F.H., Mohammadzadei, J., 1986. Solubility products of the rare-earth carbonates. J. Chem. Eng. Data 31 (1), 40–42.
Foley, N.K., Ayuso, R.A., 2013. Rare earth element mobility in high-alumina altered metavolcanic deposits, South Carolina, USA. J. Geochem. Explor. 133, 50–67.
Forst, B.R., Lindsley, D.H., 1992. Equilibria among Fe-Ti oxides, pyroxenes, olivine, and quartz: Part II. application. Am. Mineral. 77 (9–10), 1004–1020.
Frost, B.R., Chamberlain, K.R., Schumacher, J.C., 2001. Sphene (titanite): phase relations and role as a geochronometer. Chem. Geol. 172 (1–2), 131–148.
Fu, W., Li, X., Feng, Y., Feng, M., Peng, Z., Yu, H., Lin, H., 2019. Chemical weathering of S-type granite and formation of Rare Earth Element (REE)-rich regolith in South China: critical control of lithology. Chem. Geol. 520, 33–51.
Furrer, G., Stumm, W., 1986. The coordination chemistry of weathering: I. Dissolution kinetics of δ-Al2O3 and BeO. Geochim. Cosmochim. Acta 50 (9), 1847–1860.
Gaffney, J.S., Marley, N.A., Clark, S.B., 1996. Humic and Fulvic Acids and Organic Colloidal Materials in the Environment. ACS Publications.
Gammons, C.H., Wood, S.A., Williams-Jones, A.E., 1996. The aqueous geochemistry of the rare earth elements and yttrium: VI. Stability of neodymium chloride complexes from 25 to 300°C. Geochim. Cosmochim. Acta 60 (23), 4615–4630.
Ganor, J., Reznik, I.J., Rosenberg, Y.O., 2009. Organics in water-rock interactions. Rev. Mineral. Geochem. 70 (1), 259–369.
Garrels, R.M., Christ, C.L., 1965. Solutions, minerals, and equilibria. In: Harper's Geoscience Series. Harper & Row, New York, New York.
Geisler, T., 2002. Isothermal annealing of partially metamict zircon: evidence for a three-stage recovery process. Phys. Chem. Miner. 29 (6), 420–429.
Gerritse, R., 1996. Dispersion of cadmium in columns of saturated sandy soils. J. Environ. Qual. 25.
Gimeno Serrano, M.a.J., Auqué Sanz, L.F., Nordstrom, D.K., 2000. Ree speciation in low-temperature acidic waters and the competitive effects of aluminum. Chem. Geol. 165 (3), 167–180.
Gleeson, S.A., Butt, C., Elias, M., 2003. Nickel laterites: a review. SEG Newsl. 54, 1–18.
Goldich, S.S., 1938. A Study in Rock-Weathering. J. Geol. 46 (1), 17–58.
Goldschmidt, V., 1928. Om dannelse av laterit som forvitringsprodukt av norsk labradorsten. The formation of laterite as weathering product of Norwegian labradorite. Commemorative writing for H. Sørlie, Oslo: 21–24.
González-Álvarez, I., Kerrich, R., 2010. REE and HFSE mobility due to protracted flow of basinal brines in the mesoproterozoic Belt-Purcell Supergroup, Laurentia. Precambrian Res. 177 (3), 291–307.
González-Álvarez, I., Kerrich, R., 2011. Trace element mobility in dolomitic argillites of the Mesoproterozoic Belt-Purcell Supergroup, western North America. Geochim. Cosmochim. Acta 75 (7), 1733–1756.
González-Álvarez, I., Kusiak, M.A., Kerrich, R., 2006. A trace element and chemical Th–U total Pb dating study in the lower Belt-Purcell Supergroup, Western North America: provenance and diagenetic implications. Chem. Geol. 230 (1–2), 140–160.
González-Álvarez, I., Porwal, A., Beresford, S., McCuaig, T., Maier, W.D., 2010. Hydrothermal Ni prospectivity analysis of Tasmania, Australia. Ore Geol. Rev. 38 (3), 168–183.
González-Álvarez, I., Boni, M., Anand, R.R., 2016a. Mineral exploration in regolith-dominated terrains: Global considerations and challenges. Ore Geol. Rev. 73, 375–379.
González-Álvarez, I., Salama, W., Anand, R.R., 2016b. Sea-level changes and buried islands in a complex coastal palaeolandscape in the South of Western Australia: Implications for greenfield mineral exploration. Ore Geol. Rev. 73, 475–499.
González-Álvarez, I., Stoppa, F., Yang, X., Porwal, A., 2021. Introduction to the special issue, insights on carbonatites and their mineral exploration approach: a challenge towards resourcing critical metals. Ore Geol. Rev. 133, 104073.
Goodenough, K.M., Wall, F., Merriman, D., 2018. The Rare Earth Elements: demand, global resources, and challenges for resourcing future generations. Nat. Resour. Res. 27 (2), 201–216.
Gosselin, D.C., Smith, M.R., Lepel, E.A., Laul, J.C., 1992. Rare earth elements in chloride-rich groundwater, Palo Duro Basin, Texas, USA. Geochim. Cosmochim. Acta 56 (4), 1495–1505.
Goyne, K.W., Brantley, S.L., Chorover, J., 2010. Rare earth element release from phosphate minerals in the presence of organic acids. Chem. Geol. 278 (1), 1–14.
Gupta, C.K., Krishnamurthy, N., 1992. Extractive metallurgy of rare earths. Int. Mater. Rev. 37 (1), 197–248.
Haas, J.R., Shock, E.L., Sassani, D.C., 1995. Rare earth elements in hydrothermal systems: estimates of standard partial molal thermodynamic properties of aqueous complexes of the rare earth elements at high pressures and temperatures. Geochim. Cosmochim. Acta 59 (21), 4329–4350.
Han, B., Zhang, X., Liu, C., Ma, G., Guo, D., Shao, Y., Li, P., Liang, J., Fan, Q., 2023. Essential role of the interlayer of montmorillonite, vermiculite, and illite for Ni (II) sorption. J. Radioanal. Nucl. Chem. 332 (4), 1315–1323.
Harrison, T., Watson, E., 1984. The behavior of apatite during crustal anatexis: equilibrium and kinetic considerations. Geochim Cosmochim Ac 48, 1467–1477.
Hassas, B.V., Rezaee, M., Pisupati, S.V., 2021. Effect of various ligands on the selective precipitation of critical and rare earth elements from acid mine drainage. Chemosphere 280, 130684.
He, H., Huang, J., Huang, Y., Liang, X., Liu, L., Sun, M., Tan, W., Wang, Y., Zhu, J., 2023. Distribution and fractionation of Rare Earth Elements (REE) in the ion adsorption-type REE deposit (IAD) at Maofeng Mountain, Guangzhou, China. Clay Clay Miner. 71 (3), 340–361.
Heckman, K., Rasmussen, C., 2011. Lithologic controls on regolith weathering and mass flux in forested ecosystems of the southwestern USA. Geoderma 164 (3–4), 99–111.
Helgeson, H.C., 1969. Thermodynamics of hydrothermal systems at elevated temperatures and pressures. Am. J. Sci. 267 (7), 729.
Hemond, H.F., Fechner, E.J., 2022. Chemical Fate and Transport in the Environment. Academic press.
Henderson, P., 1984. Chapter 1 - General geochemical properties and abundances of the rare earth elements. In: Henderson, P. (Ed.), Developments in Geochemistry. Elsevier, pp. 1–32.
Herrington, T., Clarke, A., Watts, J., 1992. The surface charge of kaolin. Colloids Surf. A Physicochem. Eng. Asp. 68 (3), 161–169.
Herrmann, M., Söderlund, U., Scherstén, A., Næraa, T., Holm-Alwmark, S., Alwmark, C., 2021. The effect of low-temperature annealing on discordance of U–Pb zircon ages. Sci. Rep. 11 (1), 7079.
Hill, E., Wood, B.J., Blundy, J.D., 2000. The effect of Ca-Tschermaks component on trace element partitioning between clinopyroxene and silicate melt. Lithos 53 (3), 203–215.
Hoshino, M., Sanematsu, K., Watanabe, Y., 2016. Chapter 279 - REE mineralogy and resources (Editors). In: Jean-Claude, B., K, P. Vitalij (Eds.), Handbook on the Physics and Chemistry of Rare Earths. Elsevier, pp. 129–291.
Huang, D., Wu, C., Han, J., 1989. REE geochemistry and mineralization characteristics of the Zudong and Guanxi granites, Jiangxi Province. Acta Geologica Sinica-English Edition 2 (2), 139–157.
Huang, Y., He, H., Liang, X., Bao, Z., Tan, W., Ma, L., Zhu, J., Huang, J., Wang, H., 2021. Characteristics and genesis of ion adsorption type REE deposits in the weathering

crusts of metamorphic rocks in Ningdu, Ganzhou, China. Ore Geol. Rev. 135, 104173.
Ilankoon, I.M.S.K., Dushyantha, N.P., Mancheri, N., Edirisinghe, P.M., Neethling, S.J., Ratnayake, N.P., Rohitha, L.P.S., Dissanayake, D.M.D.O.K., Premasiri, H.M.R., Abeysinghe, A.M.K.B., Dharmaratne, P.G.R., Batapola, N.M., 2022. Constraints to rare earth elements supply diversification: evidence from an industry survey. J. Clean. Prod. 331, 129932.
Ingri, J., Widerlund, A., Land, M., Gustafsson, Ö., Andersson, P., Öhlander, B., 2000. Temporal variations in the fractionation of the rare earth elements in a boreal river; the role of colloidal particles. Chem. Geol. 166 (1), 23–45.
Ionic Rare Earths LTD, 2022. ASX release: substantial increase to Makuutu resources to over 500 million tonnes.
Ionov, D.A., Bodinier, J.L., Mukasa, S.B., Zanetti, A., 2002. Mechanisms and sources of mantle metasomatism: Major and trace element compositions of peridotite xenoliths from Spitsbergen in the context of numerical modelling. J. Petrol. 43 (12), 2219–2259.
Ishihara, S., Hua, R., Hoshino, M., Murakami, H., 2008. REE Abundance and REE Minerals in Granitic Rocks in the Nanling Range, Jiangxi Province, Southern China, and Generation of the REE-rich Weathered Crust Deposits. Resour. Geol. 58 (4), 355–372.
Itoh, H., Hachiya, H., Tsuchiya, M., Suzuki, Y., Asano, Y., 1984. Determination of Solubility Products of Rare Earth Fluorides by Fluoride Ion-selective Electrode. Bull. Chem. Soc. Jpn. 57 (6), 1689–1690.
Izatt, R.M., Eatough, D., Christensen, J.J., Bartholomew, C.H., 1969. Calorimetrically determined log K, ΔH°, and ΔS° values for the interaction of sulphate ion with several bi- and ter-valent metal ions. Journal of the Chemical Society a: Inorganic, Physical, Theoretical 0, 47–53.
Jaireth, S., Hoatson, D.M., Miezitis, Y., 2014. Geological setting and resources of the major rare-earth-element deposits in Australia. Ore Geol. Rev. 62, 72–128.
Janots, E., Austrheim, H., Spandler, C., Hammerli, J., Trepmann, C.A., Berndt, J., Magnin, V., Kemp, A.I., 2018. Rare earth elements and Sm-Nd isotope redistribution in apatite and accessory minerals in retrogressed lower crust material (Bergen Arcs, Norway). Chem. Geol. 484, 120–135.
Janssen, R.P.T., Verweij, W., 2003. Geochemistry of some rare earth elements in groundwater, Vierlingsbeek, The Netherlands. Water Res. 37 (6), 1320–1350.
Jayadeva, M., Sridharan, A., 1982. Double layer theory and compressibility of clays. Géotechnique 32, 133–144.
Jiang, L.-Q., Carter, B.R., Feely, R.A., Lauvset, S.K., Olsen, A., 2019. Surface ocean pH and buffer capacity: past, present and future. Sci. Rep. 9 (1), 18624.
Johannesson, K.H., Lyons, W.B., 1994. The rare earth element geochemistry of Mono Lake water and the importance of carbonate complexing. Limnol. Oceanogr. 39 (5), 1141–1154.
Johannesson, K.H., Lyons, W.B., 1995. Rare-earth element geochemistry of Colour Lake, an acidic freshwater lake on Axel Heiberg Island, Northwest Territories, Canada. Chem. Geol. 119 (1), 209–223.
Johannesson, K.H., Lyons, W.B., Stetzenbach, K.J., Byrne, R.H., 1995. The solubility control of rare earth elements in natural terrestrial waters and the significance of PO43−and CO32−in limiting dissolved rare earth concentrations: a review of recent information. Aquat. Geochem. 1 (2), 157–173.
Johannesson, K.H., Stetzenbach, K.J., Hodge, V.F., Lyons, W.B., 1996. Rare earth element complexation behavior in circumneutral pH groundwaters: assessing the role of carbonate and phosphate ions. Earth Planet. Sci. Lett. 139 (1–2), 305–319.
Johannesson, K.H., Farnham, I.M., Guo, C., Stetzenbach, K.J., 1999. Rare earth element fractionation and concentration variations along a groundwater flow path within a shallow, basin-fill aquifer, southern Nevada, USA. Geochim. Cosmochim. Acta 63 (18), 2697–2708.
Johannesson, K.H., Zhou, X., Guo, C., Stetzenbach, K.J., Hodge, V.F., 2000. Origin of rare earth element signatures in groundwaters of circumneutral pH from southern Nevada and eastern California, USA. Chem. Geol. 164 (3), 239–257.
Johannesson, K.H., Tang, J., Daniels, J.M., Bounds, W.J., Burdige, D.J., 2004. Rare earth element concentrations and speciation in organic-rich blackwaters of the Great Dismal Swamp, Virginia, USA. Chem. Geol. 209 (3–4), 271–294.
Joussein, E., Petit, S., Churchman, J., Theng, B., Righi, D., Delvaux, B., 2005. Halloysite clay minerals — a review. Clay Miner. 40 (4), 383–426.
Kanazawa, Y., Kamitani, M., 2006. Rare earth minerals and resources in the world. J. Alloys Compd. 408-412, 1339–1343.
Keller, P., Anderson, C., 2018. The Production of Critical Materials as by Products, 2, p. 14.
Kleman, J., Stroeven, A.P., Lundqvist, J., 2008. Patterns of Quaternary ice sheet erosion and deposition in Fennoscandia and a theoretical framework for explanation. Geomorphology 97 (1), 73–90.
Knox-Robinson, C.M., Wyborn, L.A.I., 1997. Towards a holistic exploration strategy: using Geographic Information Systems as a tool to enhance exploration. Aust. J. Earth Sci. 44 (4), 453–463.
Köhler, S.J., Harouiya, N., Chaïrat, C., Oelkers, E.H., 2005. Experimental studies of REE fractionation during water–mineral interactions: REE release rates during apatite dissolution from pH 2.8 to 9.2. Chem. Geol. 222 (3), 168–182.
Kohn, M.J., 2017. Titanite petrochronology. Rev. Mineral. Geochem. 83 (1), 419–441.
Kosmulski, M., 2018. The pH dependent surface charging and points of zero charge. VII. Update. Adv. Colloid Interf. Sci. 251, 115–138.
Kottek, M., Grieser, J., Beck, C., Rudolf, B., Rubel, F., 2006. World map of the Köppen-Geiger climate classification updated. Meteorol. 15, 259–263.
Kraepiel, A.M.L., Keller, K., Morel, F.M.M., 1999. A model for metal adsorption on montmorillonite. J. Colloid Interface Sci. 210 (1), 43–54.
Krauskopf, K.B., Bird, D.K., 1995. Introduction to Geochemistry, 647. McGraw-Hill, New York.
Kumari, N., Mohan, C., 2021. Basics of clay minerals and their characteristic properties. Clay Clay Miner. 24, 1–29.
Kyser, K., Hiatt, E., Renac, C., Durocher, K., Holk, G., Deckart, K., 2000. Diagenetic fluids in Paleo-and Meso-Proterozoic sedimentary basins and their implications for long protracted fluid histories. Mineralogical Association of Canada Short Course 28, 225–262.
Laird, D.A., 2006. Influence of layer charge on swelling of smectites. Appl. Clay Sci. 34 (1), 74–87.
Larsen, W., Liu, X.-M., Riveros-Iregui, D.A., 2021. Rare earth element behavior in springs and streams on a basaltic island: San Cristóbal, Galápagos. Appl. Geochem. 131, 105004.
Lasaga, A.C., Soler, J.M., Ganor, J., Burch, T.E., Nagy, K.L., 1994. Chemical weathering rate laws and global geochemical cycles. Geochim. Cosmochim. Acta 58 (10), 2361–2386.
Laveuf, C., Cornu, S., 2009. A review on the potentiality of Rare Earth Elements to trace pedogenetic processes. Geoderma 154 (1), 1–12.
Lawrence, C.R., Reynolds, R.L., Ketterer, M.E., Neff, J.C., 2013. Aeolian controls of soil geochemistry and weathering fluxes in high-elevation ecosystems of the Rocky Mountains, Colorado. Geochim. Cosmochim. Acta 107, 27–46.
Lazo, D.E., Dyer, L.G., Alorro, R.D., 2017. Silicate, phosphate and carbonate mineral dissolution behaviour in the presence of organic acids: a review. Miner. Eng. 100, 115–123.
Le Couteur, P., 2011. Geological Report on the Chambe Basin Area of Exclusive Prospecting License EPL0325/11 Mulanje Massif, Southern Malawi, East Africa. Micron Geological Ltd., Vancoucer.
Lee, J.H., Byrne, R.H., 1992. Examination of comparative rare earth element complexation behavior using linear free-energy relationships. Geochim. Cosmochim. Acta 56 (3), 1127–1137.
Leenheer, J., Malcolm, R., McKinley, P., Eccles, L.A., 1974. Occurrence of dissolved organic carbon in selected ground-water samples in the United States. J. Res. US Geol. Surv. 2 (3), 361–369.
Li, M.Y.H., Zhou, M.-F., 2020. The role of clay minerals in formation of the regolith-hosted heavy rare earth element deposits. Am. Mineral. 105 (1), 92–108.
Li, M.Y.H., Zhou, M.-F., 2023. Physicochemical variation of clay minerals and enrichment of rare earth elements in regolith-hosted deposits: exemplification from the Bankeng deposit in South China. Clay Clay Miner. 71 (3), 362–376.
Li, M.Y.H., Zhou, M.-F., 2024. Hyper-enrichment of heavy rare earth elements in highly evolved granites through multiple hydrothermal mobilizations. Am. Mineral. 109 (11), 1945–1959.
Li, M.Y.H., Zhou, M.-F., Williams-Jones, A.E., 2019. The genesis of regolith-hosted heavy rare earth element deposits: Insights from the world-class Zudong deposit in Jiangxi Province, South China. Econ. Geol. 114 (3), 541–568.
Li, M.Y.H., Zhou, M.-F., Williams-Jones, A.E., 2020. Controls on the dynamics of rare earth elements during subtropical hillslope processes and formation of regolith-hosted deposits. Econ. Geol. 115 (5), 1097–1118.
Li, M.Y.H., Kwong, H.T., Williams-Jones, A.E., Zhou, M.-F., 2022. The thermodynamics of rare earth element liberation, mobilization and supergene enrichment during groundwater-regolith interaction. Geochim. Cosmochim. Acta 330, 258–277.
Li, X., Li, W., Li, Z., 2007. Rediscussion on genetic types and tectonic significance of early Yanshan granites in Nanling. Chin. Sci. Bull. 52 (9), 981–992.
Li, Y.H.M., Zhao, W.W., Zhou, M.-F., 2017. Nature of parent rocks, mineralization styles and ore genesis of regolith-hosted REE deposits in South China: an integrated genetic model. J. Asian Earth Sci. 148, 65–95.
Liu, S.-L., Fan, H.-R., Liu, X., Meng, J., Butcher, A.R., Yann, L., Yang, K.-F., Li, X.-C., 2023a. Global rare earth elements projects: new developments and supply chains. Ore Geol. Rev. 157, 105428.
Liu, W., Li, Y., Wang, X., Cui, L., Zhao, Z., Liu, C., Xu, Z., 2022. Weathering stage and topographic control on rare earth element (REE) behavior: new constraints from a deeply weathered granite hill. Chem. Geol. 610, 121066.
Liu, Y., Hou, Z., 2017. A synthesis of mineralization styles with an integrated genetic model of carbonatite-syenite-hosted REE deposits in the Cenozoic Mianning-Dechang REE metallogenic belt, the eastern Tibetan Plateau, southwestern China. J. Asian Earth Sci. 137, 35–79.
Liu, Y., Zhang, C., Jiang, J., Zhang, Y., Wang, G., Xu, L., Qu, Z., 2023b. Interaction between groundwater and surface water in the Qujiang River Basin in China: evidence from chemical isotope measurements. Water 15 (22), 3932.
Löhr, S.C., Spandler, C., Baldermann, A., 2024. Controls on rapid rare earth element enrichment in sediments deposited by a continental-scale river system. Geochim. Cosmochim. Acta 366, 48–64.
London, D., Wolf, M.B., Morgan, G.B.V.I., Garrido, M.G., 1999. Experimental silicate–phosphate equilibria in peraluminous granitic magmas, with a case study of the Alburquerque batholith at Tres Arroyos, Badajoz, Spain. J. Petrol. 40 (1), 215–240.
Lottermoser, B.G., 1990. Rare-earth element mineralisation within the Mt. Weld carbonatite laterite, Western Australia. Lithos 24 (2), 151–167.
Lozano, A., Ayora, C., Fernández-Martínez, A., 2019. Sorption of rare earth elements onto basaluminite: the role of sulfate and pH. Geochim. Cosmochim. Acta 258, 50–62.
Luo, Y.-R., Byrne, R.H., 2004. Carbonate complexation of yttrium and the rare earth elements in natural waters, 1 1Associate Editor: D. Rimstidt. Geochim. Cosmochim. Acta 68 (4), 691–699.
Lynas Rare Earths, 2023. Annu. Rep. FY2023.
Ma, C., Eggleton, R.A., 1999. Cation exchange capacity of kaolinite. Clay Clay Miner. 47 (2), 174–180.

Ma, L., Jin, L., Brantley, S.L., 2011. How mineralogy and slope aspect affect REE release and fractionation during shale weathering in the Susquehanna/Shale Hills Critical Zone Observatory. Chem. Geol. 290 (1), 31–49.
Magoon, L.B., Dow, W.G., 1991. The Petroleum System - From Source to Trap. Journal Name: AAPG Bulletin (American Association of Petroleum Geologists); (United States); Journal Volume: 75:3; Conference: Annual meeting of the American Association of Petroleum Geologists (AAPG), Dallas, TX (United States), 7–10 Apr 1991, United States, pp. Medium: X; Size: Pages: 627.
Mahood, G., Hildreth, W., 1983. Large partition coefficients for trace elements in high-silica rhyolites. Geochim. Cosmochim. Acta 47 (1), 11–30.
Maitra, A., Chatterjee, A., Keesari, T., Gupta, S., 2020. Forming topography in granulite terrains: evaluating the role of chemical weathering. Journal of Earth System Science 129, 1–13.
Maksimov, A.I., Kovalenko, N.A., Uspenskaya, I.A., 2019. Thermodynamic modeling of the water – Nitric acid – Rare earth nitrate systems. Calphad 67, 101683.
Marini, O.J., Botelho, N.F., Rossi, P., 1992. Elementos terras raras em granitóides da Província Estanífera de Goiás. Revista Brasileira de Geociências 22 (1), 61–72.
Marquette, G.C., Gray, J.T., Gosse, J.C., Courchesne, F., Stockli, L., Macpherson, G., Finkel, R., 2004. Felsenmeer persistence under non-erosive ice in the Torngat and Kaumajet mountains, Quebec and Labrador, as determined by soil weathering and cosmogenic nuclide exposure dating. Can. J. Earth Sci. 41 (1), 19–38.
Marsac, R., Davranche, M., Gruau, G., Dia, A., 2010. Metal loading effect on rare earth element binding to humic acid: experimental and modelling evidence. Geochim. Cosmochim. Acta 74 (6), 1749–1761.
Marsac, R., Davranche, M., Morin, G., Takahashi, Y., Gruau, G., Briant, N., Dia, A., 2015. Effect of loading on the nature of the REE–humate complexes as determined by Yb3 + and Sm3+ LIII-edge EXAFS analysis. Chem. Geol. 396, 218–227.
Marsh, J.S., 1991. REE fractionation and Ce anomalies in weathered Karoo dolerite. Chem. Geol. 90 (3), 189–194.
Marshall, W.L., Jones, E.V., 1966. Second dissociation constant of sulfuric acid from 25 to 350 evaluated from solubilities of calcium sulfate in sulfuric acid solutions1, 2. J. Phys. Chem. 70 (12), 4028–4040.
Marx, S.K., Kamber, B.S., 2010. Trace-element systematics of sediments in the Murray–Darling Basin, Australia: Sediment provenance and palaeoclimate implications of fine scale chemical heterogeneity. Appl. Geochem. 25 (8), 1221–1237.
McCuaig, T.C., Hronsky, J.M., 2014. The Mineral System Concept: The Key to Exploration Targeting.
McCuaig, T.C., Beresford, S., Hronsky, J., 2010. Translating the mineral systems approach into an effective exploration targeting system. Ore Geol. Rev. 38 (3), 128–138.
McFarlane, M., 1992. Groundwater movement and water chemistry associated with weathering profiles of the African surface in parts of Malawi. Geol. Soc. Lond. Spec. Publ. 66 (1), 101–129.
McQueen, K.G., Scott, K.M., 2008. Rock weathering and structure of the regolith. Reg. Sci. 1, 105–126.
Meteoric Resources, 2023. Caldeira REE Project Maiden Mineral Resources.
Migdisov, A., Williams-Jones, A.E., Brugger, J., Caporuscio, F.A., 2016. Hydrothermal transport, deposition, and fractionation of the REE: Experimental data and thermodynamic calculations. Chem. Geol. 439, 13–42.
Migdisov, A., Guo, X., Nisbet, H., Xu, H., Williams-Jones, A.E., 2019. Fractionation of REE, U, and Th in natural ore-forming hydrothermal systems: Thermodynamic modeling. J. Chem. Thermodyn. 128, 305–319.
Migdisov, A.A., Williams-Jones, A.E., 2014. Hydrothermal transport and deposition of the rare earth elements by fluorine-bearing aqueous liquids. Mineral. Deposita 49 (8), 987–997.
Millero, F.J., 1992. Stability constants for the formation of rare earth-inorganic complexes as a function of ionic strength. Geochim. Cosmochim. Acta 56 (8), 3123–3132.
Miyawaki, R., 1995. Crystal chemical aspects of rare earth minerals. In: Rare Earth Minerals, pp. 21–40.
Mohr, E.C.J., Pendleton, R.L., 1944. The Soils of Equatorial Regions With Special Reference to the Netherlands East Indies. J.W. Edwards.
Moldoveanu, G.A., Papangelakis, V.G., 2013. Recovery of rare earth elements adsorbed on clay minerals: II. Leaching with ammonium sulfate. Hydrometallurgy 131–132, 158–166.
Moreno, T., Querol, X., Castillo, S., Alastuey, A., Cuevas, E., Herrmann, L., Mounkaila, M., Elvira, J., Gibbons, W., 2006. Geochemical variations in aeolian mineral particles from the Sahara–Sahel Dust Corridor. Chemosphere 65 (2), 261–270.
Mulrooney, D., Rivers, T., 2005. Redistribution of the rare-earth elements among coexisting minerals in metamafic rocks across the epidote-out isograd: an example from the St. Anthony complex, Northern Newfoundland, Canada. Can. Mineral. 43 (1), 263–294.
Munemoto, T., Ohmori, K., Iwatsuki, T., 2015. Rare earth elements (REE) in deep groundwater from granite and fracture-filling calcite in the Tono area, Central Japan: Prediction of REE fractionation in paleo-to present-day groundwater. Chem. Geol. 417, 58–67.
Murray-Wallace, C.V., Murray-Wallace, C.V., Steenbergen, v., 2018. Quaternary History of the Coorong Coastal Plain, Southern Australia. Springer.
Mysen, B.O., Ryerson, F.J., Virgo, D., 1981. The structural role of phosphorus in silicate melts. Am. Mineral. 66 (1–2), 106–117.
Nahon, D.B., 1991. Self-organization in chemical lateritic weathering. Geoderma 51 (1), 5–13.
Nesbitt, H.W., 1979. Mobility and fractionation of rare earth elements during weathering of a granodiorite. Nature 279 (5710), 206–210.
Nestmeyer, M., McCoy-West, A.J., 2025. Quantifying mass-dependent isotope fractionation and nuclear field shift effects for the light rare Earth elements in hydrous systems. Geochim. Cosmochim. Acta 388, 236–252.
Neumann, R., Medeiros, E.B., 2015. Comprehensive mineralogical and technological characterisation of the Araxá (SE Brazil) complex REE (Nb-P) ore, and the fate of its processing. Int. J. Miner. Process. 144, 1–10.
Nganje, T., Hursthouse, A., Edet, A., Stirling, D., Adamu, C., 2017. Hydrochemistry of surface water and groundwater in the shale bedrock, Cross River Basin and Niger Delta Region, Nigeria. Appl Water Sci 7, 961–985.
Noack, C.W., Dzombak, D.A., Karamalidis, A.K., 2014. Rare Earth Element Distributions and Trends in Natural Waters with a Focus on Groundwater. Environ. Sci. Technol. 48 (8), 4317–4326.
Norton, S.A., 1973. Laterite and Bauxite Formation. Econ. Geol. 68 (3), 353–361.
Oelkers, E.H., Poitrasson, F., 2002. An experimental study of the dissolution stoichiometry and rates of a natural monazite as a function of temperature from 50 to 230 C and pH from 1.5 to 10. Chem. Geol. 191 (1–3), 73–87.
Oelkers, E.H., Valsami-Jones, E., Roncal-Herrero, T., 2008. Phosphate mineral reactivity: from global cycles to sustainable development. Mineral. Mag. 72 (1), 337–340.
Ollier, C.D., Pain, C.F., 1996. Regolith, soils and landforms. John Wiley, Chichester.
Orris, G., Seo, Y., Briggs, D., Dunlap, D., Cocker, M., 2018. Introduction to the Global Rare Earth Element Occurrence Database. US Geological Survey. https://www.sciencebase.gov/catalog/item/5a0c5a0de4b09af898cd15d2.
Ouyang, J., Mu, D., Zhang, Y., Yang, H., 2018. Mineralogy and physico-chemical data of two newly discovered halloysite in China and their contrasts with some typical minerals. Minerals 8 (3), 108.
Owor, M., Muwanga, A., Tindimugaya, C., Taylor, R.G., 2021. Hydrogeochemical processes in groundwater in Uganda: a national-scale analysis. J. Afr. Earth Sci. 175, 104113.
Pain, C., Ollier, C., 1995. Regolith stratigraphy: principles and problems. AGSO J. Aust. Geol. Geophys. 16 (3), 197–202.
Palandri, J.L., Kharaka, Y.K., 2004. A compilation of rate parameters of water-mineral interaction kinetics for application to geochemical modeling.
Parkhurst, D.L., Appelo, C.A.J., 2013. Description of Input and Examples for PHREEQC Version 3: AA Computer Program for Speciation, Batch-Reaction, One-dimensional Transport, and Inverse Geochemical Calculations, pp. 6–A43. Reston, VA.
Patiño Douce, A.E., 1997. Generation of metaluminous A-type granites by low-pressure melting of calc-alkaline granitoids. Geology 25 (8), 743–746.
Pearson, R.G., 1988. Absolute electronegativity and hardness: application to inorganic chemistry. Inorg. Chem. 27 (4), 734–740.
Pearson, R.G., Gray, H.B., 1963. Partial ionic character of metal-chlorine bonds. Inorg. Chem. 2 (2), 358–363.
Peter Gromet, L., Silver, L.T., 1983. Rare earth element distributions among minerals in a granodiorite and their petrogenetic implications. Geochim. Cosmochim. Acta 47 (5), 925–939.
Petković, D.M., 1982. Dissociation of strong acids in aqueous solutions. J. Chem. Soc. Dalton Trans. 12, 2425–2427.
Phillips, J.D., Pawlik, Ł., Šamonil, P., 2019. Weathering fronts. Earth Sci. Rev. 198, 102925.
Pokrovsky, O.S., Schott, J., Dupré, B., 2006. Trace element fractionation and transport in boreal rivers and soil porewaters of permafrost-dominated basaltic terrain in Central Siberia. Geochim. Cosmochim. Acta 70 (13), 3239–3260.
Pope, G.A., 2015. Chapter 4 - regolith and weathering (rock decay) in the critical zone. In: Giardino, J.R., Houser, C. (Eds.), Developments in Earth Surface Processes. Elsevier, pp. 113–145.
Porwal, A., González-Álvarez, I., Markwitz, V., McCuaig, T.C., Mamuse, A., 2010. Weights-of-evidence and logistic regression modeling of magmatic nickel sulfide prospectivity in the Yilgarn Craton, Western Australia. Ore Geol. Rev. 38 (3), 184–196.
Pourret, O., Davranche, M., Gruau, G., Dia, A., 2007a. Competition between humic acid and carbonates for rare earth elements complexation. J. Colloid Interface Sci. 305 (1), 25–31.
Pourret, O., Davranche, M., Gruau, G., Dia, A., 2007b. Organic complexation of rare earth elements in natural waters: evaluating model calculations from ultrafiltration data. Geochim. Cosmochim. Acta 71 (11), 2718–2735.
Pourret, O., Davranche, M., Gruau, G., Dia, A., 2007c. Rare earth elements complexation with humic acid. Chem. Geol. 243 (1), 128–141.
Powell, H.K.J., 1974. Entropy titrations: a reassessment of data for the reaction of the sulphate ion with trivalent lanthanoid ions. J. Chem. Soc. Dalton Trans. 10, 1108.
Price, J.D., Hogan, J.P., Gilbert, M.C., London, D., Morgan, G.B., 1999. Experimental study of titanite-fluorite equilibria in the A-type Mount Scott Granite: Implications for assessing F contents of felsic magma. Geology 27 (10), 951–954.
Price, J.R., Velbel, M.A., Patino, L.C., 2005a. Allanite and epidote weathering at the Coweeta Hydrologic Laboratory, western North Carolina, U.S.A. Am. Mineral. 90 (1), 101–114.
Price, J.R., Velbel, M.A., Patino, L.C., 2005b. Rates and time scales of clay-mineral formation by weathering in saprolitic regoliths of the southern Appalachians from geochemical mass balance. Geol. Soc. Am. Bull. 117 (5–6), 783–794.
Price, J.R., Heitmann, N., Hull, J., Szymanski, D., 2008. Long-term average mineral weathering rates from watershed geochemical mass balance methods: using mineral modal abundances to solve more equations in more unknowns. Chem. Geol. 254 (1), 36–51.
Price, J.R., Nunez, J., Moore, J., 2020. Using plug-flow column reactor data to constrain calcic mineral weathering rates from watershed mass-balance methods: Lithogenic apatite dissolution and phosphorus fluxes into the Loch Vale Watershed ecosystem, Colorado, USA. Appl. Geochem. 120, 104664.

Prowatke, S., Klemme, S., 2005. Effect of melt composition on the partitioning of trace elements between titanite and silicate melt. Geochim. Cosmochim. Acta 69 (3), 695–709.
Prowatke, S., Klemme, S., 2006a. Rare earth element partitioning between titanite and silicate melts: Henry's law revisited. Geochim. Cosmochim. Acta 70 (19), 4997–5012.
Prowatke, S., Klemme, S., 2006b. Trace element partitioning between apatite and silicate melts. Geochim. Cosmochim. Acta 70 (17), 4513–4527.
Qiu, K.-F., Deng, J., Li, S.-S., Jowitt, S., Hetherington, C.J., Balen, D., 2023. Roles and perspectives of A- and I-type magmas in rare earth element and gold mineralization. GSA Bull. 136 (3–4), 1238–1250.
Ram, R., Becker, M., Brugger, J., Etschmann, B., Burcher-Jones, C., Howard, D., Kooyman, P.J., Petersen, J., 2019. Characterisation of a rare earth element- and zirconium-bearing ion-adsorption clay deposit in Madagascar. Chem. Geol. 522, 93–107.
Refsnider, K.A., Miller, G.H., 2013. Ice-sheet erosion and the stripping of Tertiary regolith from Baffin Island, eastern Canadian Arctic. Quat. Sci. Rev. 67, 176–189.
Reynolds, R.C., Johnson, N.M., 1972. Chemical weathering in the temperate glacial environment of the Northern Cascade Mountains. Geochim. Cosmochim. Acta 36 (5), 537–554.
Rose, D., 1973. Some aspects of the hydrodynamic dispersion of solutes in porous materials. J. Soil Sci. 24 (3), 284–295.
Rubel, F., Brugger, K., Haslinger, K., Auer, I., 2017. The climate of the European Alps: Shift of very high resolution Köppen-Geiger climate zones 1800–2100. Meteorol. Z. 26 (2), 115–125.
Rubin, J.N., Henry, C.D., Price, J.G., 1993. The mobility of zirconium and other "immobile" elements during hydrothermal alteration. Chem. Geol. 110 (1), 29–47.
Rudnick, R.L., Gao, S., 2003. 3.01 - composition of the continental crust. In: Holland, H. D., Turekian, K.K. (Eds.), Treatise on Geochemistry. Pergamon, Oxford, pp. 1–64.
Sadleir, S., Gilkes, R., 1976. Development of bauxite in relation to parent material near Jarrahdale, Western Australia. J. Geol. Soc. Aust. 23 (4), 333–344.
Saeger, V.W., Spedding, F.H., Commission, U.S.A.E, Laboratory, A., 1960. Some Physical Properties of Rare-earth Chlorides in Aqueous Solution. Iowa State University of Science and Technology, Ames Laboratory.
Sanematsu, K., Watanabe, Y., 2016. Characteristics and Genesis of Ion Adsorption-type Rare Earth Element Deposits.
Sanematsu, K., Kon, Y., Imai, A., Watanabe, K., Watanabe, Y., 2013. Geochemical and mineralogical characteristics of ion-adsorption type REE mineralization in Phuket, Thailand. Mineral. Deposita 48 (4), 437–451.
Sanematsu, K., Kon, Y., Imai, A., 2015. Influence of phosphate on mobility and adsorption of REEs during weathering of granites in Thailand. J. Asian Earth Sci. 111, 14–30.
Sanematsu, K., Ejima, T., Kon, Y., Manaka, T., Zaw, K., Morita, S., Seo, Y., 2016. Fractionation of rare-earth elements during magmatic differentiation and weathering of calc-alkaline granites in southern Myanmar. Mineral. Mag. 80 (1), 77–102.
Santana, I.V., Botelho, N.F., 2022. Ree residence, behaviour and recovery from a weathering profile related to the Serra Dourada Granite, Goiás/Tocantins States, Brazil. Ore Geol. Rev. 143, 104751.
Santana, I.V., Wall, F., Botelho, N.F., 2015. Occurrence and behavior of monazite-(Ce) and xenotime-(Y) in detrital and saprolitic environments related to the Serra Dourada granite, Goiás/Tocantins State, Brazil: potential for REE deposits. J. Geochem. Explor. 155, 1–13.
Sarapää, O., Sarala, P., 2013. Rare earth element and gold exploration in glaciated terrain: example from the Mäkärä area, northern Finland. Geochem.: Explor., Environ., Anal. 13 (2), 131–143.
Sassani, D., Shock, E., 1993. Estimation of Standard State Association Constants of Aqueous Complexes at 25° C and 1 Bar.
Sawka, W.N., Chappell, B.W., Norrish, K., 1984. Light-rare-earth-element zoning in sphene and allanite during granitoid fractionation. Geology 12 (3), 131–134.
Schoonheydt, R., Johnston, C., 2011. The Surface Properties of Clay Minerals, pp. 335–370.
Schoonheydt, R.A., Johnston, C.T., Bergaya, F., 2018. Clay minerals and their surfaces. In: Developments in Clay Science. Elsevier, pp. 1–21.
Schulze, R., Lartigue-Peyrou, F., Ding, J., Schebek, L., Buchert, M., 2017. Developing a life cycle inventory for rare earth oxides from ion-adsorption deposits: key impacts and further research needs. Journal of Sustainable Metallurgy 3 (4), 753–771.
Sengupta, D., Gosen, B.S.V., 2016. Placer-type rare earth element deposits. In: Verplanck, P.L., Hitzman, M.W. (Eds.), Rare Earth and Critical Elements in Ore Deposits. Society of Economic Geologists, p. 0.
Serra Verde Group, 2024. Serra Verde Enters Commercial Production.
Shakeri, A., Ghoreyshinia, S., Mehrabi, B., Delavari, M., 2015. Rare earth elements geochemistry in springs from Taftan geothermal area SE Iran. J. Volcanol. Geotherm. Res. 304, 49–61.
Shand, P., Johannesson, K.H., Chudaev, O., Chudaeva, V., Edmunds, W.M., 2005. Rare Earth Element Contents of High pCO 2 Groundwaters of Primorye, Russia: Mineral Stability and Complexation Controls. Springer.
Shannon, R.D., 1976. Revised effective ionic radii and systematic studies of interatomic distances in halides and chalcogenides. Acta Crystallogr. Sect. A: Cryst. Phys., Diffr., Theor. Gen. Crystallogr. 32 (5), 751–767.
Sherman, G.D., 1949. Factors Influencing the Development of Lateritic and Laterite Soils in the Hawaiian Islands.
Shi, Y., E, C., Peng, Q., Zhang, Z., Zhang, J., Yan, W., Xu, C., 2023. Rare earth elements in aeolian loess sediments from Menyuan Basin, northeastern Tibetan Plateau: implications for provenance. Front. Environ. Sci. 11, 1074909.
Shock, E.L., Helgeson, H.C., Sverjensky, D.A., 1989. Calculation of the thermodynamic and transport properties of aqueous species at high pressures and temperatures: Standard partial molal properties of inorganic neutral species. Geochim. Cosmochim. Acta 53 (9), 2157–2183.
Sikakwe, G.U., Otele, A., Ozibo, B.N., 2018. Chemical speciation and complexation modeling of trace and rare earth elements in groundwater of Oban Massif and Mamfe mMbayment southeastern Nigeria. Chem. Speciat. Bioavailab. 30 (1), 86–98.
da Silva Alves, M.A., Pereira, V.P., Neto, A.C.B., Menegotto, E., 2018. Weathering of the Madeira world-class Sn-Nb-Ta (cryolite, REE, U, Th) deposit, Pitinga mine (Amazon, Brazil). J. Geochem. Explor. 186, 61–76.
Simonson, R.W., 1995. Airborne dust and its significance to soils. Geoderma 65 (1), 1–43.
Skibińska, M., 2017. The sorption capability of halloysite. Annales Universitatis Mariae Curie-Sklodowska, sectio AA–Chemia 72 (1), 47.
Smedley, P.L., 1991. The geochemistry of rare earth elements in groundwater from the Carnmenellis area, Southwest England. Geochim. Cosmochim. Acta 55 (10), 2767–2779.
Smith, R.M., Martell, A.E., 1989. Critical Stability Constants: Second Supplement, 6. Springer.
Sondi, I., Bišćan, J., Pravdić, V., 1996. Electrokinetics of Pure Clay Minerals Revisited. J. Colloid Interface Sci. 178 (2), 514–522.
Sonke, J.E., Salters, V.J., 2006. Lanthanide–humic substances complexation. I. Experimental evidence for a lanthanide contraction effect. Geochim. Cosmochim. Acta 70 (6), 1495–1506.
Spedding, F., Jaffe, S., 1954. Conductances, solubilities and ionization constants of some rare earth sulfates in aqueous solutions at 25. J. Am. Chem. Soc. 76 (3), 882–884.
St. Clair, J., Moon, S., Holbrook, W.S., Perron, J.T., Riebe, C.S., Martel, S.J., Carr, B., Harman, C., Singha, K., Richter, D.d., 2015. Geophysical imaging reveals topographic stress control of bedrock weathering. Science 350 (6260), 534–538.
Steefel, C.I., Lasaga, A.C., 1992. Putting transport into water-rock interaction models. Geology 20 (8), 680–684.
Stern, J.C., Sonke, J.E., Salters, V.J., 2007. A capillary electrophoresis-ICP-MS study of rare earth element complexation by humic acids. Chem. Geol. 246 (3–4), 170–180.
Stern, O., 1924. Zur theorie der elektrolytischen doppelschicht. Z. Elektrochem. Angew. Phys. Chem. 30 (21—22), 508–516.
Stroeven, A.P., Fabel, D., Hättestrand, C., Harbor, J., 2002. A relict landscape in the centre of Fennoscandian glaciation: cosmogenic radionuclide evidence of tors preserved through multiple glacial cycles. Geomorphology 44 (1), 145–154.
Stucki, J.W., 2013. Chapter 11 - properties and behaviour of iron in clay minerals. In: Bergaya, F., Lagaly, G. (Eds.), Developments in Clay Science. Elsevier, pp. 559–611.
Stumm, W., 1997. Reactivity at the mineral-water interface: dissolution and inhibition. Colloids Surf. A Physicochem. Eng. Asp. 120 (1), 143–166.
Su, N., Yang, S., Guo, Y., Yue, W., Wang, X., Yin, P., Huang, X., 2017. Revisit of rare earth element fractionation during chemical weathering and river sediment transport. Geochem. Geophys. Geosyst. 18 (3), 935–955.
Sun, C., Liang, Y., 2013. The importance of crystal chemistry on REE partitioning between mantle minerals (garnet, clinopyroxene, orthopyroxene, and olivine) and basaltic melts. Chem. Geol. 358, 23–36.
Takahashi, T., Dahlgren, R.A., Theng, B.K.G., Whitton, J.S., Soma, M., 2001. Potassium-selective, halloysite-rich soils formed in volcanic materials from Northern California. Soil Sci. Soc. Am. J. 65 (2), 516–526.
Takehara, L., Silveira, F.V., Santos, R.V., 2016. Chapter 4 - potentiality of rare earth elements in Brazil. In: De Borges Lima, I., Leal Filho, W. (Eds.), Rare earths industry. Elsevier, Boston, pp. 57–72.
Tan, K.H., 1986. Degradation of soil minerals by organic acids. In: Interactions of Soil Minerals With Natural Organics and Microbes, 17, pp. 1–27.
Tan, X., Ren, X., Chen, C., Wang, X., 2014. Analytical approaches to the speciation of lanthanides at solid-water interfaces. TrAC Trends Anal. Chem. 61, 107–132.
Tanada, T., 1942. Hawaiian soil colloids. Hawaii Agr. Expt. Sta. Bien. Rpt 44, 56–57.
Tang, J., Johannesson, K.H., 2003. Speciation of rare earth elements in natural terrestrial waters: assessing the role of dissolved organic matter from the modeling approach. Geochim. Cosmochim. Acta 67 (13), 2321–2339.
Tang, J., Johannesson, K.H., 2010a. Ligand extraction of rare earth elements from aquifer sediments: implications for rare earth element complexation with organic matter in natural waters. Geochim. Cosmochim. Acta 74 (23), 6690–6705.
Tang, J., Johannesson, K.H., 2010b. Rare earth elements adsorption onto Carrizo sand: Influence of strong solution complexation. Chem. Geol. 279 (3–4), 120–133.
Tang, J., Qiao, J., Xue, Q., Liu, F., Fan, X., Liu, S., Huang, Y., 2021. Behavior and mechanism of different fraction lead leach with several typical sulfate lixiviants in the weathered crust elution-deposited rare earth ore. Environ. Sci. Pollut. Res. 28 (24), 31885–31894.
Tanizaki, Y., Shimokawa, T., Nakamura, M., 1992. Physicochemical speciation of trace elements in river waters by size fractionation. Environ. Sci. Technol. 26 (7), 1433–1444.
Tardy, Y., 1992. Chapter 15 - diversity and terminology of lateritic profiles. In: Martini, I. P., Chesworth, W. (Eds.), Developments in Earth Surface Processes. Elsevier, pp. 379–405.
Tarì, G., Bobos, I., Gomes, C.S.F., Ferreira, J.M.F., 1999. Modification of surface charge properties during kaolinite to halloysite-7Å transformation. J. Colloid Interface Sci. 210 (2), 360–366.
Taylor, G., Eggleton, R.A., 2001. Regolith Geology and Geomorphology. John Wiley & Sons.
Taylor, G., Eggleton, R.A., Holzhauer, C.C., Maconachie, L.A., Gordon, M., Brown, M.C., McQueen, K.G., 1992. Cool climate lateritic and bauxitic weathering. J. Geol. 100 (6), 669–677.

Taylor, R.G., Howard, K.W.F., 1999. Lithological evidence for the evolution of weathered mantles in Uganda by tectonically controlled cycles of deep weathering and stripping. CATENA 35 (1), 65–94.
Theng, B., 2012. The clay minerals. In: Developments in Clay Science. Elsevier, pp. 3–45.
Tohar, S.Z., Yunus, M.Y.M., Harun, N.B., 2024. BCR leaching procedure to evaluate the mobilization behaviour of ion adsorption type REE deposit in I-type granite weathering profiles. In: AIP Conference Proceedings. AIP Publishing.
Trench, A., Zhang, L., Groves, D.I., Crook, D., Brand, N.W., 2025. Australian critical metal exploration for analogues of Chinese ionic-clay REE deposits. Geosystems and Geoenvironment 4 (1), 100293.
Turekian, K.K., Wedepohl, K.H., 1961. Distribution of the elements in some major units of the earth's crust. Geol. Soc. Am. Bull. 72 (2), 175–192.
Uddin, F., 2008. Clays, nanoclays, and montmorillonite minerals. Metall. Mater. Trans. A 39 (12), 2804–2814.
Ueda, T., 1957. Studies on the metamictization of radioactive minerals. Mem. Coll. Sci. Univ. Kyoto. Ser. B. 24 (2), 81–120.
USGS, 1973. United States Mineral Resources. 820, Washington, D.C.
USGS, 2024. Mineral Commodity Summaries 2024. 2024, Reston, VA.
Van Gosen, B.S., Verplanck, P.L., Seal Ii, R.R., Long, K.R., Gambogi, J., 2017. Rare-earth Elements. 1802O, Reston, VA.
Vázquez-Ortega, A., Perdrial, J., Harpold, A., Zapata-Ríos, X., Rasmussen, C., McIntosh, J., Schaap, M., Pelletier, J.D., Brooks, P.D., Amistadi, M.K., Chorover, J., 2015. Rare earth elements as reactive tracers of biogeochemical weathering in forested rhyolitic terrain. Chem. Geol. 391, 19–32.
Verma, M.P., 2003. A thermodynamic assessment of dissociation constant of water, proceedings 28th workshop on geothermal reservoir engineering. Stanford University, Stanford, California.
Verplanck, P.L., 2017. The role of fluids in the formation of rare earth element deposits. Procedia Earth and Planetary Science 17, 758–761.
Viers, J., Dupré, B., Polvé, M., Schott, J., Dandurand, J.-L., Braun, J.-J., 1997. Chemical weathering in the drainage basin of a tropical watershed (Nsimi-Zoetele site, Cameroon) : comparison between organic-poor and organic-rich waters. Chem. Geol. 140 (3), 181–206.
Villaseca, C., Martin Romera, C., de la Rosa, J., Barbero, L., 2003. Residence and redistribution of REE, Y, Zr, Th and U during granulite-facies metamorphism; behaviour of accessory and major phases in peraluminous granulites of central Spain. Chem. Geol. 200 (3–4), 293–323.
Voncken, J.H.L., 2016. The Rare Earth Elements: An Introduction. Springer International Publishing AG, Cham, Switzerland.
Wall, F., 2021. Rare earth elements. In: Alderton, D., Elias, S.A. (Eds.), Encyclopedia of geology, Second edition. Academic Press, Oxford, pp. 680–693.
Wang, D.-h., Zhao, Z., Yu, Y., Dai, J.-j., Deng, M.-c., Zhao, T., Liu, L.-j., 2018. Exploration and research progress on ion-adsorption type REE deposit in South China. China Geol. 1 (3), 415–424.
Wang, F.-L., Wang, C.Y., Zhao, T.-P., 2015a. Boron isotopic constraints on the Nb and Ta mineralization of the syenitic dikes in the ~260Ma Emeishan large igneous province (SW China). Ore Geol. Rev. 65, 1110–1126.
Wang, L., Xu, C., Zhao, Z., Song, W., Kynicky, J., 2015b. Petrological and geochemical characteristics of Zhaibei granites in Nanling region, Southeast China: implications for REE mineralization. Ore Geol. Rev. 64, 569–582.
Wang, M., Li, M.Y.H., Zhou, M.-F., Zhou, J.-X., Sun, G., Zhou, Y., Li, Y., 2024. Enrichment of rare earth elements during the weathering of alkaline igneous systems: insights from the Puxiong regolith-hosted rare earth element deposit, SW China. Econ. Geol. 119 (1), 161–187.
Wang, Q., Zhu, C., Yun, J., Yang, G., 2017. Isomorphic substitutions in clay materials and adsorption of metal ions onto external surfaces: a DFT investigation. J. Phys. Chem. C 121 (48), 26722–26732.
Wang, Y., Liu, L., Sun, M., Huang, J., Huang, Y., Liang, X., Tan, W., He, H., Zhu, J., 2023. Distribution and fractionation of rare earth elements (REE) in the ion adsorption-type REE deposit (IAD) at Maofeng Mountain, Guangzhou, China. Clay Clay Miner. 71 (3), 340–361.
Wang, Z., Chen, B., Ma, X., 2014. Petrogenesis of the late Mesozoic Guposhan composite plutons from the Nanling Range, South China: implications for W-Sn mineralization. Am. J. Sci. 314 (1), 235–277.
Ward, C.P., 2017. Controls on the Enrichment of the Serra Verde Rare Earth Deposit, Brazil. Imperial College London.
Watson, E.B., Capobianco, C., 1981. Phosphorus and the rare earth elements in felsic magmas: an assessment of the role of apatite. Geochim. Cosmochim. Acta 45 (12), 2349–2358.
Watson, E.B., Green, T.H., 1981. Apatite/liquid partition coefficients for the rare earth elements and strontium. Earth Planet. Sci. Lett. 56, 405–421.
Wayland, E.J., 1934. Peneplains and some erosional landforms. In: Geological Survey of Uganda Annual Report (for year ending 31st March 1934) and Bulletin, 1, pp. 77–79.
Welch, S.A., Christy, A.G., Isaacson, L., Kirste, D., 2009. Mineralogical control of rare earth elements in acid sulfate soils. Geochim. Cosmochim. Acta 73 (1), 44–64.
Weng, Z.H., Jowitt, S.M., Mudd, G.M., Haque, N., 2013. Assessing rare earth element mineral deposit types and links to environmental impacts. Appl. Earth Sci. 122 (2), 83–96.
Whalen, J.B., Currie, K.L., Chappell, B.W., 1987. A-type granites: geochemical characteristics, discrimination and petrogenesis. Contrib. Mineral. Petrol. 95, 407–419.
White, A.F., Brantley, S.L., 1995. Weathering rates of silicate minerals. In: Chemical Weathering Rates of Silicate Minerals, Reviews in Mineralogy, 31, pp. 1–22.
Williams-Jones, A.E., Vasyukova, O., 2018. The economic geology of scandium, the runt of the rare earth element litter. Econ. Geol. 113 (4), 973–988.
Williams-Jones, A.E., Migdisov, A.A., Samson, I.M., 2012. Hydrothermal mobilisation of the rare earth elements–a tale of "ceria" and "yttria". Elements 8 (5), 355–360.
Wilson, M.J., 2004. Weathering of the primary rock-forming minerals: processes, products and rates. Clay Miner. 39 (3), 233–266.
Wones, D.R., 1989. Significance of the assemblage titanite+ magnetite+ quartz in granitic rocks. Am. Mineral. 74 (7–8), 744–749.
Wood, S.A., 1990. The aqueous geochemistry of the rare-earth elements and yttrium: 1. Review of available low-temperature data for inorganic complexes and the inorganic REE speciation of natural waters. Chem. Geol. 82, 159–186.
Wood, W.W., Smedley, P.L., Lindsey, B.D., Wood, W.T., Kirchheim, R.E., Cherry, J.A., 2022. Global Groundwater Solute Composition and Concentrations. Groundwater 60 (6), 714–720.
Wright, V.P., 1994. Losses and gains in weathering profiles and duripans. In: Quantitative Diagenesis: Recent Developments and Applications to Reservoir Geology. Springer, pp. 95–123.
Wyborn, L.A.I., Heinrich, C.A., Jaques, A., 1994. Australian Proterozoic mineral systems: essential ingredients and mappable criteria. Publication Series of the Australasian Institute of Mining and Metallurgy 5, 109–115.
Xirouchakis, D., Lindsley, D.H., 1998. Equilibria among titanite, hedenbergite, fayalite, quartz, ilmenite, and magnetite: experiments and internally consistent thermodynamic data for titanite. Am. Mineral. 83 (7–8), 712–725.
Yamamoto, Y., Takahashi, Y., Shimizu, H., 2010. Systematic change in relative stabilities of REE-humic complexes at various metal loading levels. Geochem. J. 44 (1), 39–63.
Yang, H., Zhang, Y., Ouyang, J., 2016. Physicochemical properties of halloysite. Developments in Clay Science 7, 67–91.
Yang, M., Liang, X., Ma, L., Huang, J., He, H., Zhu, J., 2019. Adsorption of REEs on kaolinite and halloysite: a link to the REE distribution on clays in the weathering crust of granite. Chem. Geol. 525, 210–217.
Yang, R., Wang, W., Zhang, X., Liu, L., Wei, H., Bao, M., Wang, J., 2008. A new type of rare earth elements deposit in weathering crust of Permian basalt in western Guizhou, NW China. J. Rare Earths 26 (5), 753–759.
Yaraghi, A., KS, A., Baharun, N., 2019. A short review on REE recovery from ion-adsorption clays. Development 8, 131–136.
Yaraghi, A., Ariffin, K.S., Baharun, N., 2020. Comparison of characteristics and geochemical behaviors of REEs in two weathered granitic profiles generated from metamictized bedrocks in Western Peninsular Malaysia. J. Asian Earth Sci. 199, 104385.
Yu, M., Du, N., Hou, W., 2021. Model prediction of the point of zero net charge of layered double hydroxides and clay minerals. Colloids Surf. A Physicochem. Eng. Asp. 611, 125860.
Yukselen, Y., Kaya, A., 2006. Prediction of cation exchange capacity from soil index properties. Clay Miner. 41 (4), 827–837.
Zhang, Z., Yang, X., Li, S., Zhang, Z., 2010. Geochemical characteristics of the Xuanwei Formation in West Guizhou: significance of sedimentary environment and mineralization. Chin. J. Geochem. 29 (4), 355–364.
Zhao, L., Dai, S., Graham, I.T., Li, X., Liu, H., Song, X., Hower, J.C., Zhou, Y., 2017. Cryptic sediment-hosted critical element mineralization from eastern Yunnan Province, southwestern China: Mineralogy, geochemistry, relationship to Emeishan alkaline magmatism and possible origin. Ore Geol. Rev. 80, 116–140.
Zhao, X., Li, N.-B., Huizenga, J.M., Yan, S., Yang, Y.-Y., Niu, H.-C., 2021. Rare earth element enrichment in the ion-adsorption deposits associated granites at Mesozoic extensional tectonic setting in South China. Ore Geol. Rev. 137, 104317.
Zhao, Z., Wang, D., Bagas, L., Chen, Z., 2022. Geochemical and REE mineralogical characteristics of the Zhaibei Granite in Jiangxi Province, southern China, and a model for the genesis of ion-adsorption REE deposits. Ore Geol. Rev. 140, 104579.
Zhou, L., Zhang, Z., Li, Y., You, F., Wu, C., Zheng, C., 2013. Geological and geochemical characteristics in the paleo-weathering crust sedimentary type REE deposits, western Guizhou, China. J. Asian Earth Sci. 73, 184–198.
Zhou, X., Sun, T., Shen, W., Shu, L., Niu, Y., 2006. Petrogenesis of Mesozoic granitoids and volcanic rocks in South China: a response to tectonic evolution. Episodes Journal of International Geoscience 29 (1), 26–33.
Ziouane, Y., Leturcq, G., 2018. New modeling of nitric acid dissociation function of acidity and temperature. ACS Omega 3 (6), 6566–6576.
Zwicker, J., Smrzka, D., Vadillo, I., Jiménez-Gavilán, P., Giampouras, M., Peckmann, J., Bach, W., 2022. Trace and rare earth element distribution in hyperalkaline serpentinite-hosted spring waters and associated authigenic carbonates from the Ronda peridotite. Appl. Geochem. 147, 105492.